Iron in modern and ancient East Antarctic snow: implications for phytoplankton production in the Southern Ocean

by

(Peter Ross) Ross Edwards, BSc. Hons.

Submitted in fulfillment of the requirements for the degree of
Doctor of Philosophy

Institute of Antarctic and Southern Ocean Studies
University of Tasmania, 1999

Supervisor(s) Dr. Peter Sedwick
Dr. Ian Allison
Dr. Denis Mackey
Mr. Vin Morgan

Declaration

This thesis contains no material which has been accepted for the award of any other degree or diploma in any University, and to the best of my knowledge contains no copy or paraphrase of material previously published or written by another person, except where due reference is made in the text.

2/1/2000

Ross Edwards

Authority of access

Ross Edwards
Date 2/1/2000

Dedicated to Peter, Brenda, Jenny and David Edwards

Introductory quote

"Upon November 12 and 13, 1902, occurred the greatest fall of matter in the history of Australia. Upon the 14th of November, it rained mud in Tasmania. It was of course attributed to the Australian whirlwinds, but according to the Monthly Weather Review, 32-365, there was a haze all the way to the Philippines, also as far as Hong Kong. It may be that this phenomenon had no special relationship with the even more tremendous fall of matter that occurred in Europe, February 1903. I think myself that in 1903, we passed through the remains of a powdered world - left over from an inter-planetary dispute, brooding in space like a red resentment ever since."

Charles Fort, *The book of the damned*, 1919.

Abstract

Iron (Fe) was measured in present-day and ancient East Antarctic snow to investigate the atmospheric flux of Fe into the Southern Ocean, the solubility of this atmospheric iron, and the level of new phytoplankton production it could support in Southern Ocean waters, given that iron is an essential micronutrient for algal growth. To investigate the present-day atmospheric Fe deposition, acid-soluble total-dissolvable Fe (TD-Fe) was measured in present-day East Antarctic snow from inland sites in Princess Elizabeth Land and marine sites in Prydz Bay, the Dumont d'Urville Sea and the Ross Sea.

To investigate temporal variations in atmospheric Fe deposition, TD-Fe concentrations were measured in glacial ice-core (i.e., ancient snow) samples of Holocene, Wisconsin-Holocene transition and Last Glacial Maximum (LGM) age from Law Dome on the coast of Wilkes Land, East Antarctica. Average TD-Fe concentrations in modern snow from Prydz Bay, Princess Elizabeth Land and the Ross Sea were similar, with a range of 612-749 pg Fe g^{-1}. Average TD-Fe concentrations in modern snow from the Dumont d'Urville Sea were an order of magnitude less (62 pg Fe g^{-1}), and comparable to TD-Fe concentrations in Holocene sections of the Law Dome ice-cores. There are significant variations in the Law Dome ice-core TD-Fe concentrations, on time scales ranging from seasonal to glacial-interglacial. Summer TD-Fe concentrations exceed winter by ~4x. Average

Holocene ice TD-Fe concentration (99 pg Fe g^{-1}) was much lower than that for the Holocene-Wisconsin transition (1100 pg Fe g^{-1}) and LGM (6700 pg Fe g^{-1}). Soluble Fe in modern East Antarctic snow was estimated from measurements of TDFe and total-filterable (0.2 μm) Fe. Soluble Fe in the samples ranged from 10-90% of TDFe, averaging ~40%. Past and present-day atmospheric Fe fluxes were estimated from average snow and ice TDFe concentrations and estimated snow accumulation rates. Present-day and late Holocene flux estimates are in the range of 0.02 -0.10 mg Fe m^{-2} yr^{-1}, with an average of 0.07 mg Fe m^{-2} yr^{-1}. The estimated LGM atmospheric Fe flux onto Law Dome ranges from 0.86 -2.15 mg Fe m^{-2} yr^{-1}, using minimum and maximum estimates of the LGM snow-accumulation rate. This is 12-30 times the average present-day atmospheric Fe flux and 16-41 times the average atmospheric Fe flux estimated from the late Holocene ice-core samples.

Assuming (1) similar atmospheric Fe fluxes exist over the Southern Ocean (south of 50°S), (2) limitation of algal production in this region by Fe deficiency (i.e., nutrient- and light-replete conditions), (3) 40% of the Fe is bioavailable, and (4) an algal C:Fe molar assimilation ratio of 33,000-500,000, then the maximum potential algal new production supported by atmospheric Fe deposition in the present-day is estimated at 0.017-0.25 mol C m^{-2} yr^{-1}. Assuming a Redfield algal C:N assimilation ratio and an upwelling flux of 12 g nitrate m^{-2} yr^{-1}, this estimated new production rate could consume 0.3-4% of the nitrate upwelled into surface waters of the present-day Southern Ocean. Similar calculations using estimated LGM atmospheric Fe flux yield potential new production of 0.2-7.9 mol C m^{-2} yr^{-1}, which could consume up to

136 % of the nitrate upwelled in the present-day Southern Ocean. Estimates of the potential increase in surface-water dissolved Fe concentration due to atmospheric Fe released from melting annual sea ice suggest that ~5 nM increases are possible in thin (~1 m deep) meltwater lenses, increases which are probably sufficient to alleviate algal Fe deficiency and allow bloom development. However, the potential total annual new production supported by atmospheric Fe released from melting sea ice is estimated as 45 Tg C, which is ~1% of the estimated total annual Southern Ocean primary production of 4414 Tg.

In summary, the results presented in this thesis are consistent with the suggestion that the present-day atmospheric Fe flux into the Southern Ocean is insufficient to support the use of the upwelled nitrate by phytoplankton, and also that the majority of algal new production in this region is supported by Fe supplied from other sources, such as upwelling and shelf sediments. However, these data indicate that atmospheric Fe inputs may support short-lived high-production events at the edge of retreating seasonal sea ice. These results are also consistent with the hypothesis that the atmospheric Fe flux into the Southern Ocean was significantly greater during the LGM, potentially supporting much greater phytoplankton new production at that time.

Acknowledgements

I am deeply indebted to Doctor Peter Sedwick for making this thesis possible. A better mentor would be impossible to find. In addition to Peter, I owe much to Dr Ian Allison, Mr Vin Morgan and Dr Denis Mackey for their support and advice. I wish to thank all those who contributed to the field program. In particular Mike Craven and Rob Kerning, who at great personal risk and hardship collected samples during the ANARE, Lambert Glacier basin traverse 94. I especially wish to thank Paul Scott, Paul Thompson, KT Bradley, Meg Humrich, Vicky Lytle, Naomi Parker, Lisette Robertson, Helen Philips, Cath Sampson, Ilse Keissling, Fiona Taylor, Jason Whitehead, Rob Massom, Brendan Buckley, Tom Trull, Martina Doblin, Petra Heil, Annie Wong, Andre Chiaradia, Kim Krebs, Mark Mooney and Jane Iseman for their support and friendship during the course of this thesis. Also special thanks to Margaret Appleton and Kelvin Michael for all their help.

This Research was supported by funding from the Antarctic CRC, APA, ANARE, Australian Antarctic Division, and DIST.

Table of Contents

List of Tables

List of Figures

Chapter 1

Introduction

1.1 Overview of the thesis

The carbon balance in the surface waters of the Southern Ocean is thought to be a dominant factor in the oceanic control of atmospheric carbon dioxide (CO_2) levels (Sarmiento and Orr, 1991). This region is characterised by the upwelling of deep water, which transports large amounts of plant nutrients to the surface (Gordon et al., 1977). Paradoxically phytoplankton in much of the present-day Southern Ocean do not appear to be nutrient limited (Martin et al., 1990b; de Baar et al., 1990; Dugdale and Wilkerson, 1992), but are unable to exhaust surface water nutrient stocks during the summer growing season (Smith, 1991; Francois et al., 1997). The polar nutrient hypothesis (Knox and McElroy, 1984; Sarmiento and Toggweiler, 1984; Siegenthaler and Wenk, 1984) postulates that if phytoplankton in the Southern Ocean could consume all of the presently unused nutrients the resulting export of carbon to the deep ocean could affect a large biological drawdown in atmospheric CO_2. This so called 'biological carbon pump', it was suggested, may have been responsible for the large variations in atmospheric CO_2 that have occurred in phase with late

Quaternary glacial cycles, as evident from air bubbles trapped in polar ice-cores (Berner et al., 1980; Neftel et al., 1982; Lorius et al., 1985; Barnola et al., 1987; Jouzel et al., 1993). Over the past decade a large body of evidence has been gathered to suggest that the availability of iron (Fe) in surface waters of the Southern Ocean may be the dominant factor controlling primary production in light replete conditions (Martin et al., 1990b; de Baar, 1990, van Leeuwe, 1997). In his 'iron hypothesis', Martin (1990) suggested that at present primary production in this region may be limited by the availability of dissolved Fe, much of which is derived from the atmospheric deposition of dust. But during glacial periods higher atmospheric fluxes of dust may have alleviated this Fe deficiency, switching on the biological carbon pump, exhausting surface water nutrients and subsequently lowering atmospheric CO_2 levels.

At present there is little quantitative data for either the Holocene or Last Glacial Maximum (LGM) atmospheric Fe flux to the Southern Ocean and its variability during these periods. Qualitative evidence for the present and paleo-atmospheric Fe flux to the Southern Ocean has been inferred from a small number of Antarctic ice-core dust and aluminum measurements, deep-sea sediments, and a limited number of atmospheric measurements (Zoller et al., 1973; Menhaut et al., 1979; Cunningham and Zoller, 1981; Tuncel et al., 1989; Wagenbach et al., 1988; Wolff et al., 1998; Dick, 1987; Dick and Peel, 1985; Dick, 1991; Kumar et al., 1995; Anderson et al., 1998). The relationship between these data and the atmospheric input of Fe to the Southern Ocean is unclear, as the major Antarctic ice-core records are from high-

altitude inland sites, which may not be representative of maritime fluxes, while the deep-sea records (e.g.; Kumar et al., 1995; Anderson et al., 1998) are difficult to interpret due to the transport of particles by ocean currents and biological processes. In addition, very little is known concerning the solubility of Fe in atmospheric dust, and hence how much will be available to phytoplankton. A further complication arises due to the presence of seasonal sea ice in both the interglacial and glacial Southern Ocean. Seasonally large areas of the Southern Ocean are covered with sea ice; on average, seasonal sea ice covers up to 15 x 10^6 km^2 at its maximum extent (Parkinson, 1992). During the months while the sea ice is present Fe will be deposited on the sea ice rather than in the ocean. Martin (1990b) suggested that the rapid melting of sea ice might provide a large episodic source of Fe to Antarctic waters.

A knowledge of the atmospheric Fe flux to the Southern Ocean during the present, Holocene, and LGM is necessary to evaluate these hypotheses. This thesis presents estimates of the atmospheric Fe flux to the Southern Ocean as determined from Fe measurements in present-day snow and ancient snow in ice-cores from East Antarctica. Specifically, the following hypotheses are examined:

(1) The present-day atmospheric Fe flux to the Southern Ocean is insufficient to allow the complete use of upwelling nitrate by phytoplankton in light replete conditions;

(2) Seasonal Antarctic sea ice may release enough Fe during melting to support a large fraction of Southern Ocean new production; and

(3) The atmospheric Fe flux to the Southern Ocean during the LGM was high enough to sustain an increase in new phytoplankton production relative to the present.

To test these hypotheses, measurements of total-dissolvable and total-filterable Fe in present-day and ancient East Antarctic snow were made. From these data the atmospheric Fe flux to the present-day and LGM Southern Ocean, the release of Fe from seasonal sea ice and the potential new phytoplankton production ensuing from these Fe fluxes are estimated.

1.2 The iron hypothesis and new phytoplankton production in the Southern Ocean

Ocean surface waters containing high nitrate concentrations but low chlorophyll*a* cover more than 20% of the world's oceans. These High Nitrate Low Chloropyll (HNLC) regions support relatively low primary production despite an abundance of the major plant nutrients nitrate and phosphate (Chisholm and Morel, 1991). Recent field studies in HNLC regions of the equatorial Pacific, the north-east Pacific and the Southern Ocean suggest that the additions of 0.5-10 nM dissolved Fe to these waters cause marked increases in algal growth and biomass (Martin and Fitzwater, 1988;

Martin et al., 1990b; de Baar et al., 1990; Helbling et al., 1991; Greene et al., 1991; Kolber et al., 1994; Price et al., 1994; Coale et al., 1998; Lindley and Barber, 1998). From these observations it has been argued that the availability of dissolved Fe exerts a primary control on phytoplankton growth and biomass, the marine food web, and the drawdown of atmospheric CO_2 in HNLC regions (Martin et al., 1990a, 1991, 1994; de Baar et al., 1995; Coale et al., 1998). This includes much of the Southern Ocean. Reliable concentration data for Fe in the HNLC waters of the Southern Ocean are few (e.g. Martin et al., 1990b, 1991; de Baar et al., 1995; Johnson et al., 1997; Sedwick et al., 1997; Sedwick and Ditullio, 1997; de Baar et al., 1999) but show that surface water dissolved Fe concentrations are typically <1 nM and are often < 0.2 nM. While the present-day atmospheric deposition of Fe to the Southern Ocean is thought to be extremely low (Donaghay et al., 1991), the flux is thought to have been significantly greater during the LGM (Kumar et al., 1995). In concert with the apparent increase in atmospheric dust during the LGM, atmospheric CO_2 concentrations as determined from ice-cores decreased from approximately 300 ppm to 200 ppm (Barnola et al., 1987). Martin (1990) proposed that while biological production in the present day Southern Ocean appears to be Fe limited, this deficiency may have been alleviated by atmospheric deposition during the LGM, causing a significant drawdown of atmospheric CO_2. Recent studies of deep-sea sediments (Kumar et al., 1993, 1995) suggest an increased atmospheric deposition of Fe to Subantarctic waters (between about 40°S and 55°S) of the Southern Ocean during Pleistocene glaciations, and a corresponding increase in phytoplankton export production. This inferred increase in primary production in phase with atmospheric

Fe deposition supports the Fe hypothesis as proposed by Martin (1990). In addition, several large scale in situ oceanic Fe fertilization experiments have been completed, showing unequivocally that the addition of Fe to HNLC waters can increase biological productivity and drive a significant local drawdown in atmospheric CO_2 (Coale et al., 1996, 1998; Martin et al., 1994; T. Trull, pers. comm., 1999; Boyd et al., 1999).

1.3. The atmosphere as a source of Fe to Southern Ocean waters

1.3.1 Atmospheric transport of mineral aerosol to Antarctica

The deposition and dissolution of Fe-bearing mineral aerosols (atmospheric mineral dust) may be the primary source of Fe in surface waters in many areas of the global ocean (Moore et al., 1984). Various aspects of mineral aerosol transport have been extensively studied over the past 20 years (see for instance: Pèwè, 1981; Gillette, 1981; Prospero, 1981a, 1981b; Leinen and Sarnthein, 1982; Morales, 1985; Buat-Menard, 1986; Chester, 1986; Pye, 1987; Tsoar and Pye, 1987; Chester and Murphy, 1990; Schütz et al., 1990; Duce et al., 1991; Goudie and Middleton, 1992; Rea, 1994; Duce, 1995; Tegen and Fung 1995). Mineral aerosols are formed by wind erosion of fine mineral particles from soils and rocks (Gillette, 1991; Duce, 1986). The primary sources of these aerosols (Figure 1.1) are the arid and semi-arid regions (Chester, 1985; Prospero, 1981a, 1981b). The Antarctic continent is nearly completely

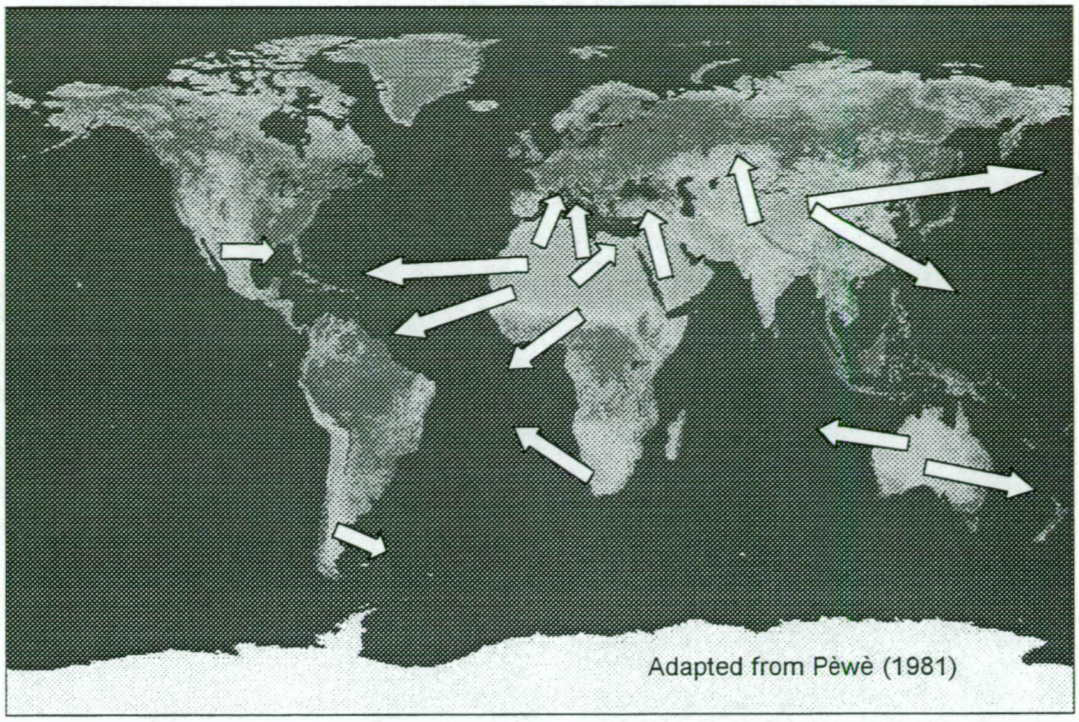

Figure 1.1 Major sources and atmospheric transport of mineral aerosols

covered with snow and ice, with no significant dust sources. Dust found in Antarctic snow is thought to mainly originate from South America. Mineralogical studies (Gaudichet et al., 1986, 1988) and isotopic fingerprinting of dust found in the East Antarctic Vostok and Dome C ice-cores (Grousset et al., 1992; Basile et al., 1997) have demonstrated the Patagonian loess of Southern Argentina to be a source of dust to East Antarctica. Lambert et al. (1990) found that atmospheric transport to Antarctica showed a seasonal variation with a minimum in winter and a maximum in summer. Atmospheric measurements of dust-derived elements at the South Pole (Cunningham and Zoller, 1981) and Neumayer station (Wagenbach et al., 1988) also show a seasonal variation with lower concentrations during winter months than during the austral summer. This atmospheric transport is thought to occur

mainly in the upper troposphere as mineral aerosols are removed from the lower troposphere by wet deposition, especially at the polar front (Shaw, 1979; Heimann et al., 1990; Lambert et al., 1990). But this transport pathway is impeded during winter by the formation of the polar vortex over the Antarctic continent. The vortex breaks up from late spring to summer allowing upper tropospheric transport to resume hence the seasonal cycle in atmospheric dust concentrations observed in Antarctica.

1.3.2 Chemical characteristics of mineral aerosols

Mineral aerosols over the remote ocean have been found to be composed largely of clay minerals (in particular, illite, chlorite, kaolinite and montmorillonite), quartz and feldspars (Chester, 1985). The clay composition of the aerosol is thought to vary with latitude as evident in oceanic sediments (Griffin et al., 1968). In particular, Southern Ocean sediments appear to be largely composed of illite and chlorite (Griffin et al., 1968). While illite appears to be a ubiquitous component of continental weathering, chlorite is characteristic of high latitude glacial weathering processes (Chester, 1985).

The solubility of the Fe deposited in the ocean is thought to be the main parameter determining its biological availability to phytoplankton (Wells et al., 1983; Rich and Morel, 1990; Morel et al., 1991). Generally, a solubility of 10% has been used to calculate the fraction of mineral dust Fe available to phytoplankton (e.g., de Baar et al., 1995), but this may be a very conservative estimate. Moore et al. (1984)

investigated the solubility of metals in mineral dust relative to aluminium (Al), assuming Al to be relatively insoluble. This study concluded that 10-12% of total Fe in the dust was soluble relative to Al. Maring (1987) investigated the seawater solubility of Al present in mineral aerosols collected from Enewetak Atoll, and found that ~5% of the mineral aerosol Al was soluble in seawater. Losno et al., (1993) found the solubility of Al in precipitation from continental and marine sites to vary between 0.2 to 91%. These results suggest that Moore et al.'s Fe solubility is probably a lower limit. Zhuang et al. (1990) used mineral aerosol particles collected over the North Pacific to investigate the dissolution of Fe-bearing aerosol in seawater. In their study, dissolved Fe was defined as that which passes through a 0.4 μm pore-size Nuclepore filter. They found that up to 40-50% of the total Fe would dissolve in seawater with dissolved Fe concentrations less than a few nmol kg^{-1}.

1.4 Estimates of the atmospheric flux of Fe to the present-day and LGM Southern Ocean

1.4.1 The present-day atmospheric Fe flux

Duce et al. (1991) estimated the present-day annual atmospheric flux of mineral dust to the world ocean at a resolution of 10° latitude × 10° longitude area. This estimate was based on calculations of wet and dry deposition using measurements of mineral dust in air and rain. Little data exists for the Southern Ocean and calculations were

largely based on atmospheric measurements from Georg-von-Neumayer station, Antarctica. From these calculations a dust flux (total mass) of 10 mg m^{-2} yr^{-1} was estimated for the Southern Ocean. Assuming that Fe comprises 3.5% of the mineral dust, Donaghay et al. (1991) calculated the atmospheric Fe flux (Figure 1.2) to the global ocean from the mineral dust fluxes of Duce et al. (1991). Annual Fe fluxes to the Southern Ocean were estimated to be of the order of 0.1 mg m^{-2} yr^{-1}. These fluxes were rounded to an order of magnitude and are lower than a direct calculation from the Duce et al. (1991) data set.

1.4.2 The atmospheric Fe flux during the LGM

The termination of the last glaciation (Stage 2 of the SPECMAP planktonic δ ^{18}O record; Winograd et al., 1997) and the penultimate deglaciation (Stage 6) were both preceded by high mineral aerosol concentrations over Antarctica and lower atmospheric CO_2 concentrations relative to the Holocene (Craggin et al., 1977; Royer et al., 1983; de Angelis et al., 1984, 1987; Petit et al., 1981, 1990; Sowers et al., 1991; Mayewski et al., 1996; Jun et al., 1998; Jouzel et al., 1993). As for the present-day, Patagonian loess has been identified as a source of mineral dust to inland East Antarctica during the LGM (Gaudichet et al., 1986, 1988; Grousset et al., 1992; Basile et al., 1997). The higher concentrations of mineral aerosol over Antarctica during the LGM have been attributed to an increased aridity in the Southern hemisphere and more extensive dust sources (Petit et al., 1981; de Angelis

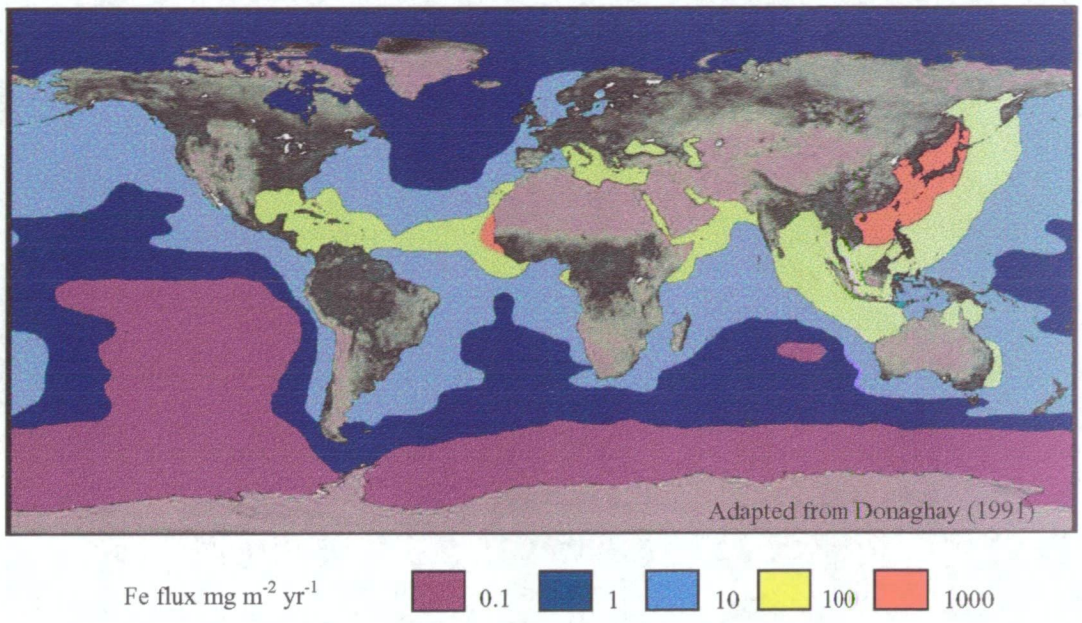

Figure 1.2 Atmospheric Fe flux to the global ocean

al., 1987, 1992), increased winds (Petit et al., 1981; Ram and Gayley, 1988) and a decrease in the hydrological cycle (Yung, et al., 1996; Anderson and Ditlevsen, 1998). During the LGM dust concentrations, (as inferred from Al concentrations) in the Vostok and Dome C ice-core records were 27-37 times that of the Holocene (Delmas, 1992). But LGM ice accumulation rates at these sites are thought to have been approximately 50% that of the Holocene (Lorius, 1989), and so higher LGM dust concentrations relative to the Holocene may in part be due to a higher ratio of dry to wet deposition (de Angelis et al., 1987). While the dust data from these ice-cores has been used to infer possible dust and hence Fe fluxes over the Southern Ocean (Martin, 1990) during the LGM, these ice cores were drilled from high altitude sites over a thousand kilometres from the coast, and it is not clear if the dust fluxes to these sites are representative of that over the ocean during the present or

LGM.

1.4.3 Seasonal Antarctic sea ice as an episodic source of Fe to the Southern Ocean

Sea ice forms seasonally over a large portion of the Southern Ocean, profoundly affecting both the overlying atmosphere and the underlying oceans. On average, Antarctic sea ice grows from a minimum of approximately 4×10^6 km^2 in February, to a maximum of approximately 18-19 $\times$ 10^6 km^2 in September or October (Parkinson, 1992). The seasonal cycle is characterised by approximately 7 months of growth (March-September) and 5 months of decay (October-February) (Worby et al., 1998). Snow cover forms a major component of the sea ice system, affecting the physical and radiative properties of the ice (Ledley, 1991). Snow is also incorporated into the sea ice as a result of snow loading, wave-induced flooding or deformation processes, forcing the ice/snow interface below sea level and flooding the base snow cover (Massom et al., 1998 and references therein). Importantly, the seasonal sea ice forms a relatively permanent surface for some 6-7 months of the year on which atmospheric dust accumulates in snow. This may be an important source of Fe to the surface ocean when the ice melts (Martin,1990; de Baar et al., 1995; Sedwick and DiTullio, 1997). The ice itself, some of which forms in coastal polynyas (Worby et al., 1998 and references therein), may also contain Fe that was present in upwelled coastal waters (Sedwick et al., 1999).

1.5 Studies of trace-metals in Antarctic snow and ice

Atmospheric heavy-metal pollution has been the main focus of trace-metal studies of Antarctic snow and ice (Murozumi et al., 1969; Boutron, 1978, 1979b, 1980; Boutron and Lorius, 1975, 1979; Boutron and Patterson, 1983, 1986, 1987; Boutron et al., 1977, 1993, 1994; Dick, 1987, 1985; Ng and Patterson, 1981; Rosman et al., 1994; Suttie and Wolff, 1992; Wolff, 1990; Wolff and Suttie, 1994). It now appears that much of the earlier trace-metal analyses suffered from contamination artefacts (Wolff and Peel, 1985). For instance, the lead, zinc and cadmium data published in Boutron (1978, 1979a, 1979b, 1980, 1981, 1982) and Boutron et al. (1977) are now known to be unreliable. Unfortunately, the majority of Fe analyses of Antarctic snow and ice were made by Boutron and Hanape before the contamination problems were resolved (Boutron, 1978, 1979a, 1979b, 1980, 1981, Boutron and Lorius, 1975, 1979; Boutron et al., 1972; Hanape et al., 1968). Measurements of Fe in Antarctic snow and ice for which contamination problems have been addressed are few, e.g Westerlund (1991), Shimamura (1995) and Barbante (1997), and are limited to a small number of samples.

Chapter 2

Experimental Methods

2.1 Introduction

The Fe, Mn and Al data presented in this thesis were measured in snow and glacial ice (ancient snow) samples collected during a number of Antarctic expeditions. These metals are present in the snow and ice at the low ng g^{-1} to pg g^{-1} concentration level, and so the analyses required special "clean" sampling procedures and highly-sensitive analytical techniques. The problems associated with collecting uncontaminated snow samples are discussed in several papers (Murozumi et al., 1969; Patterson and Settle, 1976; Ng and Patterson, 1981; Boutron and Batifol, 1985; Wolff and Peel, 1985).

Many of the recent snow samples were collected from seasonal sea ice in the vicinity of large ships. Except for Mart (1983), there are few reports of ship-contaminated snow. Given the known low concentrations of trace-metals reported in continental snow, the ships were considered as potential contamination sources. Continental samples were collected during inland traverse expeditions. Tractor trains and all-terrain vehicles were potentially the main source of contamination in this case. The

dispersion of contamination from point sources such as these are discussed by Suttie and Wolff (1993). The procedures that were used in an effort to avoid such contamination are outlined here.

The exterior layers of ice-core samples are known to be highly contaminated with trace-metals as a result of the drilling procedure and subsequent handling (Boutron and Patterson, 1986; Boutron et al., 1988; Candelone et al., 1994). In this study such samples were decontaminated by mechanically removing the outer layers of ice (Candelone et al., 1994). The ice layers were then analysed along with sub-samples from the centre of the ice core to determine the extent of contamination into the core, and hence infer the reliability of the concentration measured in the innermost sub-sample (Boutron and Patterson, 1986).

Few analytical techniques exist which have the sensitivity to quantify trace-metals in Antarctic snow. Methods that have been used include laser excited atomic fluorescence spectrometry (LEAFS; Bolshov et al., 1991), isotope-dilution mass spectrometry (IDMS), thermal-ionisation mass spectrometry (TIMS; Ng and Patterson, 1981; Rosman et al., 1994), graphite furnace atomic absorption spectroscopy (GFAAS; Boutron et al., 1991; Wolff and Peel, 1994) and Atomic fluorescence spectroscopy (AFS; Vandal et al., 1993). Except for LEAFS, these techniques have required preconcentration, such as simple evaporation (Görlach and Boutron, 1990) and adsorption on to tungsten wires (Wolff et al., 1981). More recently, high resolution inductively coupled plasma mass spectrometry (HR-ICPMS;

Shimamura et al., 1995; Barbante et al., 1997; Townsend and Edwards, 1998) and flow injection analysis (FIA; Edwards et al., 1998), which do not require preconcentration, have been employed. The Fe data presented in this thesis were determined by either FIA with spectrophotometric detection or ICPMS, and Mn and Al were determined by HR-ICPMS. Sampling procedures, general laboratory procedures and analytical methods are described in the following sections.

2.2 Reagents and equipment

2.2.1 Work areas

In an effort to reduce contamination by airborne dust, all preparation of standards and reagents, sample processing and analyses, and cleaning were performed inside laminar-flow clean air benches (Class 3.5) housed inside a conventional chemistry laboratory. Ice-cores and snow samples were decontaminated and sub-sampled in a laminar-flow clean air bench (Class 3.5) housed inside a cold room (-18 °C). These techniques were similar to those discussed by Patterson and Settle (1976), Boutron and Batifol (1985), and Candelone et al. (1994).

2.2.2 Water and reagents

Ultra-pure (>18 MΩ–cm resisitivity) deionised water (DIW) was prepared by passing prefiltered tap water (10 μm and 5 μm filters and activated-charcoal

cartridges) through a commercial water purification system (Analytical Reverse Osmosis and Polishing System, Modulab Pty Ltd). Water in this system is initially purified by reverse osmosis and then recirculated through four cartridges: an activated charcoal cartridge, two nuclear-grade ion-exchange cartridges, and an organic scavenger cartridge. Out-flowing water was passed through a 0.1 μm PTFE filter and stored in acid-cleaned low density polyethylene (LDPE) carboys. The Fe, Mn and Al concentrations of the DIW after storage were estimated from blank solution measurements by FIA and HR-ICPMS to be < 15 pg g^{-1}, < 3 pg g^{-1} and < 36 pg g^{-1}, respectively.

Acids with 4 different levels of purity were used in sample and reagent preparation and in cleaning. Samples, standards and blanks were acidified with a commercial ultrapure double quartz-distilled hydrochloric acid (Seastar chemicals). This had a supplier-assay of Fe, Mn and Al concentration of < 80 pg g^{-1}, < 3 pg g^{-1} and < 20 pg g^{-1}, respectively. However Fe analysis of the ultrapure acid, after opening and storage in a secondary container, gave an estimated Fe concentration of 4 ng g^{-1} (Sedwick et al., 1997). Singly and doubly quartz distilled hydrochloric acids (Q-HCl and 2Q-HCl, respectively) and acetic acids were used in the cleaning procedures and in the preparation of less critical reagents. These were prepared from analytical-reagent grade (or better) acids (Ajax, BDH, Reidel de Haen and Mallinkrodt) by sub-boiling distillation in a custom-built quartz still. Analytical-reagent grade (AR) acids were used for some of the cleaning steps. Ammonia hydroxide solution (NH_4OH) was purified from NH_4OH solution (AR) by isothermal distillation (also known as

isopiestic distillation) as described by Resing and Measures (1994). The Fe concentration of the purified NH_4OH solution was not determined, but is thought to be comparable to that of the DIW.

2.2.3 Equipment and cleaning procedures

Methods for the preparation and cleaning of equipment for ultra-trace-metal sampling and analyses were based on those discussed in Patterson and Settle (1976), Boutron and Patterson (1983), and Moody and Lindstrom (1977). Equipment used for the critical handling or storage of samples and reagents was either LDPE, fluorinated ethylene propylene (FEP) or polytetrafluroethylene(PTFE). Other equipment was made of either polypropylene (PP), high density polyethylene (HDPE) polycarbonate (PC), polymethyl methacrylate (acrylic) or polysulphone (PSF). Sample storage bottles (LDPE) were cleaned by soaking for 2 days in ~6 M HCl (AR) and then suspended for 2 days over the fumes of gently boiling ~6 M HCl (AR) following Tschopel et al. (1980). After cleaning, the bottles were stored for more than 3 months filled with ~0.1 M 2Q-HCl, and then rinsed liberally with DIW (4×) immediately before use. Other plasticware was cleaned by successive 2-day soakings in ~6 M HCl (AR), ~1 M Q-HCl, and ~0.1 M 2Q-HCl, with DIW rinsing between each soaking step. Pipette tips (PP) were cleaned by the latter method, but were rinsed with DIW, 2Q-HCl, then Seastar 2Q-HCl immediately before use. Tips used for pipetting ultrapure HCl were rinsed with DIW after use and reused over periods of several days.

2.2.4 Procedural blanks

Procedural blanks consisted of DIW acidified to 0.1 M with Seastar 2Q-HCl. Blanks were prepared daily during analytical work. Long-term blanks (to check for "leaching") were also prepared in 1L LDPE wide-mouth bottles, which were cleaned alongside those used for snow sampling. These were analysed regularly for Fe over a 3 year period. After 3 years the Fe concentrations of the blanks were below the FIA detection limit (15 pg g^{-1}). Estimated contributions to the blanks for Fe, Mn and Al are given in Table 2.1. Manganese and Al were determined by HR-ICPMS.

Table 2.1 Contributions to procedural blank

Stage of procedure	Method of determination	Blank contribution (pg g^{-1})		
		Fe	Mn	Al
Bottle blank	Filled with 0.1% ultra pure HCl and left for 2.5 years	< 15	< 2	< 19
Ceramic chisel	Immersed chisel blade in DIW for 30 min	< 15	n.a.	n.a
Ice-core decontamination	Decontaminated artificial ice-core made from DIW	~ 15	< 2	< 19
Pipette blank	Pipetted acid 100 times.	< 15	n.a	n.a
Acidification with HCl	Calculated for 0.1 M HCl	4*	0.003**	0.02**
	Total	< 15	< 2	< 19

n. a. = not analysed

* Assuming Fe concentration = 4 ng g^{-1} (70 nM) in Seastar 2Q-HCl

** Supplier-assay value in Seastar 2Q-HCl

2.3 Sample locations and sampling procedures

To test the 4 hypotheses presented in Chapter 1, present-day snow samples were collected from seasonal sea ice and continental sites in East Antarctica (Figure 2.1). Holocene, Holocene-Wisconsin transition and LGM age glacial ice samples were selected from ice-core sections drilled at Law Dome on the coast of Wilkes Land, East Antarctica. Samples from Prydz Bay, Princess Elizabeth Land, the Dumont

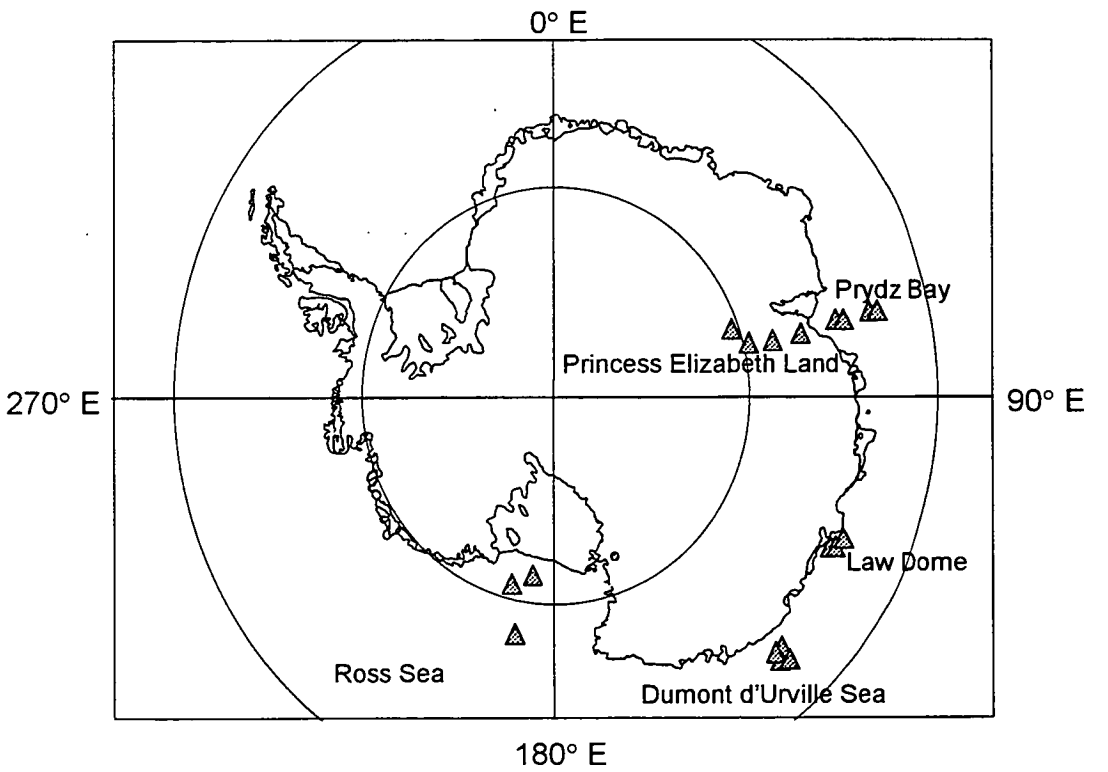

Figure 2.1 Sample site locations

d'Urville Sea and the Ross Sea were analysed to investigate Fe concentrations in marine and continental Antarctic snow over a large spatial area and ice samples from three Law Dome ice-cores were used to investigate the temporal variability in Fe concentrations in snow deposited during the Holocene, Holocene-Wisconsin transition and LGM.

2.3.1 Prydz Bay samples

Prydz Bay, the third largest embayment in Antarctica (Nunes Vaz and Lennon, 1996), is situated between approximately 70° E and 80° E longitude and covers an area of approximately 80,000 km^2. Oceanic circulation patterns in Prydz Bay are dominated by strong cyclonic circulation with current velocities (average velocity ~0.1 m s^{-1}) which increase near the perimeter, especially at the edge of the Amery Ice Shelf at the southern end of the bay (Rathburn et al., 1995). Prydz Bay is typically covered by sea ice for 9 months of the year and is characterised by a high biological productivity (Ishii et al., 1998). Snow samples were collected from pack ice in Prydz Bay in September 1994 from the ice-breaker *Aurora Australis*. These sampling sites are shown in Figure 2.2 and the site locations are given in Table 2.2. Snow samples from these sites were collected during sea-ice investigations conducted by the Antarctic CRC sea-ice sub-program. Additional information concerning sea-ice conditions and properties of these sites have been reported in Worby and Massom, (1995). These sample sites were large ridged floes with thin snow over (5-10 cm) (Massom et al., 1998).

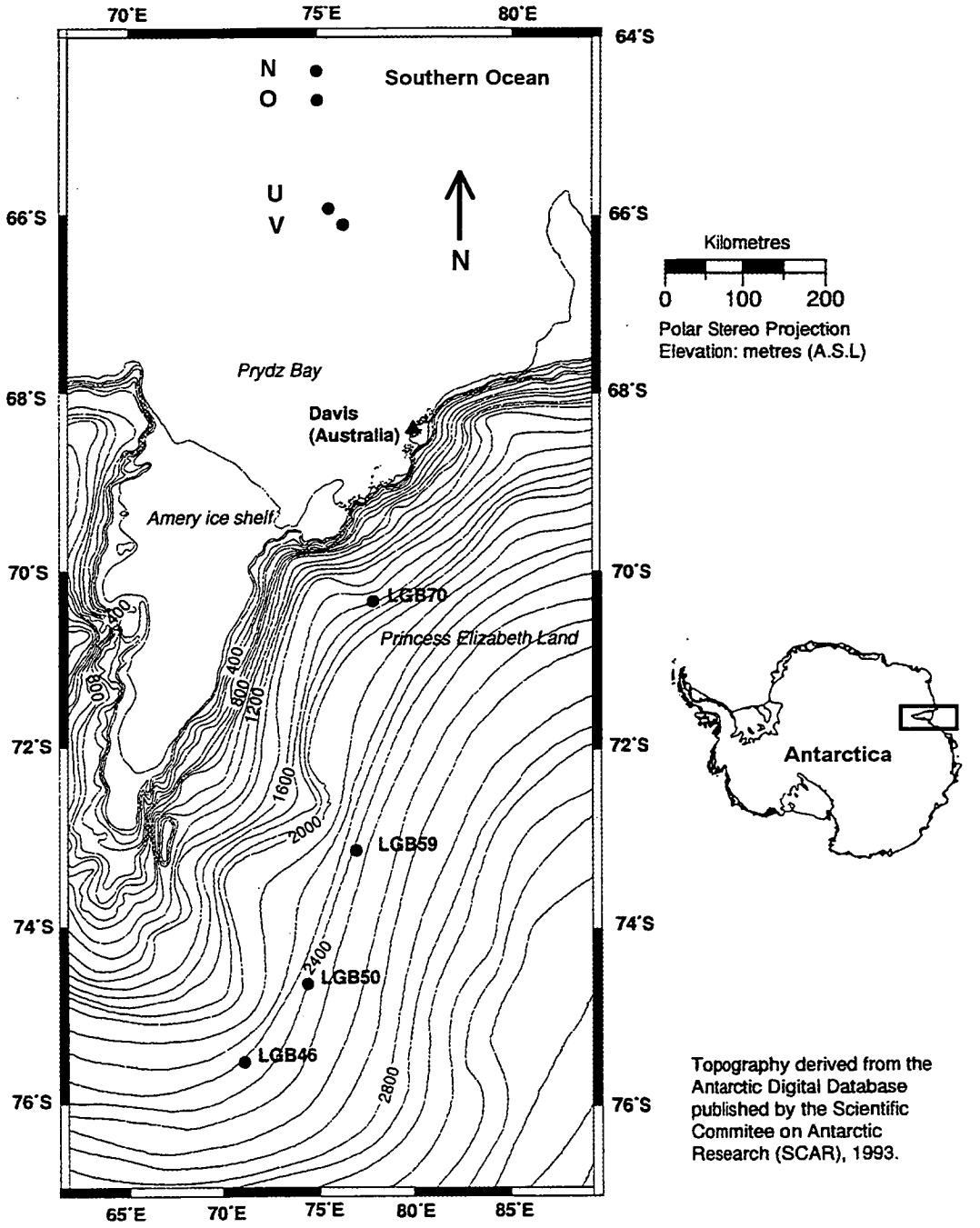

Figure 2.2 Prydz Bay and Princess Elizabeth Land sample locations

Table 2.2 Prydz Bay sample locations

Site	Lat	Long	Date sampled
N	64.57° S	74.98° E	21/9/94
O	64.90° S	75.00° E	21/9/94
U	66.12° S	75.32° E	23/9/94
V	66.30° S	75.72° E	23/9/94

2.3.2 Princess Elizabeth Land samples

The Princess Elizabeth Land snow samples were collected in 1994 from sites on the eastern periphery of the Lambert Glacier Basin (Figure 2.2) during the ANARE Lambert Glacier Basin traverse 94/95. Site locations are shown in Table 2.3. Net snow accumulation rates for these sites were calculated from snow accumulation stake measurements and are described in Higham et al. (1997).

2.3 3 Dumont d'Urville Sea samples

Snow samples were collected from sea ice in the Dumont d'Urville Sea (Figure 2.3 and Table 2.4) from the *Aurora Australis* in September 1995. As well as sampling pristine snow samples, a transect of surface snow both upwind and downwind of the ship was collected at site A, in an effort to quantify contamination emanating from the ship. Also, Site H2 was sampled on a repeat visit to the same floe as H1 (several days

Table 2.3. Princess Elizabeth Land sample locations

Site ID	Lat	Long	Elevation (m, ASL)	Date Sampled	Net snow accumulation rate (kg m^{-2} yr^{-1})
LGB 70	70.57° S	76.90° E	1650	18/11/94	163
LGB 59	73.43° S	76.52° E	2520	04/12/94	65
LGB 53	74.90° S	74.52° E	2430	12/12/94	78
LGB 46	75.85° S	71.50° E	2413	22/12/94	50

ASL = above sea level

after the first visit) to see if contamination could be detected. This floe had drifted approximately 60 km in the intervening period.

Table 2.4 Dumont d'Urville Sea sample locations

Site	Lat	Long	Date sampled
A	64.60° S	140.33° E	02/08/95
B	64.88° S	141.07° E	02/08/95
S	64.97° S	141.45° E	03/08/95
K	64.93° S	141.25° E	04/08/95
H1	65.06° S	141.58° E	03/08/95
H2	65.00° S	140.21° E	09/08/95

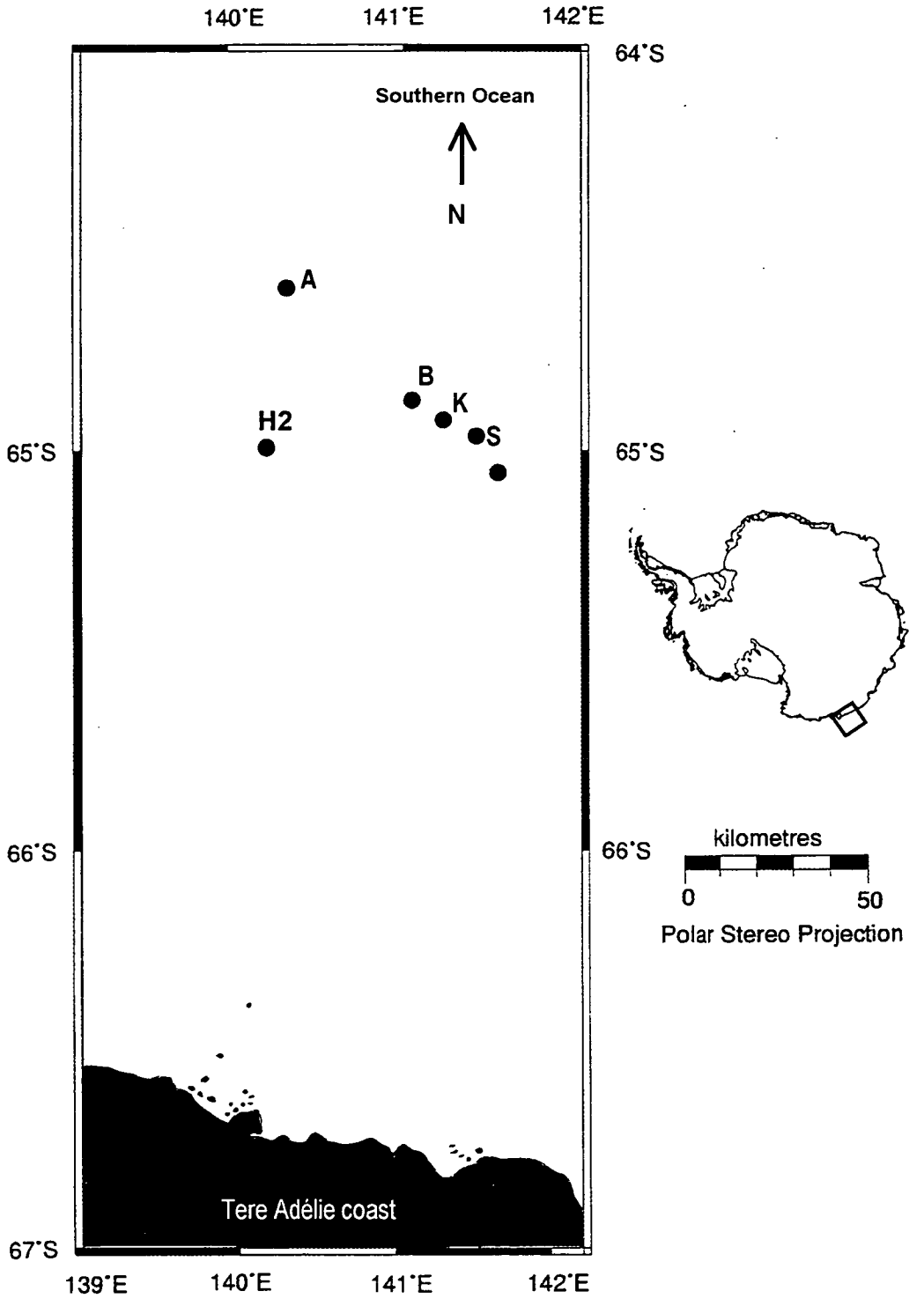

Figure 2.3 Dumont d'Urville Sea sample locations

2.3.4 Ross Sea samples

Snow samples were collected from sea ice in the Ross Sea (Figure 2.4 and Table 2.5) in November-December 1994, during a voyage of the US ice-breaker *Nathanial B. Palmer*. Like Prydz Bay, the Ross Sea is a large embayment with an ice shelf at its southern edge (Ross Ice Shelf). The western edge of the Ross Sea is bordered by the trans-Antarctic mountains and several dry valleys, which are perhaps the only significant source of mineral aerosol on the Antarctic continent (Shaw, 1979). The Ross Sea is characterised by a large gyre system (Ross Sea gyre) and is covered by sea ice for approximately 6 months of the year (Jacobs and Comiso, 1989).

Table 2.5 Ross Sea sample locations

Site	Latitude	Longitude	Date sampled
1	69.52° S	170.6° W	10/11/94
2	75.00° S	170.67° W	28/11/94
3	76.45° S	175.52° W	02/12/94

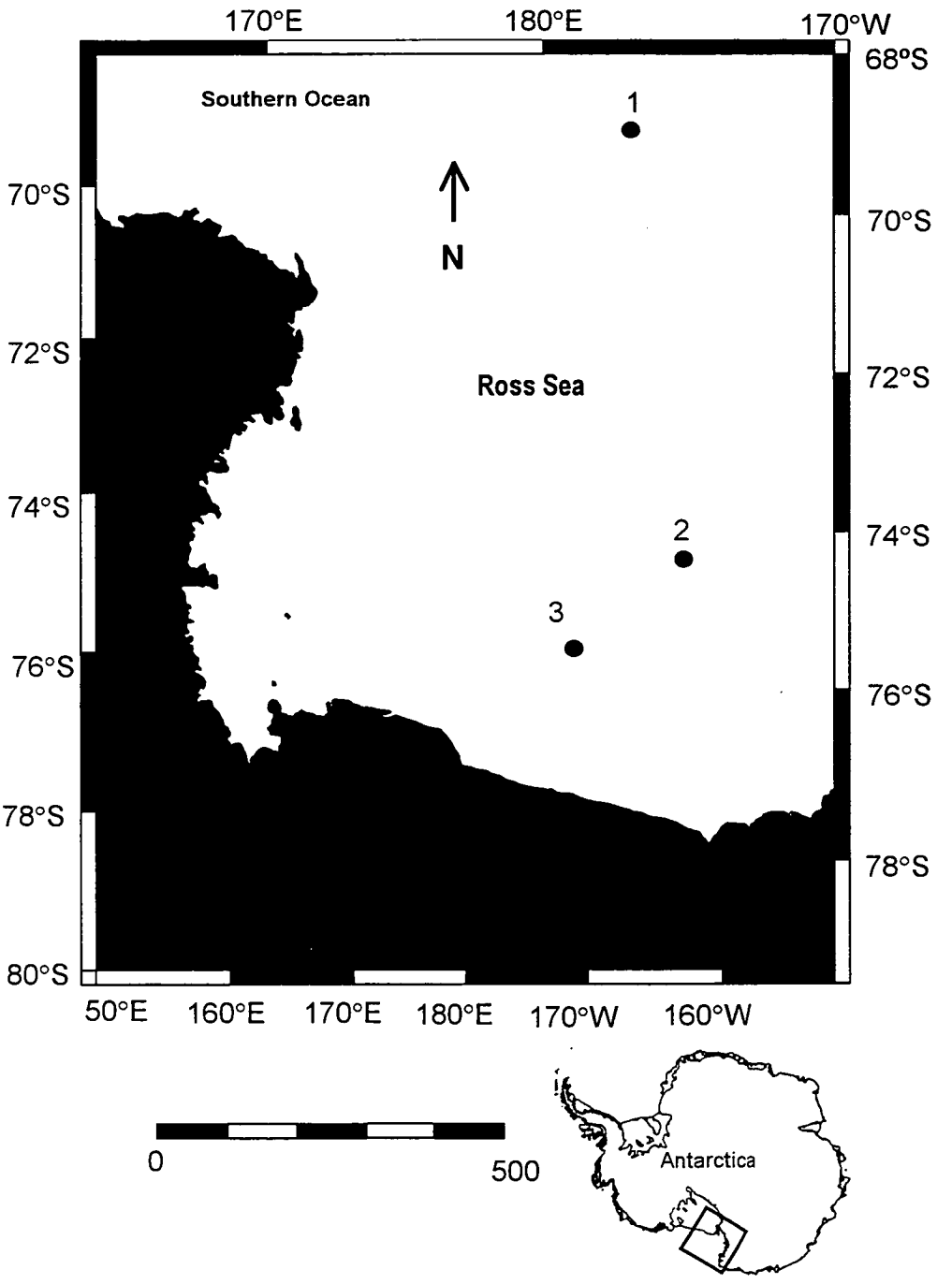

Figure 2.4 Ross Sea sample locations

2.3.5 Law Dome ice-core samples

Samples were taken from sections of ice-cores recovered from Law Dome, in Wilkes Land, East Antarctica (Figure 2.5). Law Dome is an independent ice cap approximately 200 km in diameter located on the periphery of the main Antarctic ice sheet. The Law Dome summit has an elevation of 1389 m above sea level and a maximum ice thickness of 1200 m (Hamley et al., 1986). Law Dome projects into a zone of easterly maritime atmospheric circulation. This produces a high snow accumulation rate on the eastern flank of the Dome, which then decreases across the Dome from east to west (Morgan et al., 1997).

Samples were taken from three ice-cores, DSS located 4.6 km SSW of the Dome summit, DE08 located on the eastern flank and BHC1 located near the coast to the northwest. The DSS and DE08 cores are accurately dated using $\delta^{18}O$ stratigraphy (Morgan and McCray, 1985; Morgan et al., 1997; Etheridge and Wookey, 1988) and by ice-flow modeling, BHC1 has been dated by comparing the $\delta^{18}O$ record with that of the Vostok ice core. Further details for these ice-cores are as follows:

(1) Core DSS, drilled 4.6 km SSW of the summit of Law Dome (66°46'11"S, 112°48'25"E, Figure 2.5) between 1988 and 1993. This site has an average snow accumulation rate of 640 kg m^{-2} yr^{-1} (Morgan et al., 1997). The core was drilled in two stages: a thermally drilled section (0-82 m, 200 mm diameter) and then a section drilled electromechanically in a fluid-filled bore hole (82-1200 m, 100 mm diameter).

The core reached a depth of 1200 m and covers a time span that extends back through the LGM. The ice from the LGM section is brittle and fractured and thus unsuitable for trace-metal analyses.

(2) Core DE08 thermally drilled (diameter 200 mm) 16 km east of the Law Dome summit (66°43'19"S, 113°11'58"E, Figure 2.5). The site has an extremely high surface snow accumulation rate of 1160 kg m^{-2} yr^{-1} (Etheridge et al., 1988). The core was drilled to a depth of 234 m in 1987 and spans the past 180 years. Samples from the core have been used extensively for measurements of CO_2 in trapped bubbles (Etheridge et al., 1988).

(3) Core BHC1, thermally drilled (diameter 110 mm) 110 km north west of the Law Dome summit (66°07'50"S, 110°56'17"E, Figure 2.5). This site has a low average surface snow accumulation rate of 60 kg m^{-2} yr^{-1} and is relatively close to the coast in comparison with the other sites. The core was drilled to a depth of 300 m in 1982 and was drilled along with several other cores in order to study the ice-flow mechanics of the region. Measurements of $\delta^{18}O$ along the core show a distinct Holocene-LGM transition, where average $\delta^{18}O$ values decrease by 7.0 ‰ (Morgan and McCray, 1985). Ice-flow models suggest that ice in the LGM section of this core was originally deposited near the DSS site (Budd and Rowden-Rich, 1985); oxygen isotopes from the DSS core also show a 7.0 ‰ decrease in $\delta^{18}O$ values with depth at the Holocene-LGM transition (Morgan et al., 1997).

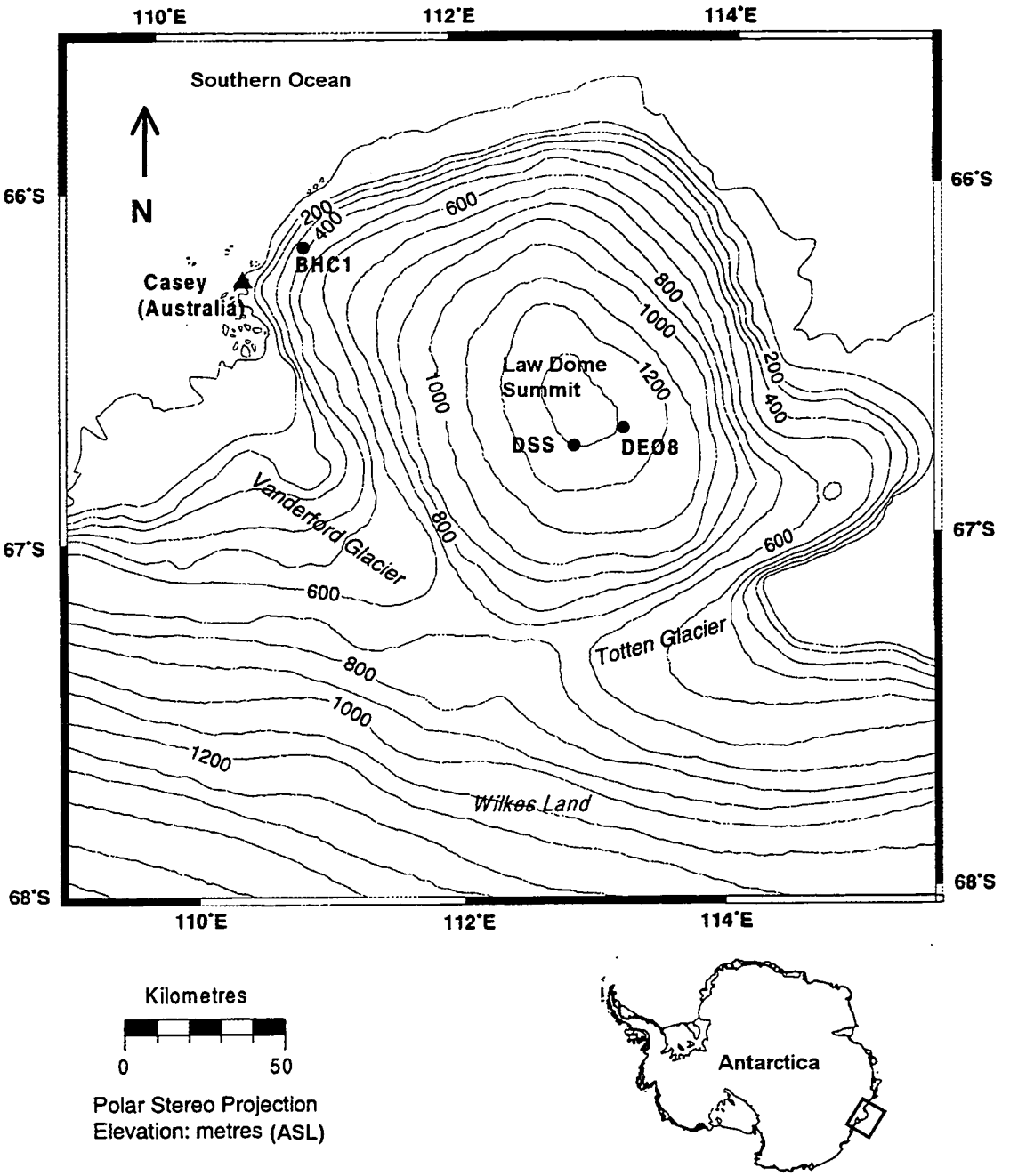

Figure 2.5 Law Dome ice-core locations

2.3.6 Snow and firn sampling

Snow and firn were sampled from seasonal sea ice and Antarctic continental sites using trace-metal clean techniques. Precautions taken to minimise contamination included approaching sample sites from downwind and the use of full clean-room apparel during sampling. Snow and firn were collected in both 1L LDPE wide-mouth bottles and acrylic tubes (id = 50 mm, length =18 mm, with PP endcaps). In designing the sampling methods, there was some initial concern that the samples may have required decontamination and that the bottles would not be able to penetrate hard, icy layers, in which case the acrylic tubes would have been well suited. On the other hand, if the snow was light and fluffy, the bottles would have been more practical. In the end both containers were used. Collection of samples from sea ice was complicated by the presence of ships (RSV *Aurora Australis* and RV *Nathanial B. Palmer*), which are potentially large sources of airborne trace-metal contamination (Mart, 1983). To access uncontaminated snow during the ship-based studies, the vessels were turned into the wind several kilometres before stopping at an ice-floe. Floes sampled from the *Nathanial B. Palmer* were accessed by inflatable boat. In both cases, once on a floe, equipment was moved further upwind before sampling. Floes sampled from the *Aurora Australis* were in areas with little open water. In this case, the sampling equipment was hauled several hundred metres upwind of the ship in a fiberglass sled before donning clean-room apparel and taking samples. Snow pits were progressively sampled in an upwind direction.

The snow pits were sampled as follows:

(1) A pit (typically 1 m wide by 0.2 m deep) was dug down to the sea ice with an acid-cleaned PP shovel or polycarbonate scoop and the upwind wall of the pit was scraped with an acid-cleaned PP scraper to ensure a clean surface;

(2) Wide-mouth bottles (1 L, LDPE) were removed from their bags and inserted into the upwind face of the snow pit. Lids were placed upwind with the inside surface in the snow. The bottles were placed so as to sample the full depth of the snow drift (Figure 2.6); and

(3) Next, the acrylic tubes were removed from their bagging and inserted vertically next to the bottles (Figure 2.6). The tubes and bottles were then excavated, capped, re-bagged and immediately put in the ship's freezer at -15° C for transportation back to Hobart.

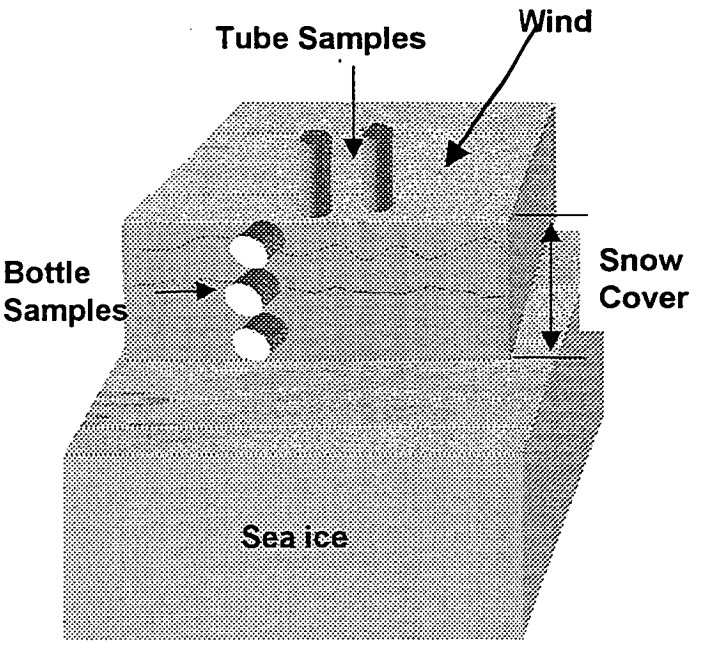

Figure 2.6 Snow sample collection from sea ice

For the continental sites, snow samples were collected during dedicated side trips from the route of the overland traverse. This involved driving all-terrain vehicles upwind approximately 5 kilometres, then walking several hundred metres further and donning clean-room attire. The sample collection protocol for these sites was the same as for the marine sites. Samples were stored in a large insulated box strapped to the outside of the traverse tractor train. The temperature inside the box was measured throughout the traverse and remained below 0° C. At the end of the traverse the samples were stored in a freezer at Mawson Base for several weeks before being shipped frozen to Hobart aboard the *Aurora Australis*.

2.3.7 Ice-core storage

After drilling, the DSS and BHC1 ice-core sections were heat sealed in LDPE bags and transported to Hobart where they were kept in cold storage at approximately –20° C. The DE08 core sections (also sealed in LDPE bags) were transported to Melbourne where they were kept at –30° C. While the DSS and BHC1 ice-cores sections stored at the Hobart repository appear to be in relatively clean condition, the DE08 sections (stored in Melbourne) surfaces were visibly contaminated with dust.

2.3.8 Sub-sampling and decontamination of ice-core sections

During drilling, handling, and storage, the exteriors of ice-core sections become highly contaminated by trace-metals (Boutron and Batifol, 1985; Boutron and Patterson, 1986; Boutron et al., 1988). To obtain uncontaminated samples, it is necessary to mechanically remove the external layers of the core, and to determine the extent to which external contamination has penetrated into the core. In this study, we used the lathe technique described by Candelone et al. (1994), where 4-5 layers of each core section, in addition to the visibly-contaminated outermost layer are successively removed using chisels under trace-metal conditions. Iron and Al were measured in meltwater sub-samples from these layers. Where the inner layers contain a relatively low and constant concentration of analyte, they are assumed to be uncontaminated (see chapter 4). The decontamination procedure was performed at the Laboratoire de

Glaciologie et Geophysique de l'Environnement (LGGE), Grenoble, France, in collaboration with Claude Boutron and Sungmin Hong, and, using a slightly modified procedure, at the Antarctic CRC in Hobart. Briefly, the procedure was as follows:

(1) Using a chisel, the first millimetre or so of the core exterior was scraped off outside the laminar-flow hood. This outer layer typically contains most of the contamination;

(2) The core sample was then fitted into a custom-built rotating clamp inside the laminar-flow bench, and the outer layer removed by shaving (using a fresh chisel) a straight line along the sample and then rotating the cleaned strip upwards (to prevent the surface from being re-contaminated). While the ice was being shaved off, the chips and shavings were collected in an LDPE scoop placed below the core;

(3). After the second layer was removed, the ice chips were transferred from the scoop into a clean 1L LDPE wide-mouth bottle, and a clean chisel and scoop were used to remove the next layer from the core section.

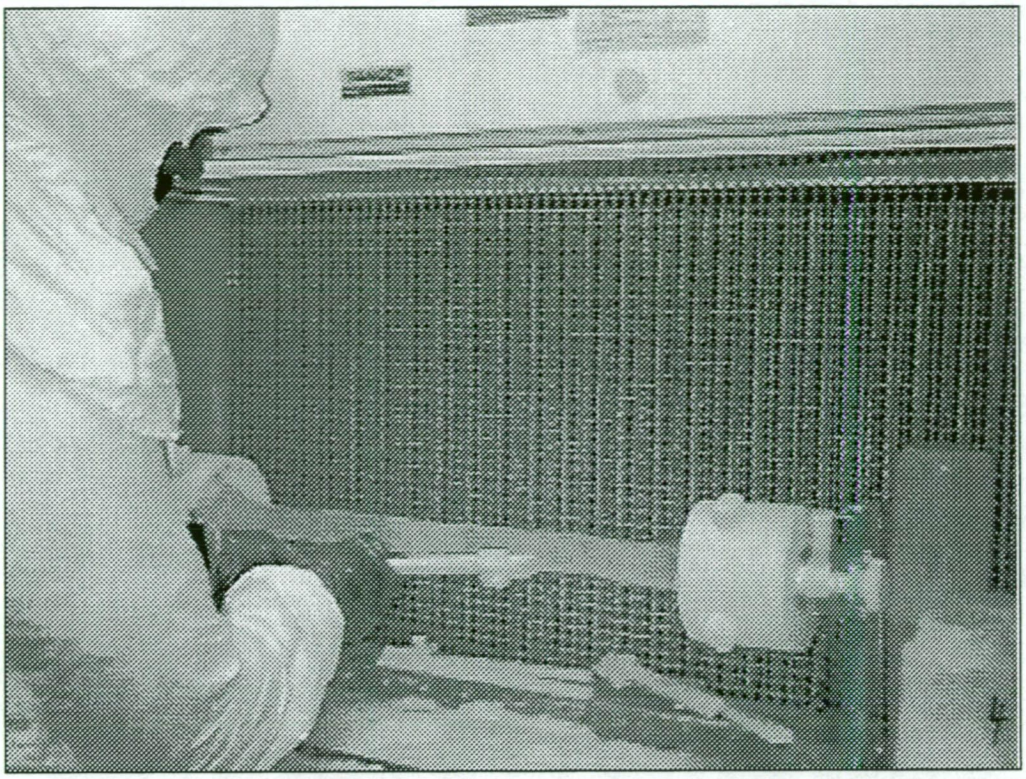

Figure 2.7 Ice-core sub-sample decontamination

(4). After 4 layers were removed and collected in this manner, the inner core was gripped near one end with a pair of plastic tongs and the other end removed with a chisel. The severed ice and clamp end were then set aside. Next, a clean 1L LDPE wide-mouth bottle was placed over the sample and the tongs were slid along the core. The ice was broken next to the tongs so that a piece of the core section fell into the bottle. This process was repeated until most of the decontaminated core section had been transferred into the bottle, except for the remaining clamped end section held in the clamp.

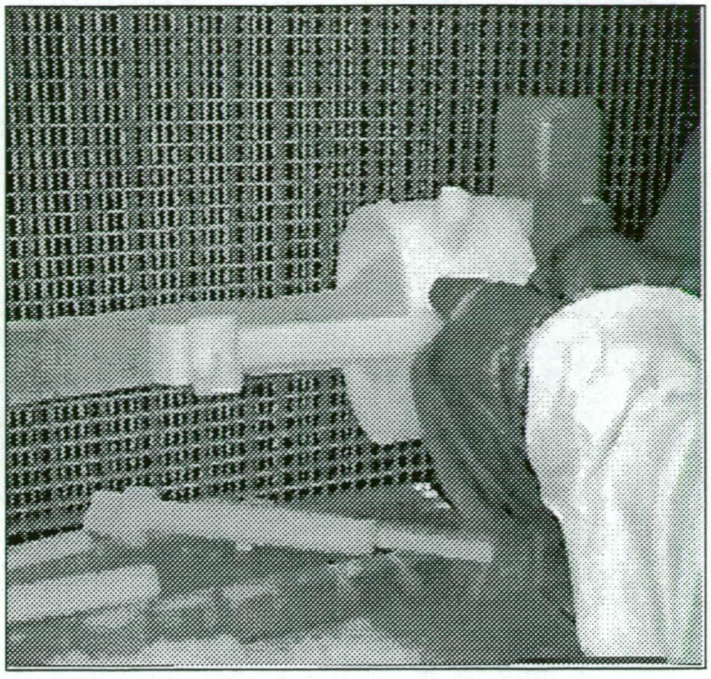

Figure 2.8 Ceramic chisel used for decontamination

The clamps used at LGGE were constructed of LDPE and are described in detail in Candelone et al. (1994). The clamps are essentially free rotating jigs on movable supports. The chisels used at LGGE have been described in Boutron and Patterson (1986) and are constructed of stainless steel (316L). Stainless steel consists primarily of Fe, however, contamination from the chisel blades was apparently eliminated by soaking them in nitric acid (HNO_3). This passivates the metal surface, making it relatively inert, and also removes contamination acquired during use. The passivity of the chisel blades appears to prevent a significant transfer of Fe from the blades to the ice. The chisels were soaked in 0.1% HNO_3 for 1 week before use, but at the time of the decontamination they had been repeatedly soaked over approximately 10 years. An ice-core clamp was constructed at the Antarctic CRC in Hobart similar to that used at LGGE. The base and supports of this lathe were constructed from acrylic

and the jigs from PTFE (Figure 2.7). Chisel blades were made from a zirconia oxide ceramic (Rojan Advanced Ceramics) and the blade holders (Figure 2.8) and ice-core tongs from LDPE.

2.4 Sample meltwater processing

2.4.1 Acidification of samples

After melting, the ice and snow meltwater samples were acidified to 0.1% with concentrated hydrochloric acid (2Q, Seastar). The acidification of samples for the ultra-trace-metal analysis of Antarctic snow and ice meltwater samples has been described in the literature (Patterson and Settle, 1976; Dick, 1987). Acid is added to the meltwater to:

(1) dissolve particles in the meltwater;

(2) prevent adsorption of trace-metals by the sample container; and

(3) maintain metals in solution.

Most of the Fe, Mn and Al in Antarctic snow and glacial ice is thought to be present as a component of clay minerals (see Chapter 1, section 1.3.2), which are only partially soluble in water at near neutral pH. Samples were acidified in an effort to determine total-dissolvable metals in the samples. It should be noted that "total-dissolvable" is an operationally-defined measurement, where dissolvable refers to

dissolution in 0.1 M HCl. Ice-core sub-samples taken during the decontamination procedure were transferred into clean 1L LDPE bottles, capped, and allowed to melt. Aliquots of these meltwaters were immediately transferred (after mixing) into tared 60 mL LDPE bottles, weighed, and acidified to 0.1 M with Seastar 2Q-HCl; the 60 mL meltwater aliquots from samples processed at LGGE were immediately refrozen (unacidified) and later transported to the Antarctic CRC, where they were re-melted and acidified. Snow samples were transported frozen (-15° C) from the field to Hobart. Snow samples collected in wide-mouth bottles were allowed to melt in the bottles, weighed and then acidified to 0.1 M with Seastar 2Q-HCl. Snow samples collected in acrylic tubes were transferred into clean LDPE wide-mouth bottles under clean-air conditions, melted, weighed and acidified as described above.

2.4.2 Extent of dissolution

All of the acidified meltwaters were stored at room temperature for at least 3 months before measurement of the operationally-defined total-dissolvable Fe (TD-Fe) concentrations. This includes both Fe^{3+} and Fe^{2+} species and also perhaps colloidal Fe species (Measures et al., 1995). This storage or "dissolution" time was chosen after using FIA to monitor the TD-Fe concentration in a number of snow samples (Figure 2.9) at various times after acidification. The measured TD-Fe concentrations of the samples all increased for up to 3 months following acidification, after which relatively constant concentrations were measured. The initial rapid increase in TD-Fe concentration is probably due to the dissolution of most of the aluminiosilcate

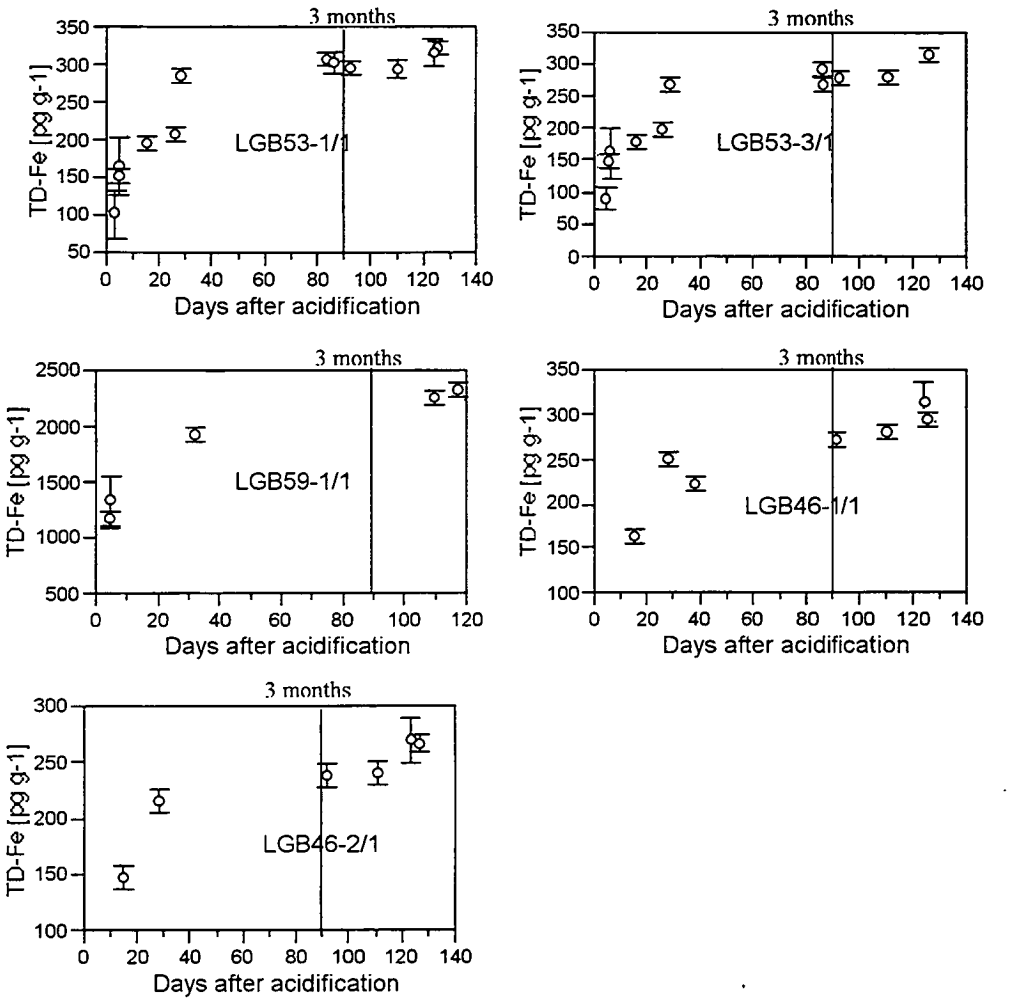

Figure 2.9 Total-dissolvable Fe vs time after acidification

(Princess Elizabeth Land snow sample meltwaters)

minerals, excluding refractory material. Procedural blanks demonstrate that this increase in TD-Fe concentration was not due to cumulative contamination from the storage bottles. No such tests were done for Mn and Al, but it is assumed that these

species also reached steady state concentrations in solution after > 3 months acidification.

2.4.3 Sample filtration

To evaluate the solubility of Fe in these samples, the meltwater from selected samples were filtered under clean-air conditions (Class 3.5) immediately after melting through acid-cleaned 0.2 μm PTFE membranes (Gelman, Acrodisc CR), with peristaltic pumping, into acid-cleaned LDPE bottles (60 mL) and acidified as in section 2.4.1. The filter line consisted of 20 cm of FEP tubing (0.3 mm id) attached to peristaltic pump tubing (PVC) followed by a filter and 15 cm of FEP tubing. Between samples the filter line was stored as a closed loop filled with 10% Q-HCl (typically for 1 week). Before use, the filters were preconditioned by pumping DIW through the line for approximately 2 hr. At the end of the preconditioning, a DIW blank was collected in an acid-cleaned LDPE bottle (60 mL) and acidified as in section 2.4.1. All blanks from the filtering procedure were found to be less than the Fe detection limit (i.e., 15 pg g^{-1}). Iron determined in the filtered samples is operationally-defined as "total-filterable" Fe (TF-Fe) in the following sections and Chapters, and presumably provides a measure of the fraction of total Fe in the snow which is readily soluble at the natural pH of the meltwaters.

2.5 Determination of Fe by FIA

2.5.1 Analytical method and modifications

Total-dissolvable Fe was determined by FIA with spectrophotometric detection following a modification of the procedure described by Measures et al. (1995). This procedure has been used successfully in the analysis of dissolved and TD-Fe in Southern Ocean seawater (Sedwick et al., 1997; Sedwick and DiTullio, 1997). The chemistry of the method is described by Hirayama and Unohara (1988) and is based on the catalytic action of Fe(III) on the oxidation of N,N-dimethyl-p-phenylenediamine (DPD) with hydrogen peroxide (H_2O_2). Two reddish semiquinone derivatives are formed from the oxidation of DPD and are detected spectrophotometrically by absorbance at a wavelength of 514 nm. In the catalytic cycle, Fe(III) reacts with DPD (forming the semiquinone derivatives) and is reduced to Fe(II). Iron (II) then reacts with H_2O_2 to form Fe(III). Hence both dissolved Fe(III) and Fe(II) are detected (and perhaps also colloidal and inorganic complexed Fe). The system described by Measures et al. (1995) included an in-line preconcentration system comprised of a poly vinyl chloride (PVC) column packed with 8-hydroxyquinoline immobilised on vinyl polymer gel (Landing et al., 1986). However, survey analyses of snow meltwaters suggested adequate sensitivity of this method without preconcentration. Hence the preconcentration components of the system were removed and replaced by a sample loop (approximately 100 μL). The acidified seawater carrier used in the Measures et al. (1995) system was replaced with

DIW acidified to 0.1 M with 2Q-HCl. This eliminated an aberrant peak and dip in absorbance signal caused by the difference between the refractive index of the carrier and sample. This effect was, however, apparent in the analysis of relatively saline snow samples collected from sea ice. This salinity effect was investigated by raising the salinity of a low-salinity snow sample with pelagic Southern Ocean seawater (TD-Fe below the detection limit). The dilution-corrected results of this experiment are shown in Figure 2.12. It was found that a significant salinity error was introduced for salinities greater than 3 ‰. To counter this problem, meltwaters with a salinity greater than 3 ‰ were determined by the method of standard additions. Finally, the Measures et al. (1995) system was modified by placing an immobilised 8-hydroxyquinoline "clean-up" column in the DPD reagent line (the least pure reagent) in order to remove Fe from this reagent. The spectral absorbance of the semiquinone end products (at 514 nm) were measured in-line by a UV/VIS spectrophotometer (Shimadzu, liquid chromatography series, model: SPD-10 AV). Peak detection and quantification were obtained by using a PC-74 A/D board (Boston Technologies) and the flow injection analysis software package FCS (A-Chem Technologies, Grahame Cross) running on an IBM-compatible 286 PC. The temperature of the reaction coil was maintained at 20° C by a water bath fitted with a thermoregulator. A 12 channel peristaltic pump (Alitea, model: XV) was used to drive the flow system.

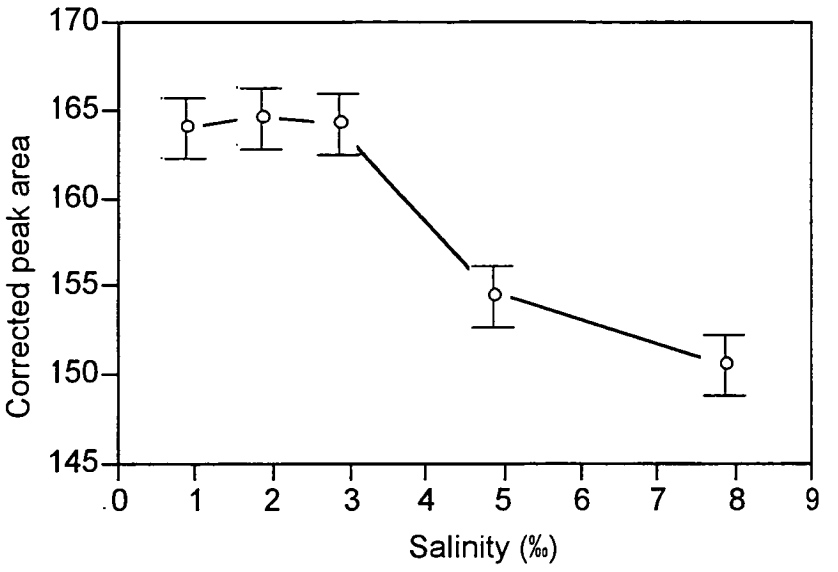

Figure 2.10 Effect of sample salinity on FIA peak area for TD-Fe method

The FIA manifold (Figure 2.11) was constructed of FEP tubing, inside diameter (id) 0.3 mm and PEEK tees, unions and fittings with Kel-F ferrules (Upchurch). The reaction and mixing coils were constructed from FEP tubing (0.3 mm id) by a modification of the knitting method of Selavka et al. (1987). The DPD clean-up column was packed with 8-hydroxyquinoline immobilised on vinyl polymer gel, as described by Resing et al. (1992). A sample loop (42 cm, FEP, approximately 100 μL) was substituted for the sample preconcentration column, and no sample buffer used.

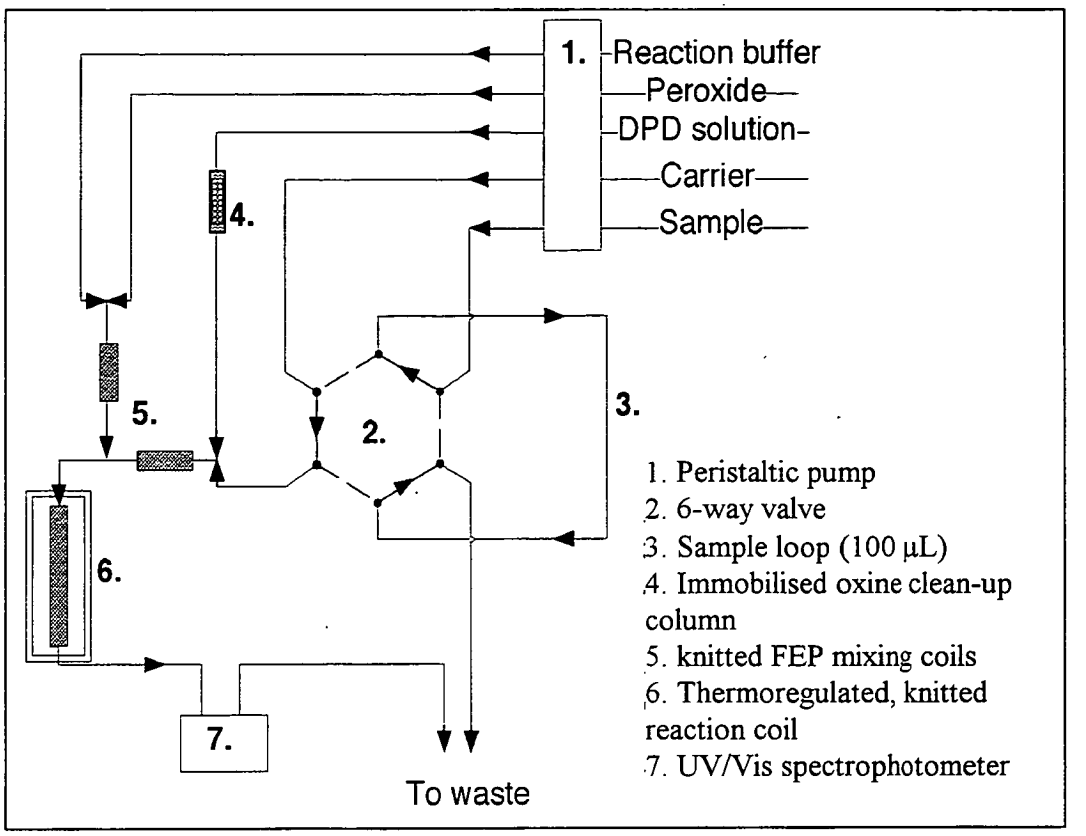

Figure 2.11 Fe FIA manifold

The manifold valve was a 6 port, PTFE rotary valve (Rheodyne, type 50) which was modified by replacing the stainless steel backing plate with a PTFE backing plate attached with nylon screws. The FIA reagents and samples were housed in a laminar-flow bench (Class 3.5) and the reagent and sample lines fed outside to the FIA manifold and associated instrumentation, which was set up on the laboratory bench.

2.5.2 Reagents and standards

Brij-35 surfactant (15%) was prepared by dissolving solid Brij-35 (Aldrich) in DIW. Ultrapure H_2O_2 (5%) was prepared by dilution of 30% ultrapure H_2O_2 solution (Ultrex, J.T. Baker) with DIW. DPD solution was prepared daily by dissolving approximately 0.5 g of N,N-dimethyl-p-phenylenediamine dihydrochloride (Fluka) in 60 mL of DIW and 50 µL of 2Q-HCl. The reaction buffer was prepared as follows: 250 mL of isothermally-distilled NH_4OH solution was added to 115 mL of doubly-distilled acetic acid and diluted to approximately 1 L with DIW. After cooling, the solution was adjusted to pH = 6.3 ± 0.1 with doubly-distilled acetic acid and NH_4OH solution to which was added 3 mL of 15% Brij-35 followed by 100 µL of 10% triethylene tetramine (Fluka). The carrier was DIW acidified to 0.1 M with 2Q-HCl. Standards were prepared in DIW acidified to 0.1 M with Seastar 2Q-HCl by serial dilution from 1 mg g^{-1} Fe (III) nitrate atomic absorption standards (Spectrosol, Ajax chemicals). Low standards (< 100 pg g^{-1}) were stored for a maximum time of 1 month.

2.5.3 Analysis procedure

The standard operating conditions are shown in Table 2.6. Before and after use, the system was cleaned by pumping 1 M Q-HCl through the reagent and sample lines for approximately 1 hr followed by DIW for 20 minutes. This also regenerated the DPD clean-up column. If a sample concentration several hundred pg g^{-1} higher in Fe than

the others was encountered during an analysis, then a shortened cleaning procedure was repeated for the sample line. Duplicate sample measurements repeated if the relative standard deviation on the average absorbance area exceeded 10%. Mid-range standards were run after every 6 samples, and the system recalibrated if they were not within ± 10% of their initial absorbance. A blank was measured after every batch of 10 samples. Calibrations were highly linear, over several orders of magnitude (Figure 2.12).

Table 2.6 FIA operating conditions

Wavelength	514 nM
Reaction temp:	20° C
Pump speed:	18.5% of max.

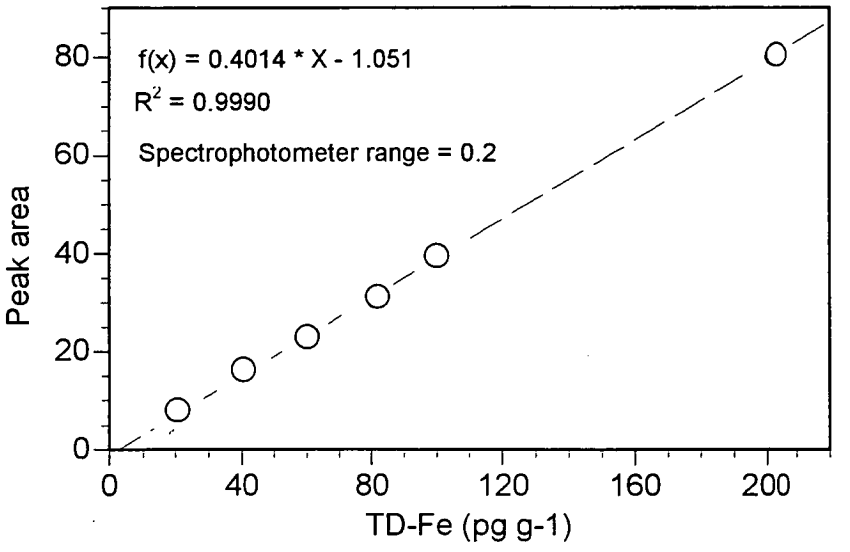

Figure 2.12 Example FIA calibration curve

2.5.4 Detection limit and uncertainty of FIA method

The detection (DL), here defined as the lowest concentration level that is statistically different from a blank at a specified level of confidence (Currie, 1988), was calculated from equation 3 and 4 of Skoog (1984).

$$S_m = \overline{S_{bl}} + 3 \times s_{bl} \qquad (1)$$

$$DL = (S_m - S_{bl})/m \qquad (2)$$

where S_m = the minimum analytical signal

S_{bl} = the blank signal

$\overline{S_{bl}}$ = the mean blank signal

s_{bl} = the standard deviation of the blank signal

k = one sided critical value of the standard normal variate

m = the slope of the calibration curve

As there was no observable blank for the FIA Fe method, Sm and DL were determined from the peak area of 12 replications of a 40 pg g^{-1} standard. In this case $\overline{S_{bl}} = 20$, $s_{bl} = 2.6$, m = 2 and k= 3 for a confidence level of 95% and 11 degrees of freedom. The minimum analytical signal was estimated to be an absorbance area of 7.7 (arbitrary units) and DL = 15 pg g^{-1}. The analytical uncertainty (indeterminate error) for the Fe determinations was estimated from the standard deviation of duplicate analyses and the standard deviation of the slope and intercept of the

calibration curve linear equation from the propagation of errors (Skoog 1984). The analytical uncertainty for the FIA method was estimated to be 30% on the mean at 20 pg g^{-1}, 10% at 50 pg g^{-1} and 5% for concentrations ≥ 300 pg g^{-1}.

2.6 Determination of ultra-trace-metals by HR-ICP-MS

2.6.1 HR-ICPMS method

Total-dissolvable Al, TD-Mn and TD-Fe were determined by HR-ICPMS in collaboration with Dr A. Townsend of the Central Science Laboratory, University of Tasmania (Townsend and Edwards, 1998). Total-dissolvable Fe was determined by this method in addition to FIA, so that the reliability of both methods could be assessed. The analysis of trace-metals in polar snow and ice by HR-ICPMS has been described by Shimamura et al. (1995), Barbante et al. (1997), and Townsend and Edwards (1998). The HR-ICPMS technique is extremely sensitive, with detection limits at the femtogram per gram (fg g^{-1}) level, for many elements. In addition, the instrument has a mass resolution of up to 7500 (m/Δm, 10% valley definition), and is readily able to resolve Fe and Mn from isobaric interferences. Determinations were made using a Finnigan-MAT Element HR-ICPMS housed in a positive-pressure HEPA-filtered room. The instrument is equipped with a double focussing sector-field mass spectrometer of reversed Nier-Johnson geometry with resolution settings of 300, 3000 and 7500 (m/Δm, 10% valley definition). Table 2.7 gives typical operating parameters used in the analyses. The isotopes determined are shown in Table 2.8,

along with the resolution used and potential interferences. The nebuliser gas-flow rate was optimised daily using Al^{27}, Fe^{56} or Pb^{208}. Samples were introduced into the instrument using a microconcentric nebuliser (MCN-100, CETAC Technologies) and cooled with a Scott-type spray chamber maintained at 5° C. The nebuliser was run in free-aspiration mode to avoid using potentially-contaminating PVC peristaltic pump tubing. To avoid artefacts due to differential aspiration between samples, the introduced sample volume and sample inlet line depth was kept constant. The MCN-100 nebuliser system is highly efficient and required only small sample volumes, typically 30-50 $\mu L\ min^{-1}$, with little loss of signal sensitivity relative to standard nebulisers. One drawback of using this type of nebuliser was that samples with salinities > 3 ‰ blocked the nebuliser with salt. Thus only samples with salinities less than 3 ‰ were analysed using this method. The sampling cone, torch and spray chamber were cleaned by soaking in 10 M HNO_3 (AR) for several days and then rinsed with DIW. These components remained installed for the duration of the study. Prior to analysis, the instrument was purged three times for 8 hr with alternating solutions of 2.5 M 2Q-HCl and 2Q-HNO_3. Solutions were aspirated for 1 hr followed by DIW for 5 min. At the end of the third 8 hr, 0.1 M 2Q-HCL was aspirated for 2 hr to precondition the system, after which samples were run. The sample introduction system was cleaned after each sample or standard by aspirating 2.5 M 2Q-HCl and 2Q-HNO_3 for 3 min each. DIW was aspirated before and after each acid. A total rinsing time of 10-15 min was typical between each sample. A similar rinsing protocol has been reported by Shimamura et al. (1985). We found this sequential acid rinse

Table 2.7 Typical instrument setting for HR-ICP-MS

RF power:	1250 W
Gas flow:	Plasma gas (Ar): 12-13 L min^{-1} Auxiliary (Ar): 0.8 - 1 L min^{-1} Sample (Ar): 0.8 - 1.2 L min^{-1}
Torch:	Fassel-type
Nebuliser:	Microconcentric nebuliser (MCN-100, CETAC Technologies)
Spray chamber:	Scott (double-pass type) cooled to 3.5-5° C
Cones:	Ni sampler (1.1 mm orifice id) and skimmer (0.8 mm orifice id)
Sample uptake:	Free aspiration, pumping for waste only
Instrument tuning:	Performed using a 1 ng mL^{-1} multi-element solution
Ion transmission:	100 000 counts s^{-1} per ng g^{-1} indium (average peak intensity)
Scan type:	Magnetic jump with electric scan over small mass range
Number of sample scans:	100-200 (depending on element, resolution and concentration)
Ion sampling depth	Adjusted to obtain maximum signal intensity
Ion lens setting:	Adjusted to obtain maximum signal intensity

Table 2.8 Isotopes determined and potential interferences

Isotope	Natural Abundance (%)	Resolution (m/Δm, 10% valley)	Potential isobaric interferences
^{27}Al	100	300	Fe^{2+}, CNH and CN
^{55}Mn	100	3000	ArN and ArNH
^{56}Fe	91.72	3000	ArO and CaO

combination to be most effective at lowering the background signals for the most problematic elements (e.g., Al and Fe) analysed in this study.

2.6.2 Standards, blanks and precision

Multi-element standards were prepared by gravimetric serial dilution from 10 μg g^{-1} Perkin-Elmer mixed element ICP standards (product number N930-0233 with 29 elements including Al, Mn and Fe). Blanks were prepared by acidifying DIW to 0.1 M with Seastar 2Q-HCl. Linear correlation coefficients for the calibration curves were in excess of 0.99 for all elements discussed here. Fresh blanks were prepared daily, while standards were prepared weekly. Standard solutions and blanks were analysed at regular intervals throughout each analysis to check for contamination

and/or instrumental drift. Typically, ten measurements were performed on blank solutions during the course of each analysis (typically 20 samples). The analytical precision for Mn was estimated from five consecutive measurements of a 50 pg g^{-1} standard solution, while the analytical precision for Al and Fe were estimated using 500 pg g^{-1} solutions. These concentrations were selected as they were believed to be close to the average concentrations occurring in the samples. Measurement reproducibility was routinely found to be with in 5-10% Relative Standard Deviation (RSD) on the mean for each element considered.

2.6.4 Instrument background signal

Relatively large background signals were initially observed for all the elements considered. Further tests indicated that some of this background was due to contamination from the gas lines. By placing a 0.5 μm in-line gas filter (Nupro) after the gas regulator and rinsing the gas line with DIW, this contamination was reduced by a factor of 3 for Al and Fe, (the most problematic elements). The background signal was further reduced by aspirating HCl and HNO_3, as previously described. A recalcitrant small background signal remained for Al and Fe. Sub-micron particles small enough to pass through the gas filter are suspected to have been the source of this residual background contamination.

2.6.5 Detection limit and blanks for HR-ICPMS method

Detection limits for the three elements were estimated from DIW blanks (9 replications) using equations 1 and 2 (section 2.5.4). The detection limits for Mn, Al and Fe were estimated to be 2, 19 and 30 pg g^{-1} respectively, with blanks of 3, 36 and 15 pg g^{-1} respectively. The analytical uncertainty for the method was estimated from the standard deviation of duplicate analyses and the standard deviation of the slope and intercept of the calibration curve linear equation by propagation of errors (Skoog, 1984). These estimated analytical uncertainties were:

Mn, 50% on the mean at 10 pg g^{-1}, 30% at 30 pg g^{-1} and 5% for concentrations $\geq$ 100 pg g^{-1};

Al, 50% at 50 pg g^{-1}, 18% at 100 pg g^{-1} and 10% for concentrations $\geq$ 300 pg g^{-1};and

Fe, 50% at 60 pg g^{-1}, 20% at 100 pg g^{-1} and 10% for concentrations $\geq$ 300 pg g^{-1}.

2.6.6 Spectral interferences

The determination of Mn and Fe at ultra-trace concentrations is often difficult with conventional quadrupole ICP-MS instruments, because of overlap from isobaric molecular ions, e.g., ArNH and ArO interfere with the determination of Mn and Fe respectively (Moens et al., 1994). However, the HR-ICPMS instrument was able to easily resolve the elemental signals from nearby polyatomic interferences. Manganese and Fe were measured in the medium resolution mode ($m/\Delta m=3000$). It should be noted that a trade off for this increased resolution is a reduction in signal intensity (Moens et al., 1995), typically 10-15%, depending on instrument settings. As a result, longer signal acquisition times were used for the analysis of these elements. Aluminium was analysed in low-resolution mode ($m/\Delta m=300$). Interferences from Fe^{2+}, $C^{12}N^{14}H^{1}$, $C^{13}N^{14}$ and $C^{12}N^{15}$ with Al^{27} were found to be negligible from surveys performed in medium resolution mode (the contribution from CNH and CN was found to be <0.4% of the Al blank signal).

2.6.7 Comparison of ICPMS results with FIA measurements

As standard reference materials for polar snow and ice are unavailable (Barbante et al., 1997), it was useful to compare the Fe determinations from HR-ICPMS and FIA. Total-dissolvable Fe concentrations ([Fe]) determined by the two techniques were found to be in good agreement ($[Fe]_{HR\text{-}ICPMS} = 1.039 \times [Fe]_{FIA} + 25$ pg g^{-1}, $R^2 = 0.987$ for n= 24). Figure 2.7 shows a comparison between the concentrations measured by

the two techniques. While it is difficult to assess the accuracy of the results without a reference standard for polar snow, the Fe determinations from both methods were in close agreement, suggesting that the data are reliable. The HR-ICPMS Fe data are systematically higher (slope 1.039 and intercept of 25 pg Fe g^{-1}), with an offset of approximately 30 pg Fe g^{-1} for an FIA Fe concentration of 100 pg Fe g^{-1}. The difference is probably due to the variability in the HR-ICPMS background and/or possibly particulate Fe that is determined by the ICPMS. Only the FIA Fe determinations are considered in the remainder of the thesis, rather than HR-ICP-MS, data, which required some background corrections.

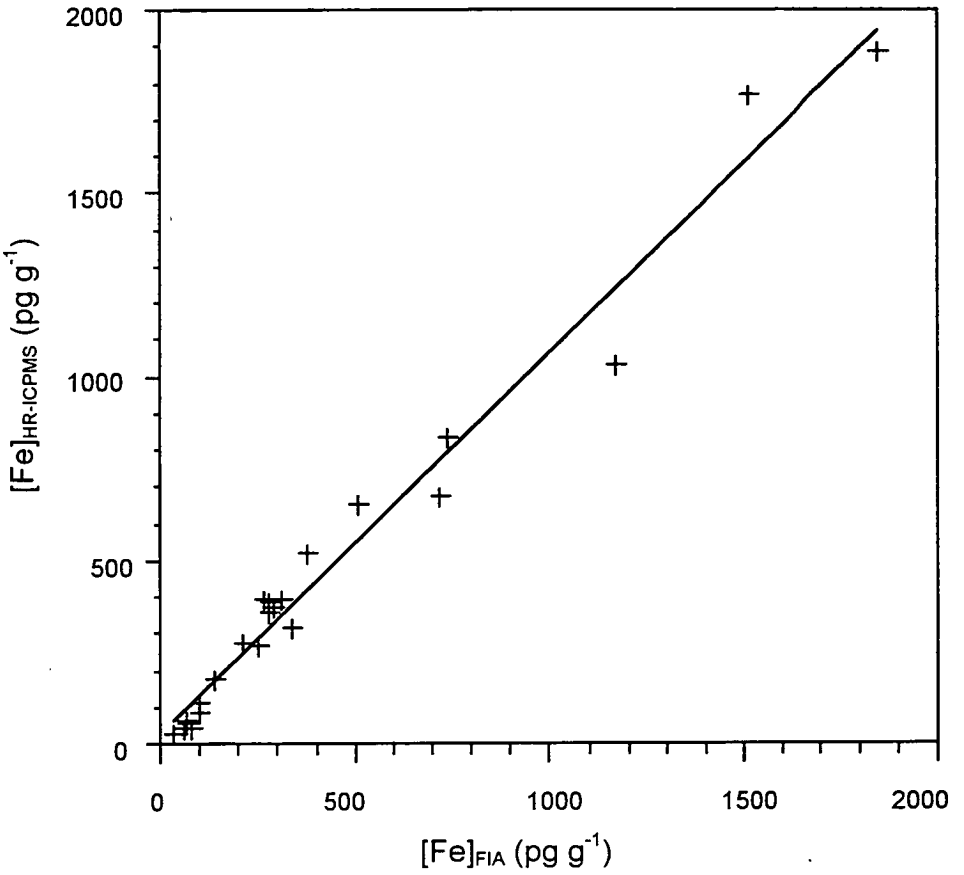

Figure 2.13 $[Fe]_{HR\text{-}ICPMS}$ vs $[Fe]_{FIA}$

Chapter 3

Results

3.1 Introduction

In this chapter, trace metal data for samples from the five locations described in Chapter 2 are presented. Raw data can be found in appendix A. The results for TD-Fe and, for selected samples, TF-Fe, TD-Al and TD-Mn are shown here. In addition, data concerning the reliability of the measurements are presented. These data include an evaluation of ship-derived contamination at an ice floe location, and the penetration of surface contamination into the ice-core samples.

3.2 Prydz Bay and Princess Elizabeth Land

During September, November and December 1994, snow samples were collected from East Antarctic locations in Prydz Bay and Princess Elizabeth Land. In total 8 sites were sampled, 4 on seasonal sea ice in Prydz Bay and 4 on the eastern periphery of the Lambert Glacier Basin in Princess Elizabeth Land (see Chapter 2). One aim of this fieldwork was to examine the latitudinal variability of atmospheric Fe deposition along a thin longitudinal band. The longitude of sampling locations varied between

71.50° E and 76.91° E, and the distances between sampling sites ranged from centimetres to several hundred kilometres.

3.2.1 Prydz Bay data

Total-dissolvable Fe concentrations for Prydz Bay snow samples are presented in Table 3.1. Iron concentrations at these sites varied from 69 to 1776 pg g^{-1}, with an arithmetic mean of 612 pg g^{-1}. Sample concentrations within individual snow pits varied by up to two orders of magnitude. This variability was present both horizontally and vertically (Figures 3.1 to 3.4), and no clear trends were observed. Several measurements were also made of TD-Al and TD-Mn (Table 3.2) in low-salinity samples. Aluminium concentrations covered a similar range to Fe, but with an arithmetic mean (AM) roughly twice as large (TD-Al AM = 1238 pg g^{-1}). Total-dissolvable Mn concentrations were, on average, more than an order of magnitude lower than both TD-Fe and TD-Al concentrations, but varied over one order of magnitude in range.

3.2.2 Princess Elizabeth Land data

Total-dissolved Fe, TD-Al and TD-Mn concentrations are presented in Tables 3.3 to 3.7. The arithmetic means for TD-Fe, TD-Al and TD-Mn concentrations were 858, 1514 and 25 pg g^{-1}, respectively. The trace metal concentrations within individual pits varied over an order of magnitude (Figures 3.5 to 3.8), and were comparable to

Table 3.1 Prydz Bay snow, TD-Fe concentrations

Site	N	O	U	V	All sites
	64.57° S, 74.98° E	64.90° S, 75.00° E	66.12 °S, 75.32° E	66.30° S, 75.72° E	
TD-Fe [pg g^{-1}]					
AM	634 (533)	824 (409)	429 (264)	643 (514)	612 (441)
Range	69-1539	260-1426	151-1077	268-1767	69-1767
N	10	8	12	9	39

AM = Arithmetic mean, standard deviation in brackets

N = number of samples

(Bar length represents depth of snow integrated by sample, 0 depth = snow surface)

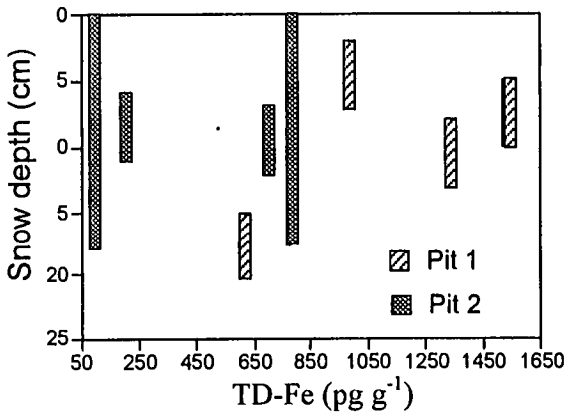

Figure 3.1 Prydz Bay site N, TD-Fe

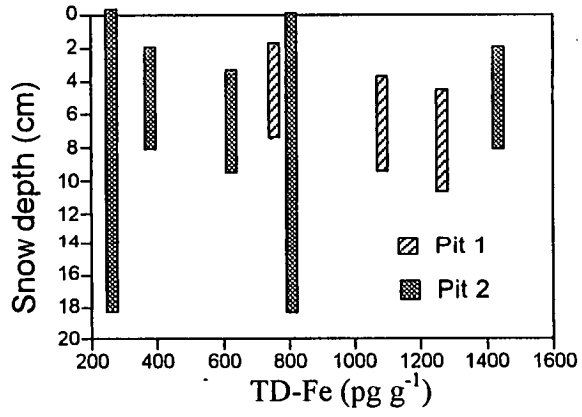

Figure 3.2 Prydz Bay site O, TD-Fe

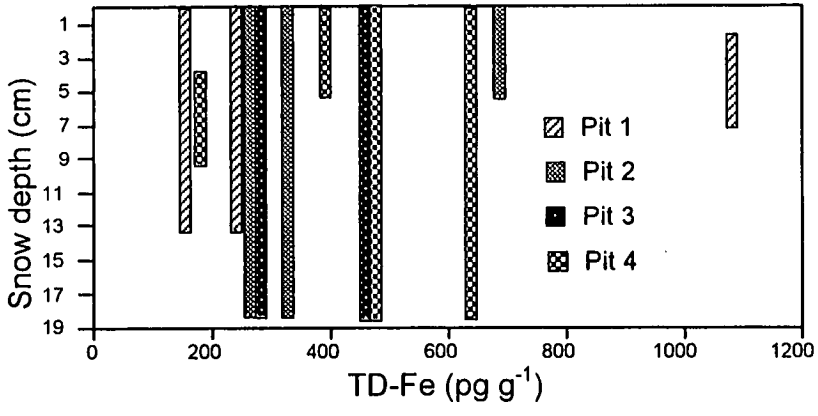

Figure 3.3 Prydz Bay site U, TD-Fe

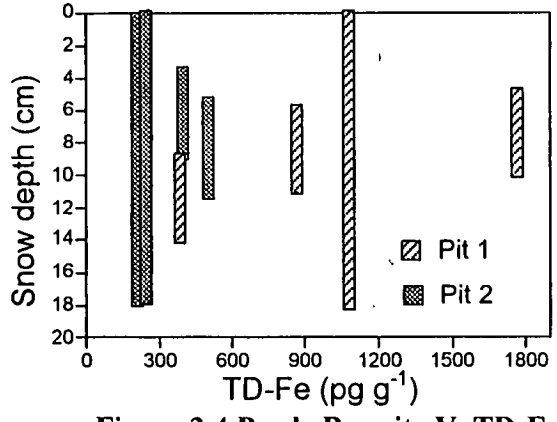

Figure 3.4 Prydz Bay site V, TD-Fe

Table 3.2 Prydz Bay snow, TD-Al and TD-Mn concentrations

All sites	TD-Al [pg g^{-1}]	TD-Mn [pg g^{-1}]
AM	1238 (1610)	42(69)
Range	170-4397	7-166
N	6	5

Standard deviation in brackets

AM = Arithmetic mean

N = number of samples

the ranges found in Prydz Bay, samples but with slightly less variability within individual pits. There is no obvious trend in the mean concentrations with either latitude or elevation of the sampling locations.

Table 3.3 Site LGB 70, total-dissolvable trace-metal concentrations

Element	TD-Fe [pg g^{-1}]	TD-Al [pg g^{-1}]	TD-Mn [pg g^{-1}]
70.57°S, 76.90°E, 1650 m			
AM	643 (488)	948(337)	21 (3)
Range	174-1550	174-1550	18-24
N	6	4	4

Table 3.4 Site LGB 59, total-dissolvable trace-metal concentrations

Element	TD-Fe [pg g^{-1}]	TD-Al [pg g^{-1}]	TD-Mn [pg g^{-1}]
73.43° S, 76.52° E, 2520 m			
AM	1461 (1003)	2024 (1210)	41 (32)
Range	346-2947	1169-2880	11-86
N	6	2	4

Table 3.5 Site LGB 53, total-dissolvable trace-metal concentrations

Element	TD-Fe [pg g^{-1}]	TD-Al [pg g^{-1}]	TD-Mn [pg g^{-1}]
74.90° S, 74.52° E, 2430 m			
AM	928 (908)	1007 (433)	18 (7)
Range	314-2479	622-1513	14-28
N	8	4	4

Table 3.6 Site LGB 46, total-dissolvable trace-metal concentrations

Element	TD-Fe [pg g^{-1}]	TD-Al [pg g^{-1}]	TD-Mn [pg g^{-1}]
75.85° S, 71.50 E, 2413 m			
AM	537 (211)	2281 (2319)	18 (7)
Range	266-845	698-1854	11-27
N	9	4	4

Table 3.7 Combined Princess Elizabeth Land, total dissolvable trace-metal concentrations

Element	TD-Fe [pg g^{-1}]	TD-Al [pg g^{-1}]	TD-Mn [pg g^{-1}]
AM	858 (751)	1514 (1844)	25 (18)
Range	174-2947	555-5676	11-86
N	29	14	16

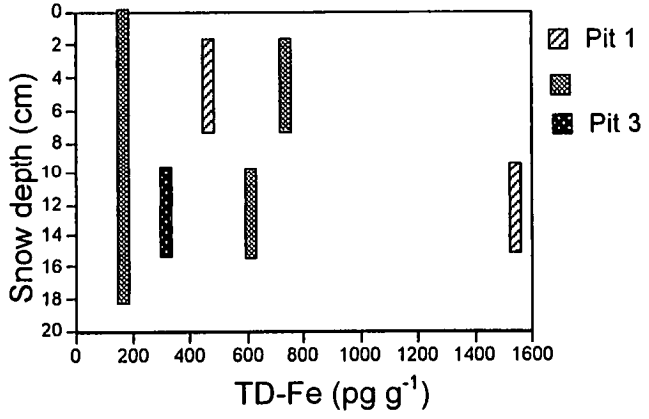

Figure 3.5 Princess Elizabeth Land site LGB 70, TD-Fe

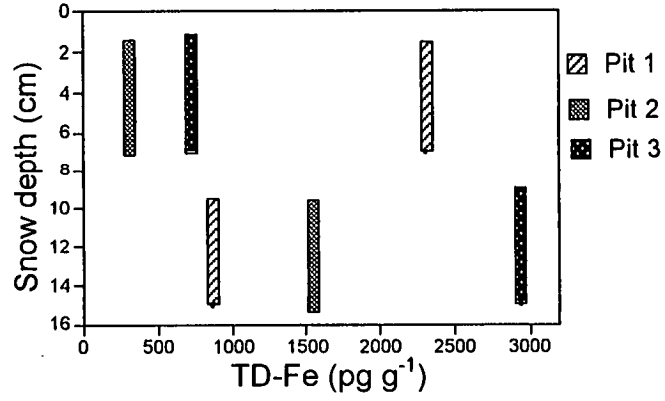

Figure 3.6 Princess Elizabeth Land site 59, TD-Fe

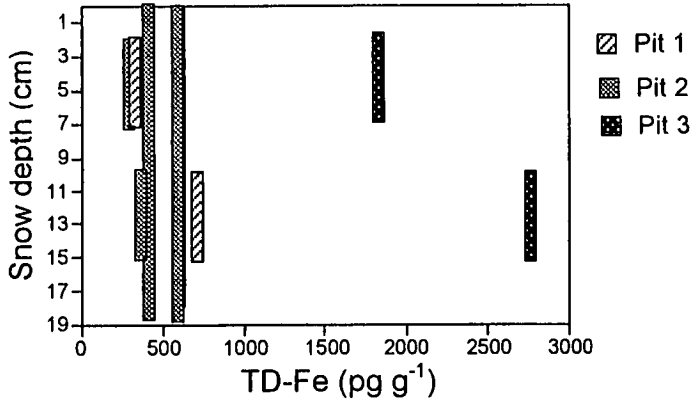

Figure 3.7 Princess Elizabeth Land site LGB 53, TD-Fe

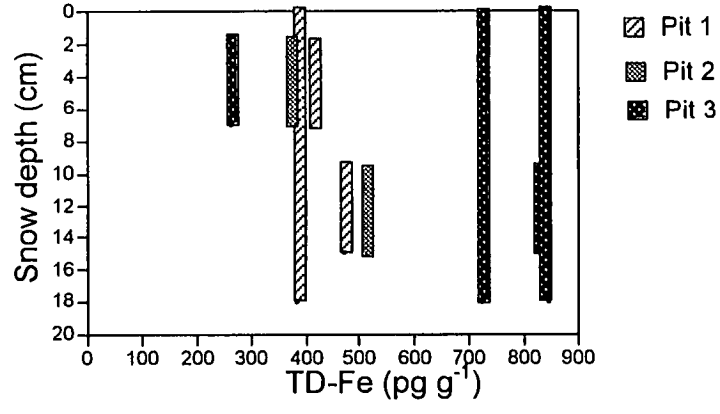

Figure 3.8 Princess Elizabeth Land site LGB 46, TD-Fe

Table 3.8 Prydz Bay and Princess Elizabeth Land, total-dissolvable Trace-metal concentrations

Element	TD-Fe [pg g^{-1}]	TD-Al [pg g^{-1}]	TD-Mn [pg g^{-1}]
AM	717 (601)	1275(1236)	22 (18)
Range	69-2947	170-5676	11-166
N	68	19	20

3.2.3 Combined Prydz Bay and Princess Elizabeth Land data set

Statistics for the combined Prydz Bay and Princess Elizabeth Land trace-metal data sets are shown in Table 3.8.

3.3 Dumont d'Urville Sea

During August 1995, snow samples were collected from sea ice in the Dumont d'Urville Sea off the coast of Terre Adélie, East Antarctica (see Figure 2.3, Chapter 2). These sample locations were several thousand kilometres East of those sampled in Prydz Bay during 1994. In addition to sampling snow from the "clean" area upwind of the ship, samples from downwind were collected at site A, to investigate

the possibility of contamination being introduced by the ship (e.g., in soot from the ship's stacks).

3.3.1 Ship-derived contamination investigation

An upwind/downwind transect of snow was sampled at site A as depicted in Figure 3.9. TD-Fe concentrations in snow from the transect TD-Fe data are shown in Table 3.9. Upwind, TD-Fe concentrations were extremely low (18 to 125 pg g^{-1}). In contrast, downwind concentrations were up to two orders of magnitude higher than the upwind samples. The high TD-Fe concentrations downwind of the ship and low concentrations upwind, suggest that snow is significantly contaminated by material carried in the air from the ship. Therefore, it is assumed that snow downwind of the ship is contaminated, whereas pristine concentrations are assumed for samples collected upwind of the ship.

3.3.2 Dumont d'Urville Sea data

With the exceptions of site H2 samples and downwind samples from station A, relatively low TD-Fe concentrations (arithmetic mean of 73 pg g^{-1}) were found in the snow samples from the Dumont d'Urville Sea.

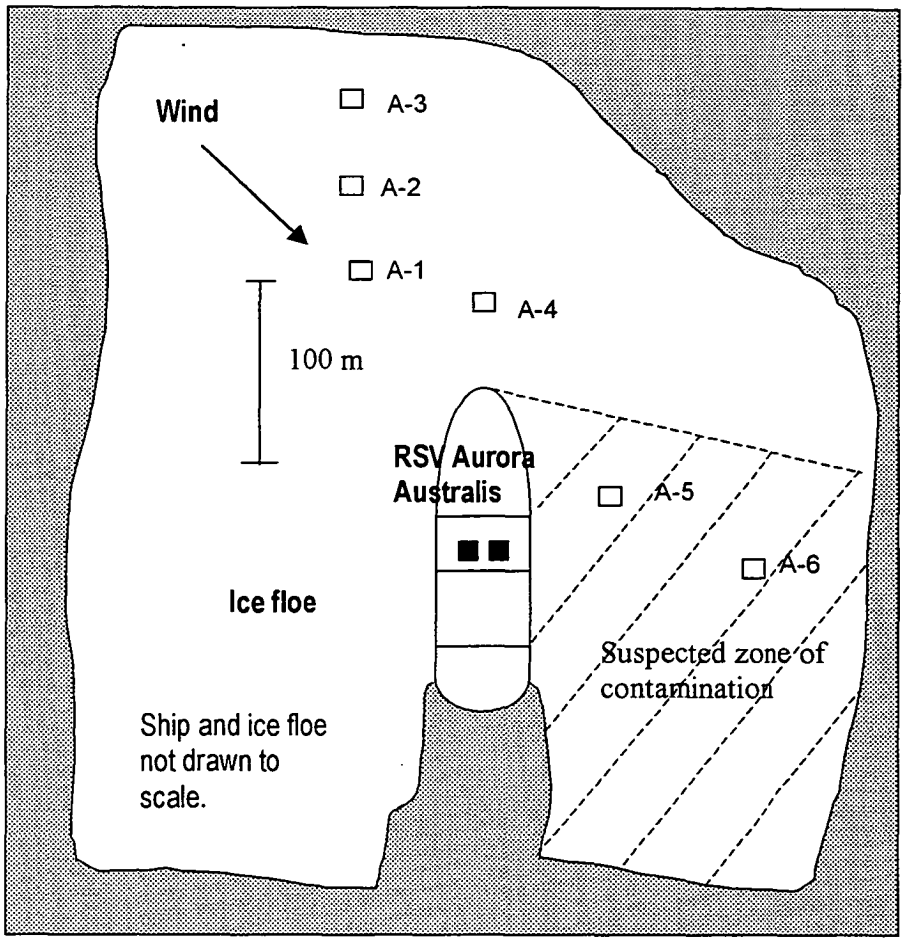

Figure 3.9 Dumont d'Urville Sea, site A snow pit locations

Table 3.9 Dumont d'Urville, site A transect, surface snow TD-Fe concentrations

Pit no.	A-1	A-2	A-3	A-4	A-5	A-6
AM	57	30	45	80	2187	2558
Range	50-64	30	18-125	66-94	266-4108	116-5000
N	2	2	10	2	2	2

The samples from site H2 were collected during a second visit to this ice floe (no samples were collected during the first visit), and the pit location was near what appeared to be a frozen ship track. Given the potential for ship-derived contamination suggested by the site A data, these samples are assumed to be contaminated, and are not used in the calculation of the regional mean concentrations. As for the Prydz Bay and Princess Elizabeth Land locations, there appears to be little correlation of TD-Fe concentrations with depth within the pits (Figures 3.10 to 3.14).

Table 3.10 Dumont d'Urville Sea snow TD-Fe concentrations

Site	A 64.60° S, 140.33° E	B 64.88° S, 141.07°E	K 64.93° S, 141.25°E	S 65.06° S, 141.58°E	H2 65.00° S, 141.21°E	All sites
			TD-Fe [pg g^{-1}]			
AM	45 (34)**	81 (80)	84 (8)	89 (35)	*226 (146)	73 (41)
Range	18-125	25-172	78-90	27-142	28-396	18-172
N	10	3	2	9	6	24

* not used to calculate mean.
** excluding samples A5 and A6

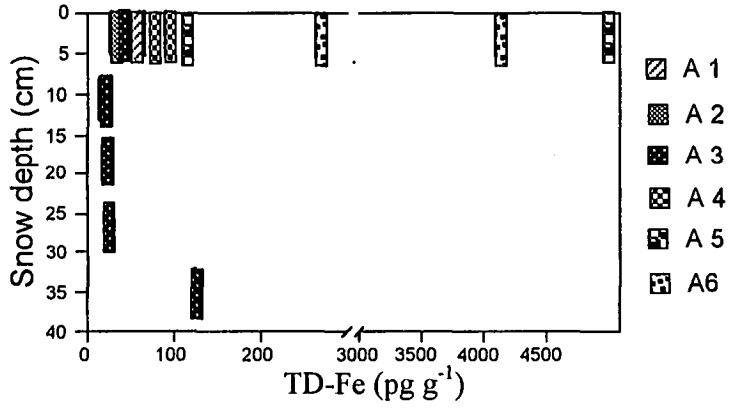

Figure 3.10 Dumont d'Urville Sea site A, TD-Fe

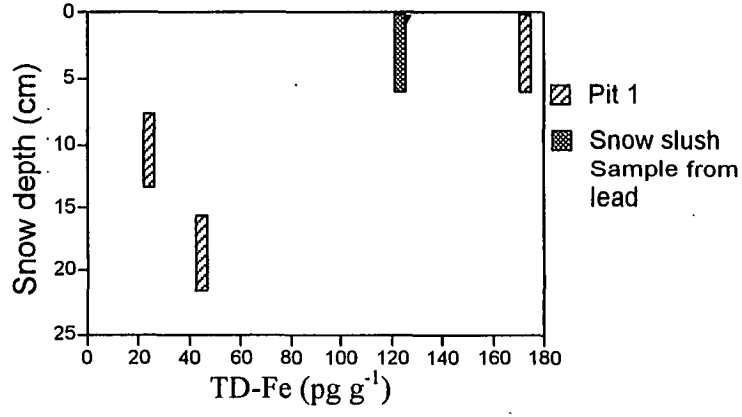

Figure 3.11 Dumont d'Urville Sea site B, TD-Fe

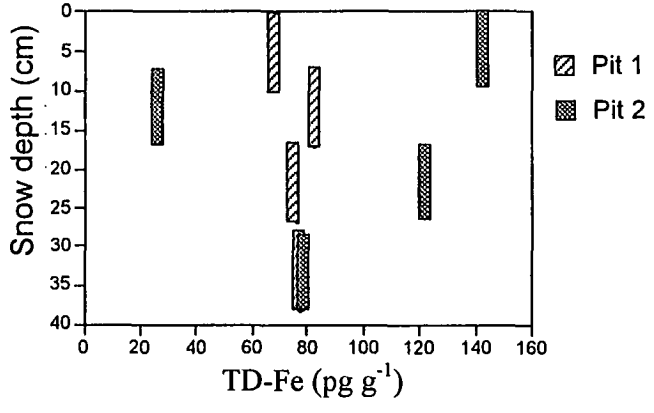

Figure 3.12 Dumont d'Urville Sea site S, TD-Fe

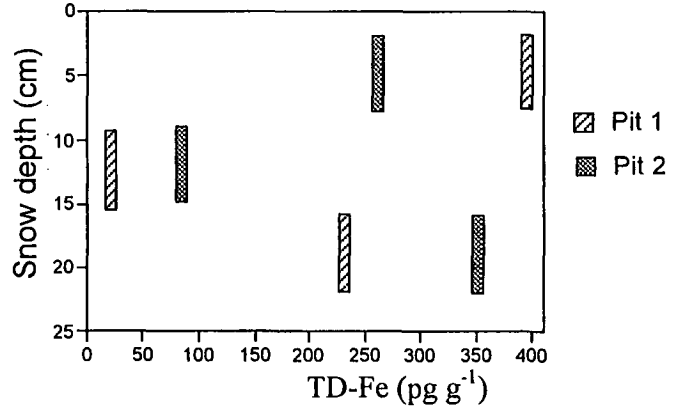

Figure 3.13 Dumont d'Urville Sea site H2, TD-Fe

3.4 Ross Sea data

A small number of snow samples were collected from sea ice in the Ross Sea in November and December 1994. The results from this area are shown in Table 3.11. The TD-Fe concentrations ranged from 709 to 1054 pg g^{-1}, and had an arithmetic mean of 894 pg g^{-1}, which is comparable to the mean TD-Fe concentrations for the Prydz Bay and Princess Elizabeth Land samples. However, the range of concentrations from each site are smaller than for samples from Prydz Bay and Princess Elizabeth Land.

Table 3.11 Ross Sea snow TD-Fe concentrations

Site	**1** 69.52° S, 170.6° W	**2** 75.00° S, 170.67° W	**3** 76.45° S, 175.52° W	**All sites**
		TD-Fe [pg g^{-1}]		
AM	749 (57)	1035 (127)	987 (94)	894 (136)
Range	709-790	855-1035	921-1054	709-1054
N	2	2	2	6

3.5 Law Dome ice-core samples

Sub-samples of three ice-cores from Law Dome (See Chapter 2) were used to investigate the temporal variability in TD-Fe concentration in snow over the period from the recent past back to the LGM. The estimated ice core sample ages before present (BP, 1997) are shown in Figure 3.14. Each sample was decontaminated, and cross-core trace-metal profiles were constructed to assess the reliability of the inner sample concentrations, as discussed in Chapter 2.

3.5.1 Evaluation of the decontamination procedure

The TD-Fe concentrations measured in sub-samples from the decontamination of six ice-core sections (DE08 55B, DSS 28A1-3, DSS 1165, BHC1 129A, BHC1 132A and BHC1 137B) are shown in Figures 3.15 to 3.20. Relatively low and constant TD-Fe concentrations were measured in meltwaters from the three innermost layers of each ice-core section, which suggests that the decontamination procedures were successful in each case. The concentrations assigned to the inner-most layer of DSS 28A 1-3, DSS 1165, DE08 55B, DE08 77A, BHC1 129A and BHC1 137B are an average of a number of sub-samples from larger sections which were decontaminated (see Appendix, Table A.6).

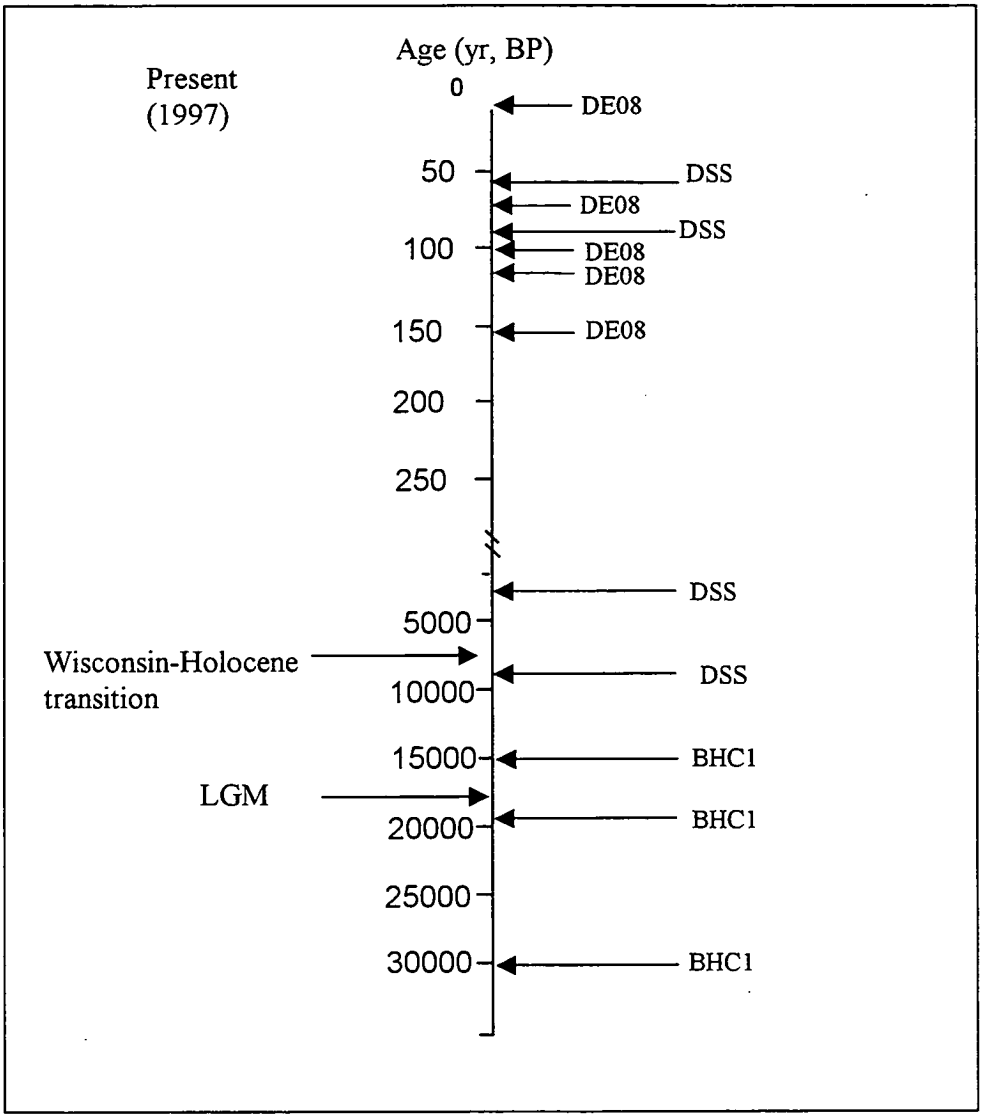

Figure 3.14 Estimated ages of Law Dome ice-core samples used in this study

(BHC1 ages were estimated by comparison of the BHC1 $\delta^{18}O$ record with that of the Antarctic Vostok ice-core, and are uncertain to several 1000 years). The TD-Fe variability in these sub-samples was significant for the DSS 28 A 1-3 and DE08 55B sections (the youngest sections), with standard deviations of approximately 50% on

the mean. This variability is believed to be due to the seasonality of the atmospheric Fe deposition to the sites. The sub-sample TD-Fe standard deviations from the DSS 1165, DE08 77A, BHC1 129A and BHC1 137B sections were less than 35% on the mean. With the exception of DE08 77A these sub-samples are believed to integrate more than 1 yr deposition. High TD-Fe concentrations were measured in the exterior layers of core section DSS 1165 (Figure 3.16). At the time this core section was drilled, the DSS bore hole was filled with a kerosene-based fluid to prevent it from closing, whereas the other core samples were obtained from dry bore holes. This may explain the high external contamination of this section in comparison to the other samples. The external TD-Fe concentrations of core section BHC1 132A (Figure 3.19) is also significantly higher than for the other samples (with the exception of DSS 1165). This is thought to be a product of both the higher uncontaminated TD-Fe levels in this core section (from the LGM) and the cumulative contamination of the core during storage and handling, given that BHC1 was drilled earlier than the other cores. However, the TD-Fe concentration measured in the centre of this core section is thought to be reliable, and is corroborated by particle measurements in sections of the DSS core of similar age (Jun et al., 1998). In addition to TD-Fe, TD-Al was determined in core section 55B (Figure 3.18). As with the TD-Fe core-profile for this sample, a clear concentration plateau was found for TD-Al, suggesting that this core was successfully decontaminated for Fe and Al. Effective decontamination for Fe is assumed for the other core sections for which data are presented, based on the decontamination profiles for Al, which was measured independently at LGGE (S. Hong, personal communication).

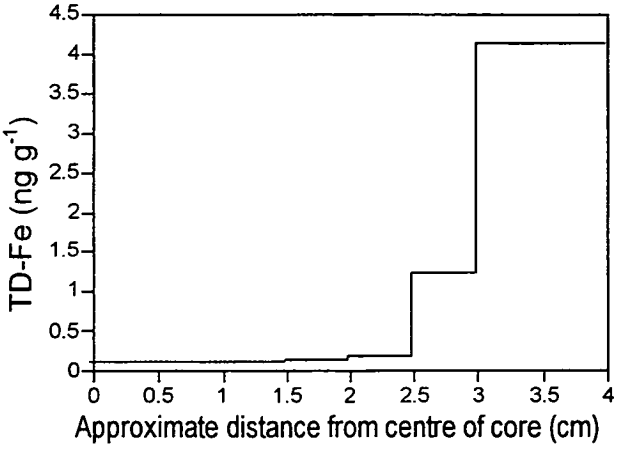

Figure 3.15 DSS 28A TD-Fe decontamination profile

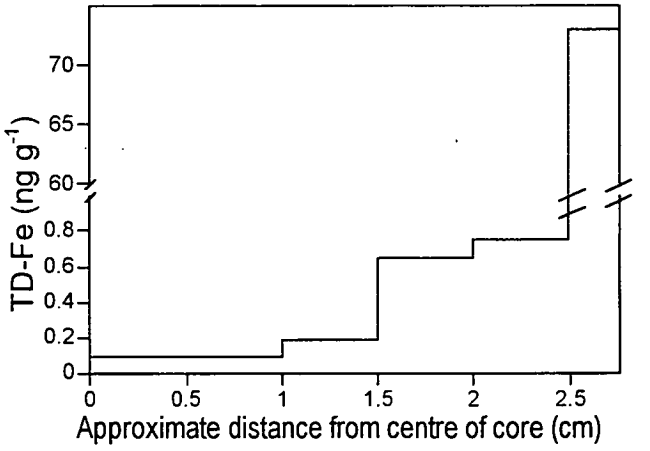

Figure 3.16 DSS 1165 TD-Fe decontamination profile

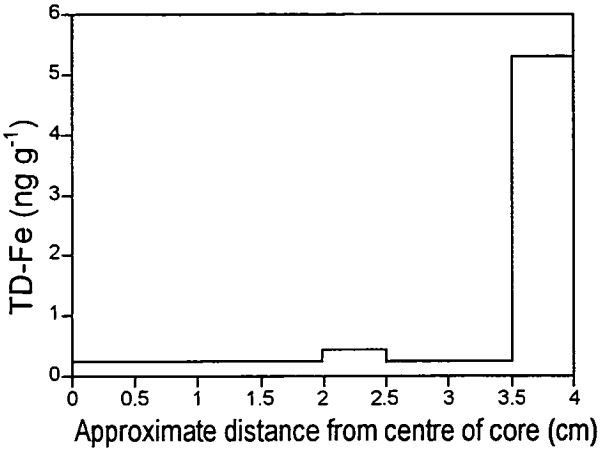

Figure 3.17 DE08 55B TD-Fe decontamination profile

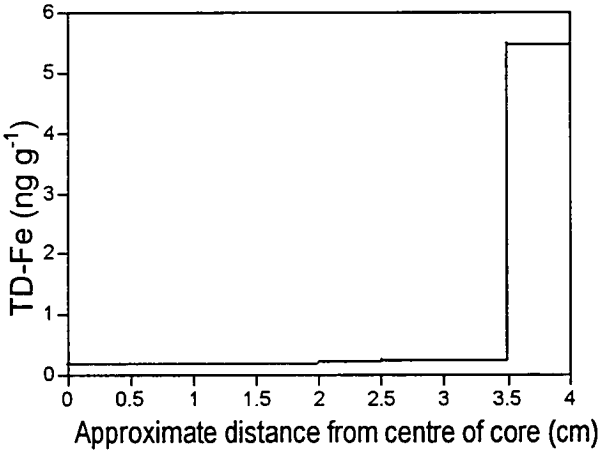

Figure 3.18 DE08 55B TD-Al decontamination profile

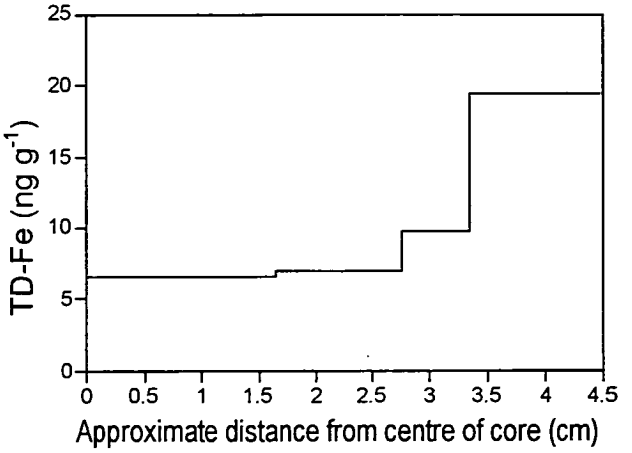

Figure 3.19 BHC1 132A TD-Fe decontamination profile

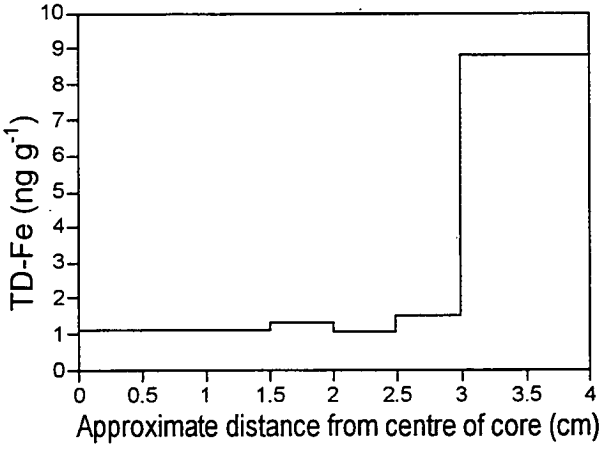

Figure 3.20 BHC1 137A TD-Fe decontamination profile

3.5.2 Ice-core data

Holocene Ice-core TD-Fe concentrations (Figure 3.21) were generally low (27-139 pg g^{-1}), with the exception of DE08 sections 55A and 55B, which ranged from 100-340 pg g^{-1} (Appendix, Table A.6). In contrast Wisconsin-Holocene transition and Wisconsin age TD-Fe concentrations were up to two orders of magnitude higher with the highest concentration (6700 pg g^{-1}) determined for a sample dating from the LGM (Appendix, Table A.6).

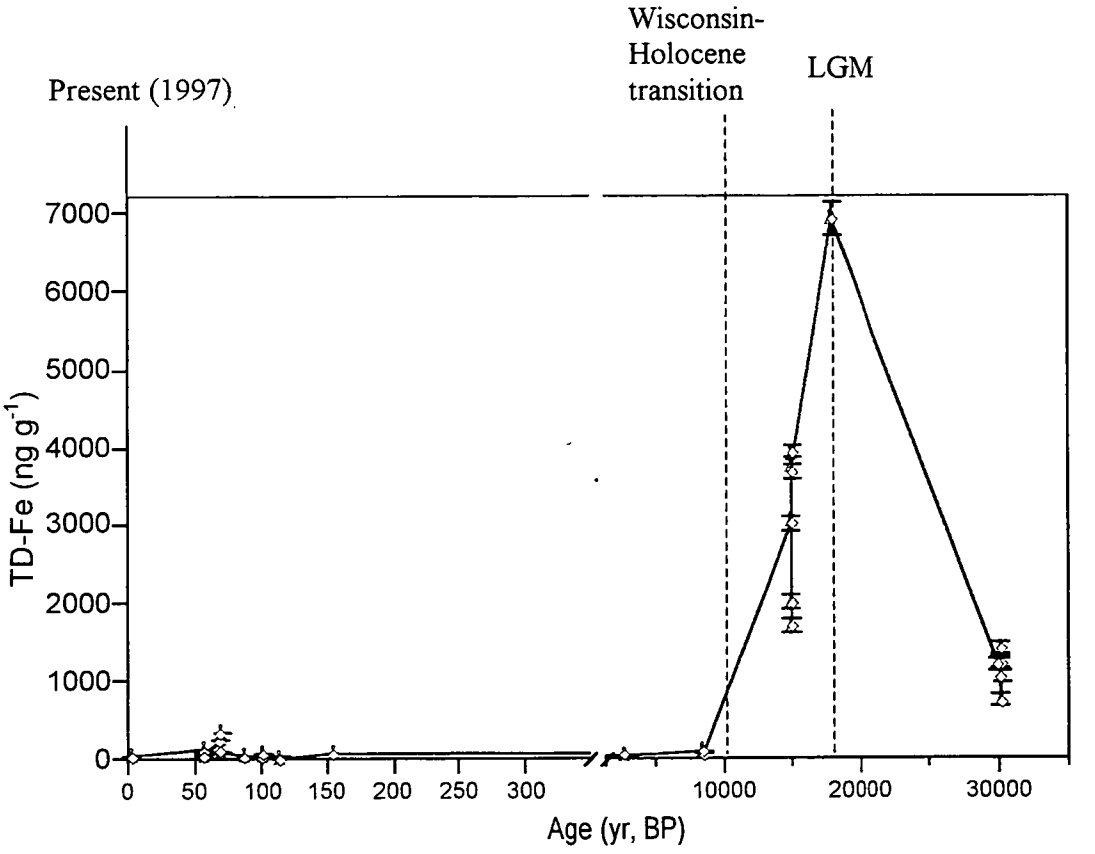

Figure 3.21 Law Dome Holocene and Wisconsin age ice-core TD-Fe concentrations

(Error bars show analytical uncertainty)

3.6 Fe and Mn enrichment factors

Mineral dust formed by crustal weathering is thought to be the principle source of Fe in the marine atmosphere. To determine whether this is the main source, crustal enrichment factors (EF) are calculated (Chester, 1986). Using Al as the crustal reference element these are calculated by equation 3 (Chester, 1985 and references therein).

$$EF_{crust} = \frac{(Element/Al)_{snow}}{(Element/Al)_{crust}} \qquad (3)$$

Assuming Fe/Al_{crust} and Mn/Al_{crust} = 0.841 and 0.017 respectively (Taylor and McClennan; 1985)

Enrichment factors for snow and ice-core TD-Fe and TD-Mn were calculated, and the data summarised in Table 3.12. Excluding a potentially contaminated sample (Dumont d'Urville Sea sample, A 5/2) average EF's of 1 were calculated for both Fe and Mn suggesting a crustal source for these elements. Enrichment factors of 14 for Fe and 7 for Mn were calculated for sample A 5/2, which appear to be contaminated (section 3.3.1). Aluminium was not determined for samples from the Dumont d'Urville site H2 and therefore suspected contamination of this site cannot be confirmed.

Table 3.12 Enrichment factors for Fe and Mn

Elemental	Fe	Mn
AM EF	1.0 (0.7)	1.4 (1.0)
Range	0.2-3	0.3-2.3
N	30	21

3.7 Soluble Iron fraction present in snow

Soluble Fe was calculated as the ratio of TF-Fe to TD-Fe, and is given as a percentage of TD-Fe in Table 3.13. Soluble Fe ranged from 10 to 90% with an arithmetic mean of 41% and a geometric mean of 30%.

Table 3.13 Soluble Fe fraction present in snow samples

Soluble Fe fraction (% TD-Fe)	
AM	41 (25)
GM	30
Range	10-90
N	23

GM = geometric mean

Chapter 4

Discussion

The following chapter discusses the trace-metal data shown previously, from which the present and LGM atmospheric input of Fe onto the Southern Ocean are estimated. The solubility of this atmospheric Fe input, its possible impact on algal production, and the role of sea ice in modulating the delivery of this Fe into the surface ocean are also discussed.

4.1 The Fe content of modern and ancient East Antarctic snow

4.1.1 Enrichment factors and source of Fe and Mn

Enrichment factors were calculated for TD-Fe and TD-Mn relative to TD-Al (see Chapter 3 section 3.6). Average enrichment factors of 1 for both Fe and Mn (i.e. not enriched relative to the mean crustal abundances) suggest that the source of these elements is terrigenous dust, as assumed. In comparison, the snow sample A-5/2, which was collected from surface snow down wind of the *Aurora Australis,* was found to be highly enriched in both Fe and Mn relative to Al with EF's of 14 and 7

respectively. This sample appears to have been contaminated by material, which contains more Fe and Mn relative to Al, (soot, rust etc) blowing from the ship.

4.1.2 Variations in present-day snow TD-Fe concentrations

Standard deviations on mean TD-Fe concentrations for the individual sampling sites (σ_s) ranged from 39 to 97% of the average TD-Fe concentration, much higher than the estimated 5% uncertainty of the FIA analysis (σ_a) used to determine the Fe concentrations. There are several possible interpretations of the high values for σ_s, including:

(1) Random contamination at the sampling sites and during the analysis;

(2) The estimated value of σ_a is too low; and

(3) The high σ_s represents the actual variability of TD-Fe concentration in the snow samples.

Random contamination during sampling is a possibility, considering the low levels of Fe encountered in this study. As described in Chapter 2, the major source of contamination at the sampling sites was expected to come from ships during the sea ice sampling, and from the tractor trains, generators etc during the continental sampling. Of these, the marine expeditions probably posed a greater potential for

contamination, due to the proximity of the ships to the sampling sites. The contaminated sample collected from downwind of the ship at site A in the Dumont d'Urville Sea suggest that the downwind sampling protocol was effective in avoiding gross ship-derived contamination. The unusually high TD-Fe concentration found in snow at the Dumont d'Urville Sea site H2 also suggests gross contamination from the ship, which is assumed to have been avoided in pristine upwind sites.

It is also possible that random contamination may have occurred during the sample preparation and analysis, but no significant contamination was ever found in either day-to-day analytical blanks, or long-term storage blanks used to identify Fe leaching from the sample bottle containers. There is then no evidence of significant contamination of samples during collection, processing and analysis (except where indicated).

It is conceivable that our estimate of σ_a may be too low, as the precision of the technique was determined from Fe standards and not from the repeat analysis of actual samples over time. As discussed in Chapter 2, Fe was leached from the dust particles in the samples over a period of 3 months before analysis. If the percentage of leachable Fe in the dust particles were not constant after 3 months, then this may account for some of the variability; however fairly reproducible TD-Fe vs time curves obtained in the leaching study (section 2.4.2) strongly argue against this being responsible for the very large (order of magnitude) variations in Fe at a single site. Also the excellent agreement between the FIA and ICPMS analyses carried out at

different times argues against analytical or processing artefacts as the source of the observed variability. Thus, the most likely explanation is that the large range in TD-Fe concentrations represents natural small-scale spatial variability of mineral aerosol content in the snow. The sites sampled were extremely complex in terms of snow cover. The marine sites were composed of many small sea ice floes frozen together. The fresh snow on the floes was highly mobile, and built up around ice ridges or on existing small snow dunes. These features were composed of snow of various age, wetness and crystal structure. The snow samples were preferentially taken from these features due to the shallow snow depth in other areas of the floes, and it is possible that the snowdrifts represent a mixture of snow from several months of deposition with quite different dust contents. Sastrugi and other complex features were observed at the continental sites. Figure 4.1 shows two adjacent TD-Fe profiles for a snow-pit at site S in the Dumont d'Urville Sea. While the TD-Fe concentrations vary little with depth in profile 1, there is a significant amount of variability in profile 2, approximately 15 cm away from profile 1 as shown in Figure 4.1. The difference in the two profiles could be explained if, for example, the snow dune was formed by four separate snowfall events, each with a different Fe concentration (Figure 4.2). Unfortunately, this hypothesis cannot be tested due to a lack of detailed stratigraphy from the snow pits. However it seems likely that much of the variability in the Fe concentrations is due to variability between different snow layers at the sites, or mixing of different batches of snow due to sea ice movement, wind etc.

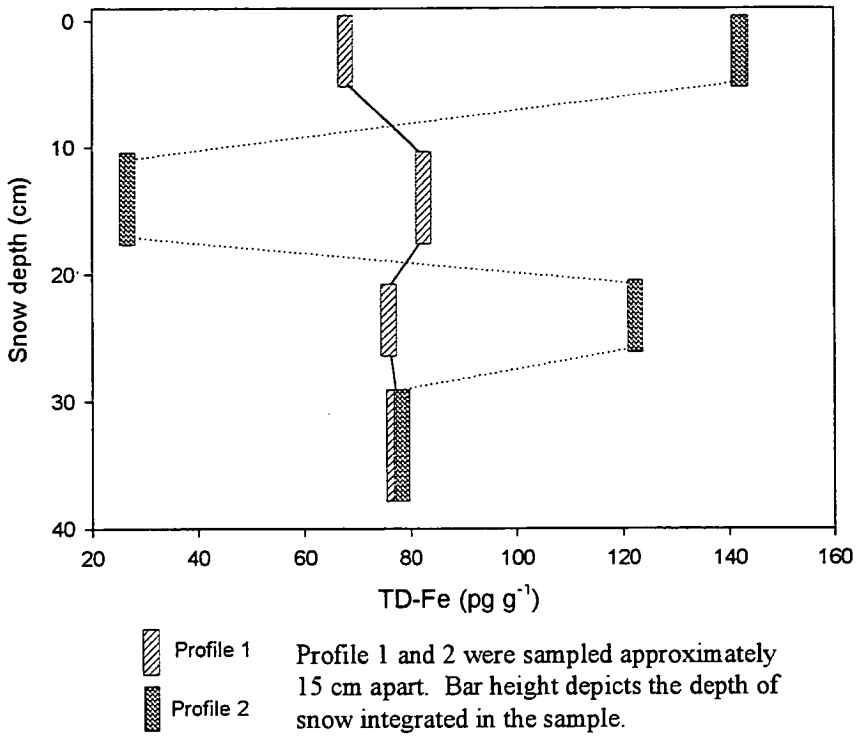

Figure 4.1 Adjacent TD-Fe profiles of snow pit B, Dumont d'Urville Sea

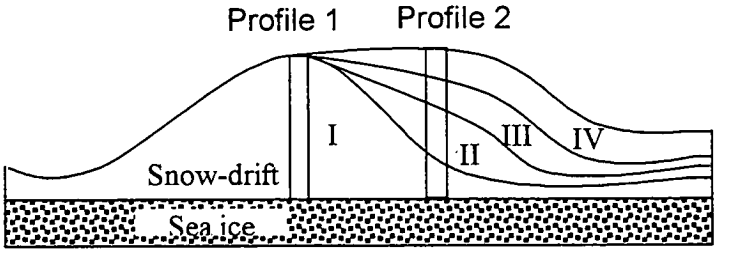

I: Initial basal snow layer, II – IV: later separate snow falls

Figure 4.2 Possible scenario to explain two depth profiles

In comparison to the variability within individual pits, the variability between average site concentrations was considerably less, with standard deviations ranging from 12-40% on the TD-Fe regional mean. The Prydz Bay and Princess Elizabeth Land range over distances of approximately 1200 km, from the marine sites in Prydz Bay to the high Antarctic plateau site LGB 46. With the exception of the Princess Elizabeth Land site LGB 59, site average TD-Fe concentrations were comparable. In addition, similar TD-Fe concentrations were found for snow from the Ross Sea, and similar TD-Fe snow concentrations for Antarctic snow have been reported by Westerlund and Ohman (1991) and Shimamura et al. (1995). With the exception of LGB 59, there appears to be very little variability between the sampling sites suggesting that it is reasonable to combine site averages in order to calculate regional averages for these areas.

4.1.3 Seasonal variations in the TD-Fe concentration of late-Holocene ice-core samples

Because of high snow accumulation rates at the DSS and DE08 drilling sites, the annual layer thickness in the upper sections of these cores are relatively large. As a consequence, the recent Holocene samples studied do not integrate an entire year's deposition (Table 4.1). The chronologies for these ice-core sections have been constructed by counting annual layers as defined by oxygen isotope ($\delta^{18}O$) stratigraphy (Etheridge et al., 1988; Morgan et al., 1997), and display a well defined summer peak and winter trough in $\delta^{18}O$ at these sites. The seasonality of the sub-

samples were estimated by dividing the annual $\delta^{18}O$ signal into equal summer, autumn, winter and spring components. Four samples from the DSS 28A section provide a record of atmospheric Fe deposition over almost an entire year (Figure 4.3): from late summer to autumn 1939 (DSS 28A-1), winter 1939 (DSS 28A-2), early spring 1939 (DSS 28A-3) and late-summer to winter 1939/40 (DSS 28A-4). Analysis of these samples reveal summer TD-Fe concentrations to be higher than winter by a factor of around 4. The seasonal variability of TD-Fe concentrations in the sections could be due to either seasonal variations in the snow accumulation rate at the site, or to the atmospheric transport of Fe to the site (ie, dust concentration in atmosphere). Changes in the snow accumulation rate may affect the TD-Fe concentration of snow by changing the ratio of dry deposition to wet deposition. While dry deposition is generally thought to be less efficient than wet deposition (Davidson, 1989), Fe deposited by this pathway could become concentrated at the surface of the snow pack increasing the determined Fe concentration. Davidson (1989) estimated the percentage of dry deposition of crustal elements to Greenland to be 10% for high accumulation sites and 35% for low accumulation sites. If the relationship between wet and dry deposition in Greenland is valid in Antarctica, then a reduction in snow accumulation during the isotopic spring/summer could account for some of seasonal variability. But there does not appear to be an effect of a seasonal bias in snow accumulation at the DSS site: on the basis of peroxide concentrations (which also displays seasonal cycle at the sites) and oxygen isotope measurements spanning the past 684 years, van Ommen and Morgan (1997) conclude that it is reasonable to assume that there was no systematic seasonal bias in

the accumulation of snow at the DSS site. More recently, snow accumulation at the DSS site has been measured by an automatic weather station (I. Allison, personal communication, 1999). Preliminary snow-accumulation data from the weather station is shown in Table 4.2. While data for several years accumulation are needed to confidently describe seasonal variations, the preliminary data in Table 4.2 suggests that there is no significant bias between winter and summer accumulation rates. This suggests that the variability of the Fe concentrations in these ice-core sub-samples is due to changes in atmospheric dust concentrations over the site. Although data are lacking from late-spring (1939) to summer (1940), these preliminary results suggest a seasonal cycle with a maximum atmospheric Fe flux in summer, decreasing to a low in winter. A similar seasonal cycle has been found for atmospheric measurements of crustal elements Mn at Neumayer station (Wagenbach, 1988) on the coast of Dronning Maud Land, and scandium at the South Pole (Tuncel, 1989). This seasonality is also suggested by dust concentrations in snow and ice at several Antarctic sites (Marshall, 1962; Hamilton, 1969; Taylor, 1964; Bull, 1971). This implies that there may be a seasonal bias to the snow samples that were collected during winter, perhaps explaining the very low TD-Fe concentrations in the Dumont d'Urville samples, collected in July.

Table 4.1 Modern ice-core samples, isotopic season and TD-Fe concentrations

Core ID	Depth (m)	Date BP (1997)	Annual layer thickness (m, ice equivalent)	Time span
DSS 28A-1	46.64-46.82	56	0.54	spring summer
DSS 28A-2	46.82-46.98	56	" "	winter
DSS 28A-3	46.98-47.08	56	" "	autumn
DSS 28A-4	47.17-47.54	57	" "	spring summer
DE08 55A	96.01-96.29	69	1.24	spring summer
DE08 55B part (a)	96.41-96.55	70	1.39	spring
DE08 55B part(b)	96.55-96.69	70	" "	winter spring
DSS 41B	72.95-73.20	88	0.64	winter
DE08 77A part (a)	136.02-136.16	102	1.19	winter autumn
DE08 77A part (b)	136.16-136.30	102	1.16	autumn
DE08 85-A	150.90-151.42	115	1.17	winter
DE08 108A	192.80-193.08	155	0.97	summer

Annual layer thickness data from Tas van Ommen, personal communication, 1999)

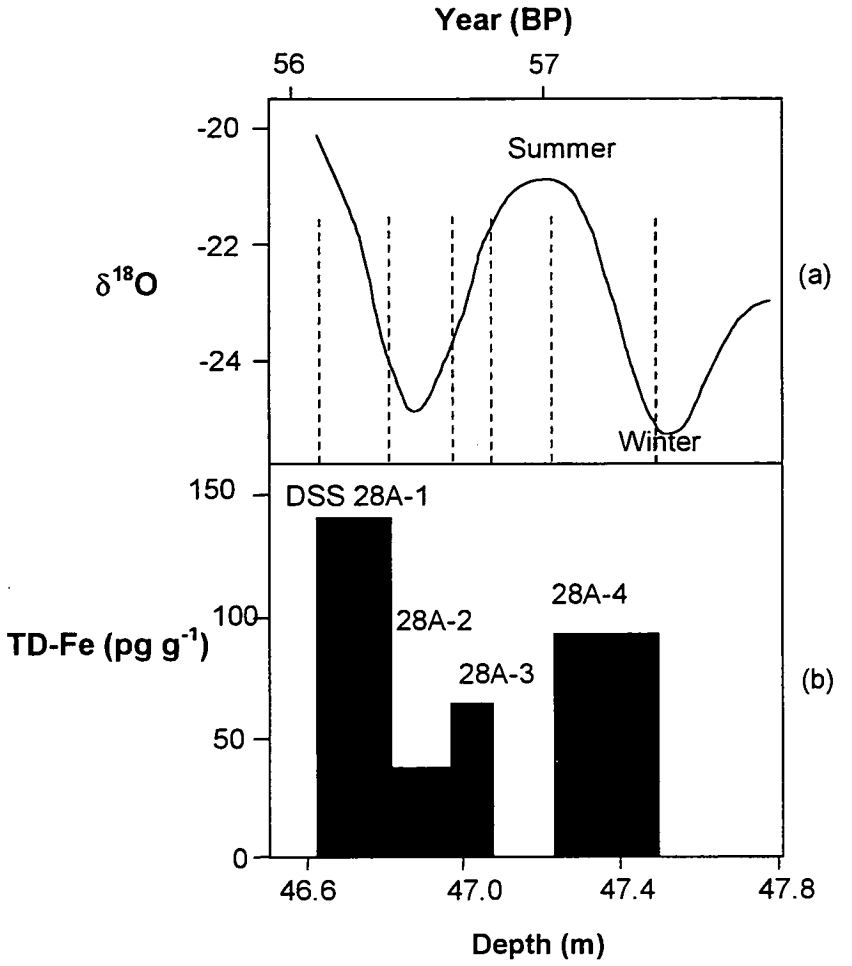

Figure 4.3 (a) DSS 28A sub-sample depth with respect to a generalized seasonal $\delta^{18}O$ signal for the DSS core. (b) Sub-sample Fe concentrations as a function of depth in core

Table 4.2 Net snow accumulation at the DSS site, Law Dome, during 1998

(I. Allison, personal communication, 1999)

Month	Snow accumulation (m)
Jan	0.20
Feb	0.20
Mar	0.05
Apr	0.12
May	0.35
Jun	0.10
Jul	0.13
Aug	0.33
Sep	-0.24
Oct	0.19
Nov	0.29

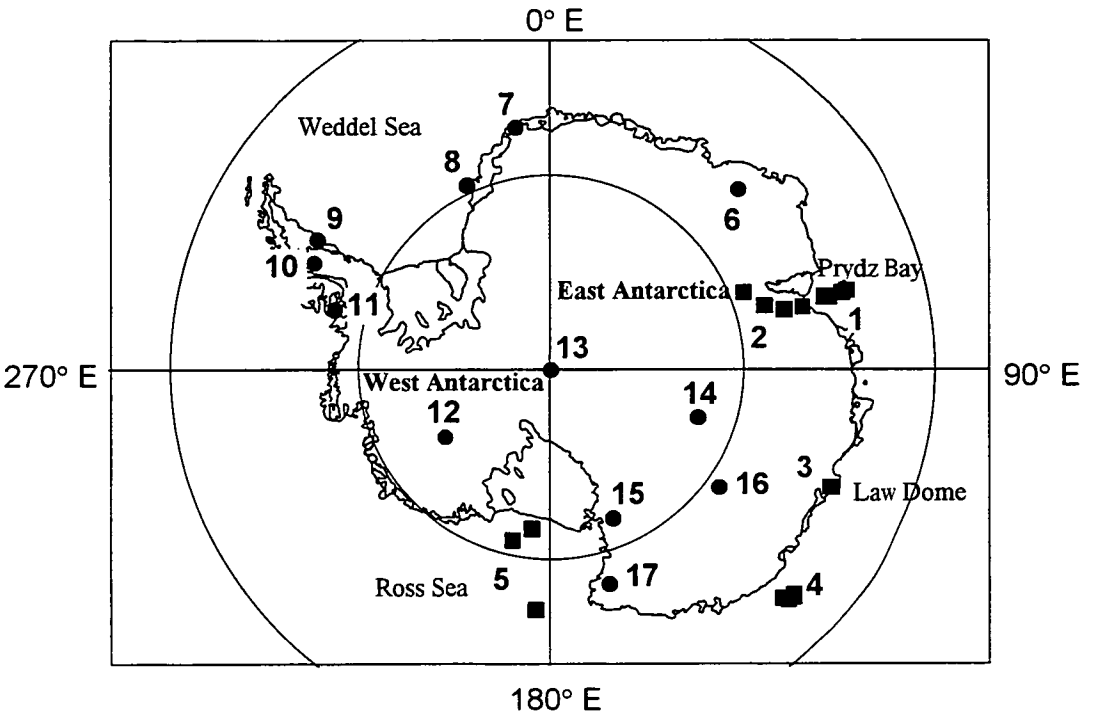

1. Prydz Bay; 2. Princess Elizabeth Land; 3. Law Dome; 4. Dumont d'Urville Sea; 5. Ross Sea; 6. Mizuho ice-core drill site; 7. Neumayer Station; 8. Westerlund and Ohman (1991) sample sites; 9., 10. and 11. Dick (1991) sample sites; 12. Byrd ice-core drill site; 13. South Pole; 14. Vostok ice-core drill site; 15. Taylor Dome ice-core drill site; 16. Dome C ice-core drill site; 17. Maggi and Petit (1998) firn-core drill site.

Figure 4.4 Locations of mineral-dust and trace-metal studies

4.1.4 Regional variability of present day and late Holocene TD-Fe concentrations

Regional average TD-Fe concentrations for the Dumont d'Urville Sea, Ross Sea, Prydz Bay, Princess Elizabeth Land and Law Dome (late-Holocene samples) locations are shown in Table 4.3 along with TD-Fe concentrations reported in the literature for Antarctic snow (see Figure 4.4 for locations). With the exception of the Dumont d'Urville Sea and the Law Dome Holocene ice-core sections, TD-Fe concentrations appear to be remarkably uniform over most of Antarctica. The Dumont d'Urville Sea and Holocene Law Dome average TD-Fe concentrations were found to be an order of magnitude lower than those of the Ross Sea, Prydz Bay and Princess Elizabeth Land. Several hypotheses may be offered to explain the lower TD-Fe levels found in the Dumont d'Urville Sea and the modern Law Dome ice-core sections. The Dumont d'Urville Sea samples were collected in July, and thus may be seasonally biased due to a minimum in atmospheric dust concentrations during the austral winter (see section 4.1.3). If these samples represent a seasonal minimum for the region and the snow concentrations vary seasonally by a factor of 4, as suggested by the late-Holocene Law Dome ice-core samples, then the estimated seasonal maximum snow TD-Fe concentration would be approximately 300 pg Fe g^{-1}. This estimated maximum Fe concentration is still approximately 50% of the average TD-Fe concentrations found at the other regions. While a seasonal bias cannot be ruled out for the Dumont d'Urville Sea samples, the similarity between the average TD-Fe concentration for this region and the modern Law Dome ice-core (which integrate an entire year) sections suggest there may be some real regional variability in snow

TD-Fe concentrations. Dick (1991) found extremely low levels of Al, a mineral dust tracer, in air from Gipps Ice Rise on the Antarctic Peninsula. The concentrations (44-644 pg Al m^{-3}) were up two orders of magnitude lower than those found at the South Pole, Neumayer station on the coast of Enderby Land, and two Antarctic Peninsular sites, Beethoven Peninsula and Crescent scarp (Cunningham and Zoller, 1981; Dick, 1985; Wagenbach et al., 1988) (see Figure 4.4). Samples from the Beethoven Peninsula and Crescent scarp were later found to contain contributions from local sources of exposed rock. However, the South Pole and Neumayer sites are much further from exposed rock than the Antarctic Peninsular sites, and local contributions are not expected. Dick (1991) postulated that if the transport of mineral dust to the Antarctic occurs in the upper troposphere, as is thought (Shaw, 1979; Heimann et al., 1990; Lambert et al., 1990), then the higher concentrations found at the South Pole may be due to the high altitude. Atmospheric radon studies (Lambert et al., 1990) suggest that mineral aerosols in the lower troposphere are removed by precipitation in the vicinity of the Polar Front and Antarctic Convergence Zone. While Neumayer site is at sea level, the higher concentrations there may be explained by air descending from the polar plateau. Dick argued that the air masses over the Peninsula sites were in contrast affected by low pressure systems from over the Southern Pacific Ocean, and that mineral aerosols may have been removed from this air by earlier precipitation. Prydz Bay and in particular the Ross Sea are regions likely to be affected by outflowing air from the inland Antarctic continent (Parish and Bromwich, 1991; Bromwich et al., 1993a, 1993b and references therein, 1996; Bromwich and Liu, 1996).

Table 4.3 Average Fe content of Antarctic snow

Location	Arithmetic average TD-Fe ($pg\ g^{-1}$)	Reference
Dumont d'Urville Sea	73	This work
Law Dome	62	This work
Ross Sea	749	This work
Prydz Bay	612	This work
Princess Elizabeth Land	646	This work
Weddell Sea	550	Westerlund and Ohman (1991)
Enderby Land	630	Shimamura et al. (1995)
South Pole	714*	Boutron (1982)

* Possibly contaminated

It is possible that the Fe in snow at the Prydz Bay and Ross Sea sites was derived from air masses descending from the polar plateau, hence the relative uniformity in TD-Fe concentrations. In contrast, the meteorological conditions during the sampling period in the Dumont d'Urville Sea were dominated by northerly air masses, and are thus unlikely to be affected by air draining off the continent. Similarly, Law Dome projects into a predominantly easterly maritime airflow (Morgan et al., 1997), which would also be expected to be depleted in mineral dust relative to the air descending from the Antarctic interior. Thus the Fe content of

Antarctic snow is likely highly dependent on regional atmospheric circulation patterns.

4.1.5 Iron concentrations in Wisconsin-Holocene transition and LGM ice-core samples

As discussed in Chapters 2 and 3, samples from the Law Dome BHC1 ice-core dating from around the LGM were decontaminated and analysed for Fe. In an ideal situation, these samples would have come from the DSS ice-core, which was drilled near the dome summit. Unfortunately, the LGM ice from the DSS core was fractured soon after being removed from the drill, and is unsuitable for decontamination. Instead, Wisconsin-Holocene transition and LGM ice sub-samples were selected from the BHC1 core (Section 2.3.5). However as discussed in section 2.3.5 the BHC1 LGM ice composition should be directly comparable to that in the DSS core. Total-dissolvable Fe concentrations from the BHC1 sections are shown in Table 4.4. Significantly higher Fe concentrations were found for the Wisconsin-Holocene transition and LGM age ice relative to the DSS and DE08 Holocene samples were found (Figure 3.21). In particular, the ice dated from approximately 18,000 yrs BP (LGM) was more than two orders of magnitude higher in TD-Fe concentration than the average for the Holocene DSS and DE08 samples (62 pg g^{-1}). A similar decrease in the number of insoluble particles (presumably dust) from LGM to Holocene age samples has been reported for the Law Dome DSS core (Jun et al., 1998).

Table 4.4 Holocene-Wisconsin transition and LGM ice-core sample TD-Fe concentrations

Core ID	No. of samples	Date BP (1997)	Estimated time span (yr)	TD Fe (pg g^{-1})
BHC1 129	5	~ 15000	10	*2900 (1000)
BHC1 132A	1	~18000	~ 10	6700
BHC1 137B	5	~30000	>10	*1100 (300)

* average, standard deviation in brackets

4.2 Estimated atmospheric Fe fluxes to the present-day and glacial Southern Ocean

4.2.1 Holocene atmospheric iron flux estimated from the Law Dome ice-core record

The total-dissolvable Fe concentrations measured in sixteen decontaminated core sections are presented in Table 4.5, together with estimates of the age of each core section, the time interval spanned by the sample, and the estimated atmospheric TD-Fe flux (estimated as the TD-Fe concentration multiplied by the accumulation rate). These Fe fluxes are slightly different to those published in Edwards et al (1998), in which average accumulation rates for DSS and DE08 were used in the calculations. More recently, reliable annual layer-thickness data have become available (T. van Ommen, personal communication, 1999) for these sections (Table 4.1), excluding DSS 940 and DSS 1165, for which the average annual accumulation rate of 640 kg

m^{-2} yr^{-1} is used. From the DSS 28A data, and an annual accumulation rate of 496 kg m^{-2} yr^{-1}, we calculate an average atmospheric Fe flux of 0.040 ± 0.022 mg m^{-2} yr^{-1} for the calendar year 1939 (average of seasonal fluxes). This estimated average flux falls within the range of 0.020-0.070 mg m^{-2} yr^{-1} calculated for the other Holocene ice-core sections, excluding sections DE08 55A, DE08 55B-1 and DE08 55B-2 (calendar year 1929-30), where significantly higher atmospheric Fe fluxes of 0.126-0.430 mg m^{-2} yr^{-1} are calculated. The data for DE08 55A, DE08 55B-1 and DE08 55B-2 are thought to be reliable (e.g., see decontamination profile for DE08 55B-1, Figure 3.15), and thus it is suggested that these ice-core sections record anomalously high dust transport to this site during 1929. Maggi and Petit (1998) report increased dust concentrations dating from 1932 to 1942 (AD) in a firn core from Hercules Neve (Figure 4.4). These authors attribute the increased dust concentrations to a drought in South America during that period. Mosley-Thompson and Thompson (1982) also report a considerable increase in dust deposition to the Ross Ice Shelf over the calendar years 1920-1940, and suggest a possible local source and/or an increase in the atmospheric transport to the region. The average value of the estimated atmospheric Fe fluxes for the Holocene is 0.092 ± 0.1 mg m^{-2} yr^{-1} (n = 15), and 0.046 ± 0.02 mg Fe m^{-2} yr^{-1} (n = 12) if the possibly "anomalous" data from 1929-30 (AD) are excluded. We tentatively use the latter value as an estimate of the Holocene atmospheric Fe flux onto the Law Dome area and surrounding Southern Ocean waters. This flux is within the range (0.025-0.1 mg Fe m^{-2} yr^{-1}) of Fe fluxes estimated from reported Antarctic Holocene dust and trace-metal data (Table 4.6).

Table 4.5 Ice-core section data and estimated atmospheric Fe flux

Core ID	Core depth (m)	Date BP (1997)	Time span	TD-Fe ($pg\ g^{-1}$)	TD-Fe flux ($mg\ m^{-2}\ yr^{-1}$)
DSS 28A-1	46.64-46.82	56	spring summer	139	0.069
DSS 28A-2	46.82-46.98	56	winter	36	0.018
DSS 28A-3	46.98-47.08	56	autumn	64	0.032
DSS 28A-4	47.17-47.54	57	Spring summer	86	0.043
DEO8 55A	96.01-96.29	69	spring summer	250	0.282#
DEO8 55B part (a)	96.41-96.55	70	spring	340	0.430 #
DEO8 55B part(b)	96.55-96.69	70	winter spring	100	0.126#
DSS 41B	72.95-73.20	88	winter	34	0.020
DEO8 77A part (a)	136.02-136.16	102	winter autumn	64	0.070
DE08 77A part (b)	136.16-136.30	102	autumn	62	0.066
DEO8 85-A	150.90-151.42	115	winter	29	0.031
DEO8 108A	192.80-193.08	155	summer	77	0.069
DSS 940	895.74-895.99	§ 2729	~ 2 years	36	0.023
DSS 1165-1	1106.76-1106.94	§ 8518	~ 16 years	110	0.070
DSS 1165-2	1106.94-1107.04	§ 8530	~ 10 years	70	0.045

Fe fluxes were calculated using an accumulation rate of 640 kg m^{-2} yr^{-1} for DSS 940 and DSS 1165. (§) - age estimated from an ice flow model (V. Morgan, personal communication, 1998). (#) - data not included in Holocene average.

4.2.2 Atmospheric Fe fluxes from present-day snow samples

Atmospheric TD-Fe fluxes for the snow sampling sites were calculated from average TD-Fe concentrations (for each site) and estimated net snow accumulation rates (Table 4.7). Net accumulation rates for the Princess Elizabeth Land sites were estimated from snow accumulation stake measurements (Higham et al., 1997). These stakes were placed at the sites during 1993 and the snow depth of the stakes measured in 1994. The net annual snow accumulation rates for the marine sites have not been measured. Instead, the long term average (11 yr) net annual accumulation rates of Cullather et al. (1998) are used. These estimates were derived from the atmospheric moisture budget (precipitation minus evaporation/sublimation) of the European Centre for Medium-Range Weather Forecasts (ECMWF) analyses. The highest estimated atmospheric Fe flux was estimated for Prydz Bay, followed by the Ross Sea. The atmospheric Fe flux to the Dumont d'Urville Sea was low, and comparable to the southern most sites in Princess Elizabeth Land. Total-dissolvable Fe fluxes for sites from Prydz Bay to the southernmost Princess Elizabeth Land site are shown in Figure 4.5. The estimated Fe fluxes appeared to be relatively constant from the Prydz Bay sites (average flux = 0.09 mg Fe m^{-2} yr^{-1}) to the Princess Elizabeth Land site LGB 59, but then decreased by approximately a factor of 3 from LGB 59 to LGB 46.

Table 4.6 Antarctic ice dust fluxes estimated from ice-cores

Site	Dust conc. ($ng\ g^{-1}$)	Dust conc. reference	Method	Ice accum. Rate ($m\ H_2O$ equiv. yr^{-1})	Ice accum. rate reference	Dust flux ($mg\ m^{-2}\ yr^{-1}$)	Fe flux ($mg\ m^{-2}yr^{-1}$)
Byrd (80°S, 120°W)	19	Cragin et al., 1977	Al	0.16	Lorius, 1989	0.003	0.1
Dome C (75°S, 120° W)	34	Petit et al., 1981	Al	0.034	Lorius, 1989	0.001	0.035
	26	Royer et al., 1983	Dust vol.			0.0009	0.03
Vostok	30	de Angelis et al., 1984.	Al	0.023	Lorius, 1989	0.0007	0.025
South Pole (90°S)	20	Estimated from average Fe concentration, Boutron, 1982	Fe	0.080			0.06

Notes:

Al concentration measured, dust concentration calculated from Al assuming 8% of the dust mass is Al. Dust volume measured by laser light scattering and the dust concentration calculated assuming a dust density of $2g\ cm^{-3}$. Fe flux calculated by assuming 3.5% of dust mass is Fe.

Table 4.7 Estimated present-day atmospheric Fe fluxes

Site location	Net annual accum. rate ($kg\ m^{-2}\ yr^{-1}$)	Average TD-Fe ($pg\ g^{-1}$)	Estimated Fe flux ($mg\ m^{-2}\ yr^{-1}$)
Prydz Bay	*150	612	0.09
Princess Elizabeth Land:			
LGB 70	163	643	0.10
LGB 59	65	1461	0.09
LGB 53	78	928	0.07
LGB 46	50	537	0.03
Dumont d'Urville Sea	*400	73	0.03
Ross Sea	*100	749	0.07

* Estimated net annual snow accumulation from Cullather et al., 1998.

With the exception of LGB 59 which was found to have a relatively low accumulation rate (65 kg m^{-2} yr^{-1}), but high average TD-Fe concentration (1461 pg g^{-1}), the accumulation rate appeared to be the dominant factor determining the atmospheric Fe flux to the sites (i.e. average TD Fe concentrations were comparable for these sites). While the estimated fluxes are sensitive to the accuracy of the net snow accumulation rates, the estimated Fe flux to the most inland site (LGB 46) is comparable to the estimated Fe fluxes for the inland Vostok and Dome C ice-core sites of 0.025 and 0.035 mg Fe m^{-2} yr^{-1}, respectively.

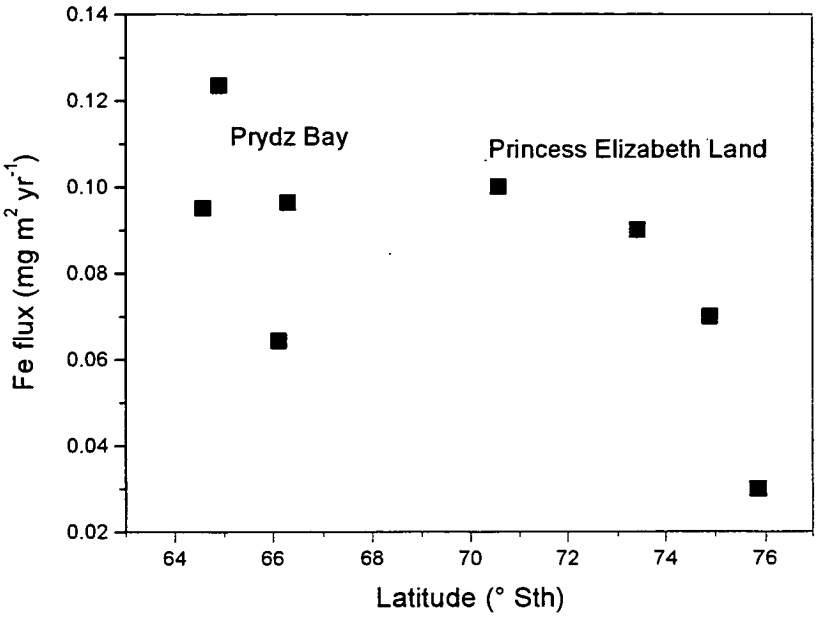

Figure 4.5 Estimated atmospheric Fe fluxes for Prydz Bay and Princess Elizabeth land vs latitude

Holocene atmospheric Fe fluxes estimated from the literature and from the ice-core and snow data shown in this thesis are depicted in Figure 4.6. It should be noted that the Prydz Bay, Dumont d'Urville Sea and Ross Sea snow accumulation rates were derived from a computer model, with large uncertainties, and are probably uncertain to an order of magnitude, so the Prydz Bay, Dumont d'Urville Sea and Ross Sea flux estimates are probably uncertain to an order of magnitude.

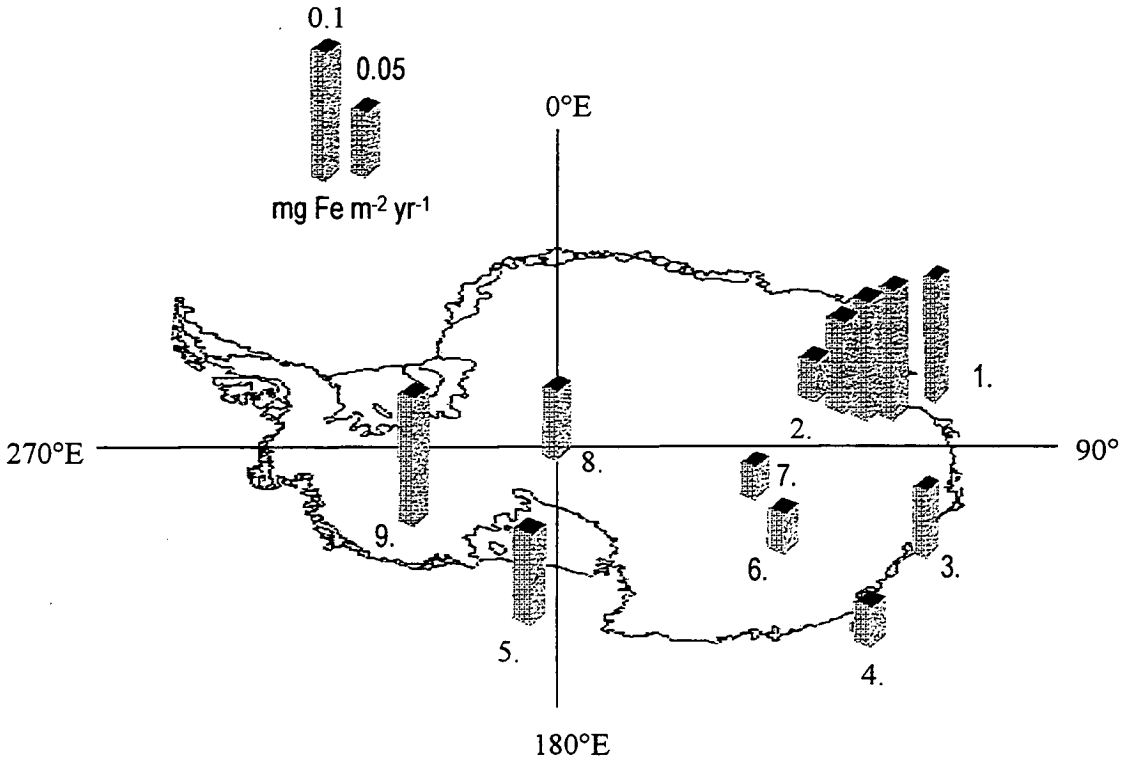

1. Prydz Bay, snow samples
2. Princess Elizabeth Land, snow samples
3. Law Dome, ice-core samples
4. Dumont d'Urville Sea, snow samples
5. Ross Sea, snow samples
6. Dome C, ice-core samples
7. Vostok, ice-core samples
8. South Pole, snow samples
9. Byrd, ice-core samples

Figure 4.6 Estimated atmospheric Fe fluxes to Antarctica

With the exception of the Law Dome and Dumont d'Urville locations, the estimated inland fluxes are much lower than that of the coastal and marine sites, presumably due to lower accumulation rates. This raises the questions as to whether inland ice-cores, such as Dome C and Vostok, are representative of atmospheric dust fluxes and hence Fe fluxes to the Southern Ocean. More data is required from both marine and continental locations to determine the relationship between the atmospheric Fe fluxes to these areas. Using both the estimated snow and Holocene ice-core TD-Fe data (not including fluxes estimated from the literature), an average Holocene atmospheric flux for East Antarctica and the adjacent Southern Ocean is estimated to be 0.06 mg Fe m^{-2} yr^{-1}. This estimated flux maybe considered a lower limit given that:

(1) The fluxes to the Antarctic continent may be lower than those over the ocean;

(2) the Dumont d'Urville sea sites may be seasonally biased and;

(3) the Law Dome ice core data excluded several high values which were thought to be anomalous.

However, if the Dumont d'Urville Sea and continental Princess Elizabeth Land data are excluded (leaving the Prydz Bay, Ross Sea and Law Dome data) the average flux is little different, estimated is to be 0.07 mg Fe m^{-2} yr^{-1}. This flux agrees well with the Fe flux of 0.1 mg m^{-2} yr^{-1} for the Southern Ocean estimated by Donaghay et al.

(1991), which was derived from the dust flux calculations of Duce et al. (1991) (See Chapter 1.0).

4.2.3 Atmospheric Fe flux to Law Dome during the LGM

While the TD-Fe concentration for Law Dome LGM ice was found to be approximately 100 times that of the Holocene, a significantly lower LGM snow accumulation rate of between 128 and 320 kg m^{-2} yr^{-1} has been estimated from $\delta^{18}O$ stratigraphy and ice-flow models (T. van Ommen, personal communication, 1999), assuming that the BHC1 LGM section originated near the DSS site. Using these estimated snow accumulation rates, a LGM atmospheric Fe flux of between 0.860 and 2.15 mg m^{-2} yr^{-1}, is estimated, which is roughly 16-41 times the estimated average Holocene flux for the Law Dome site, or 12-30 times the estimated present-day average calculated from the combined snow and late-Holocene ice data. This increase in the atmospheric Fe flux during the LGM can be compared with dust flux estimates derived from measurements of Al in ice-cores from Vostok and Dome C (Delmas, 1992), which imply LGM dust fluxes 14-18 times greater than Holocene value. This work thus suggests an LGM Fe flux comparable to or greater than these previous estimates.

4.3 Estimates of planktonic new production supported by atmospheric Fe deposition to the present day and glacial Southern Ocean

4.3.1 Solubility of Fe in East Antarctic snow and ice

Only the readily water-soluble fraction of Fe deposited to the ocean appears to be bioavailable to phytoplankton (Wells et al., 1983; Rich and Morel, 1990; Morel et al., 1991). The soluble fraction of Fe in mineral aerosols has been assumed to be approximately 10% (Duce et al., 1991; Donaghay et al., 1991), but with the exception of the data shown in this thesis, there have been no solubility measurements of Fe in Antarctic snow or precipitation onto the Southern Ocean.

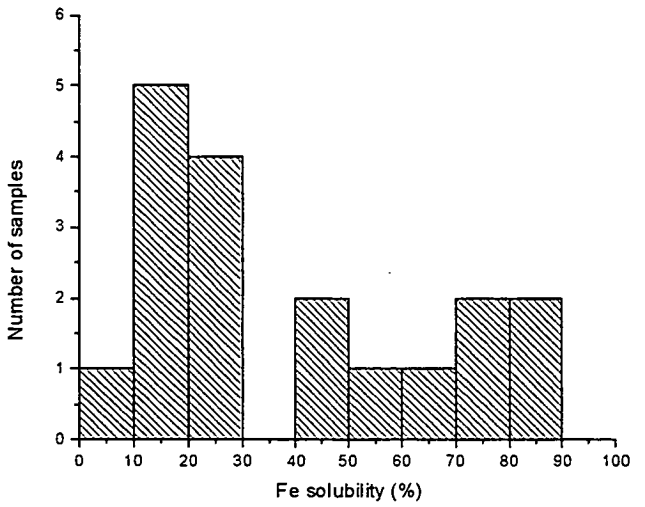

Figure 4.7 Frequency histogram of Fe solubility

Selected samples were filtered through a 0.2 μm pore-size PTFE membrane filter immediately after melting in order to estimate the percentage "Fe solubility", from the ratio of total-filterable Fe to total-dissolvable Fe (Section 2.4.2). This operationally-defined soluble Fe fraction ranged from 10 to 90%, almost the entire spectrum, with half of the solubility's between 10 and 30%. A frequency histogram of the Fe solubility is shown in Figure 4.7. The frequency distribution is positively skewed (skew = 0.35) and in this case the geometric mean (30%, section 3.7) provides a better indication of the central tendency of the data set than the arithmetic mean (40%). While a larger data set is required to adequately describe the solubility distribution of Fe in Antarctic snow, this initial data set suggests that the Fe solubility is typically between 10-30%. The mean solubility determined in this study falls within the range of recent estimates (6-50%, Zhu et al., 1997; Zhang et al., 1990) for atmospheric waters over the remote ocean. The large range of solubility's found in this study have also been found for Fe in Greenland ice core samples (Laj et al., 1997). Using a combination of particle induced X ray emission and scanning electron microscope/ X ray dispersive analysis, Laj et al., (1997) estimated the solubility of Fe to range between 10 and 60% with an arithmetic mean of 40 ± 20%. The Fe solubility data determined by Laj et al. also appears to be positively skewed and the arithmetic average probably over estimates the mean solubility (which appears to lie between 20 and 30%).

4.3.2 Estimates of new production in the present-day Southern Ocean supported by atmospheric Fe deposition

The basic requirements for primary production in the sea are light and nutrients. Iron is essential for algal growth and may be considered as a nutrient (Raven, 1988, 1990). When light of the correct wavelengths and intensity is available, the ensuing production from the introduction of nutrients into the photic zone is considered new production (Dugdale and Wilkerson, 1992 and references therein). In contrast to new production (NP), regenerated production is based upon nutrients recycled in the photic zone. An estimate of the potential NP in the Southern Ocean (expressed as carbon) ensuing from the soluble component of the atmospheric Fe flux can be calculated using algal carbon (C) to Fe molar assimilation ratios (Table 4.8). The C:Fe assimilation ratios reported in the literature range from 33,000: 1 to 500,000:1, and appear to vary with both species and environment (Sunda et al., 1995). Assuming (1) similar atmospheric Fe fluxes exist over the Southern Ocean (south of 50°S) as those estimated here, (2) limitation of algal production in this region by Fe deficiency (i.e., nutrient and light replete conditions), and (3) 30% of the Fe is bioavailable, an estimate of potential NP can be made from the reported C:Fe ratios and the estimated present-day atmospheric Fe flux (0.07 mg Fe m^{-2} yr^{-1}) using equations 4 and 5.

Table 4.8 Literature plankton cellular C:Fe ratios

C:Fe	Species/habitat	Reference
33,000:1	T. weissflogii	Martin et al. (1989)
*93,200:1	E. huxleyi, T. oceanica, P. calceolata, T. pseudonana, T. weissflogii, P. minimum. Same species in both coastal and oceanic conditions	Sunda et al. (1995)
100,000:1	T. weissflogii	Anderson and Morel (1982)
500,000:1	T. pseudonana and T. Oceanica	Sunda et al. (1991)

* average of 74 values

$$\text{Soluble Fe deposited} = \frac{\text{Fe flux (g m}^{-2}\text{ yr}^{-1})}{\text{Molecular weight}} \times \text{Solubility factor} \qquad (4)$$

$$= \frac{7 \times 10^{-5}\text{ (g m}^{-2}\text{ yr}^{-1})}{55.85\text{ (g mol}^{-1})} \times 0.3 \quad = 3.8 \times 10^{-7}\text{ mol Fe m}^{-2}\text{ yr}^{-1}$$

Assuming algal C:Fe = 500,000:1, then

$$\text{Maximum NP} = 3.8 \times 10^{-7}\text{ (mol Fe m}^{-2}\text{ yr}^{-1}) \times 500{,}000 \qquad (5)$$

$$= 0.19\text{ mol C m}^{-2}\text{ yr}^{-1}$$

For the maximum reported C:Fe assimilation ratio, the potential NP ensuing from the soluble fraction of the estimated atmospheric Fe flux is estimated to be 0.19 mol C m^{-2} yr^{-1}. While this estimate does not take into account that the phytoplankton

growing season is approximately 6 months long (Comiso et al., 1993), it is still less than 2% of the average Southern Ocean primary production (PP) of approximately 10 mol C m^{-2} yr^{-1} estimated by Arrigo et al. (1998). Arrigo et al. (1998) used a bio-optical algorithm to estimate Southern Ocean primary production from algal pigment fields determined using the Nimbus-7 coastal zone color scanner (CZCS). The algorithm was validated by comparison with the ^{14}C based productivity dataset of Behrenfeld and Falkowski (1997). Primary productivity predicted by the algorithm ranged from 2 -120 mol C m^{-2} yr^{-1}. The low end of this range is comparable with the minimum rate determined by Rubin et al. (1998) for the Pacific Sector of the Southern Ocean (2 mol C m^{-2} yr^{-1}). Even for this minimum rate the estimated atmospheric Fe flux could only support 9% of the productivity. Phytoplankton assimilation ratios of C and N in Antarctic waters have been found to be Redfieldian (Redfield, 1958) i.e., C:N =6.6 (Rubin et al., 1998, Hoppema et al., 1999). Given the potential NP of 0.19 mol C m^{-2} yr^{-1} supported by the atmospheric Fe flux, phytoplankton could consume 0.03 mol N m^{-2} yr^{-1} of nitrate (0.19 mol C m^{-2} yr^{-1} / 6.6). This is approximately 4% of the estimated upwelling flux of nitrate (0.8 mol N m^{-2} yr^{-1}) in the Southern Ocean (Francois et al., 1997). In addition to nitrate, dissolved Fe will also be brought to the ocean surface by upwelling. Martin et al.(1990) estimated the Fe flux to the Southern Ocean from upwelling to be approximately 91 μmol Fe m^{-2} yr^{-1} assuming an Fe concentration of 0.1 μmol Fe m^{-3} and an average upwelling velocity of 91 m yr^{-1} for the Southern Ocean. But this upwelling velocity appears to be much higher than recent estimates (20-45 m yr^{-1}) (Francois et al., 1997; Grotov et al., 1998; Hoppema et al., 1999). Recalculating the

upwelling Fe flux using an upwelling velocity of 30 m yr^{-1} (Francois et al., 1997) and the upwelling seawater Fe concentration (0.1 μmol Fe m^{-3}) of Martin et al. (1990) gives an average upwelling Fe flux to the Southern Ocean of 3 μmol Fe m^{-2} yr^{-1}. Assuming that 100% of this Fe is soluble, then following the same reasoning as equations 3 and 4 the potential NP from this flux is estimated to be 1.5 mol C m^{-2} yr^{-1}(C:Fe of 500,000:1) which could consume approximately 27% of the estimated nitrate flux. The total potential NP ensuing from both the atmospheric flux and upwelling flux of Fe is estimated at 1.7 mol C m^{-2} yr^{-1} approximately 30% of the nitrate flux. In comparison, if the PP of 10 mol C m^{-2} yr^{-1} estimated by Arrigo et al. (1998) were NP, > 100% of the estimated nitrate flux would be consumed suggesting that a large percentage of PP is recycled production. Similar calculations for a range of C:Fe ratios are shown in Table 4.9. If this estimate is multiplied over the surface area of the Southern Ocean south of 50°S (3.81×10^{13} m^2, Smith, 1991) the maximum total new production comes to 777 Tg C yr^{-1}. This estimate is approximately 18 % of the annual primary production rate of 4414 Tg C yr^{-1} for the Southern Ocean (south of 50°S) estimated by Arrigo et al. (1998). These estimates are consistent with hypothesis 1 and suggest that the present-day atmospheric Fe flux into the Southern Ocean is far insufficient to support the full use of the upwelled nitrate by phytoplankton, and also that the majority of algal NP in this region is supported by Fe supplied from other sources, such as upwelling, and that much of the PP is recycled production.

Table 4.9 Potential new production in the present-day Southern Ocean supported by Fe

C:Fe	Atmospheric Fe NP (mol C m^{-2} yr^{-1})	Upwelling Fe NP (mol C m^{-2} yr^{-1})	Total Fe NP (mol C m^{-2} yr^{-1})	Southern Ocean, NP (Tg C yr^{-1})	Percentage of potential NP (%)
33,000:1	0.013	0.10	0.11	50	2
*93,200:1	0.036	0.28	0.32	142	5
100,000:1	0.038	0.30	0.34	155	6
500,000:1	0.19	1.50	1.7	777	30

* = average C:Fe ratio

Note - this ignores sediment inputs, which may be important, e.g.; polar front region in South Atlantic (de Baar et al., 1995)

4.3.3 Release of Fe from Antarctic seasonal sea ice

Surface-water Fe concentrations in the ice-free pelagic Southern Ocean surrounding Antarctica have been found to be of the order of 0.1-0.2 nmol (Martin et al., 1990; Sedwick and Ditullio, 1992), away from sources such as shelf sediments (eg; deBaar et al., 1995). Hence, sea ice formed from these waters is not expected to contain significant amounts of Fe. However, during the seasonal growth of the sea ice, atmospheric Fe will be deposited in snow on the ice instead of into the ocean surface waters. Thus the growth and melting of the ice will temporally refocus the atmospheric input of Fe into the ocean releasing it over a relatively short period of time when the ice melts. Martin (1990) calculated the amount of Fe released by Antarctic sea ice during its meltback to be 3.9 Gg Fe, but this calculation assumed the entire volume of sea ice to have an Fe concentration of 30 nM. While some of the snow that falls on the sea ice becomes incorporated into the sea ice (Massom et al., 1998; Worby et al., 1998), it is unlikely that the entire sea ice Fe content would be this high if the Fe is only derived from atmospheric deposition. However an exception may be where the ice originates in coastal polynyas where the upwelled seawater may be quite rich in TD-Fe (Sedwick et al., in press). The amount of atmospheric Fe released from the sea ice can be calculated from the maximum surface area of the seasonal sea ice zone (SSIZ), its growth time, and the estimated atmospheric flux of Fe to the SSIZ of the ocean.

This ignores Fe trapped in the sea ice itself, and so is probably a very conservative estimate. For a maximum SSIZ surface area of 15 x 10^{12} m^2 (Parkinson, 1992) and atmospheric Fe flux of 0.07 mg Fe m^{-2} yr^{-1}, the amount of Fe released from the ice melting comes to approximately 1.1 Gg Fe, 27 % of that calculated by Martin (1990). However, this estimate ignores the fact that the sea-ice growth period is approximately 6 months (Parkinson, 1992) and assumes that all atmospheric Fe flux is retained on the ice. In reality the Antarctic seasonal sea ice zone contains a significant amount of open water, even at maximum sea ice extent. At maximum, the potential NP per unit area supported by the atmospheric Fe content of the ice will be same as that calculated in the previous section (4.2.5). Assuming the maximum phytoplankton C:Fe ratio of 500,000:1, the potential maximum NP = 0.19 mol C m^{-2} yr^{-1}, or 34 Tg C for the entire Antarctic SSIZ. This is an insignificant amount of production in comparison to the estimated total annual Southern Ocean primary production of 4414 Tg (Arrigo et al., 1998). Estimated increases in the surface seawater dissolved Fe concentration from the sea ice melting are shown in Table 4.10, for various mixing depths. If the Fe released from the melting sea ice is concentrated in a thin lense of melt-water, 10 cm deep, the Fe concentration will

Table 4.10 Increase in seawater Fe concentration from melting sea ice

Mixing depth of added Fe (m)	Increase in Seawater dissolved Fe concentration (nM)
0.1	4
1.0	0.4
30.0	0.01

increase by approximately 4 nM. Additions of 4 nM Fe to seawater have been shown to alleviate phytoplankton Fe limitation in both bottle-incubation and open ocean Fe-fertilization experiments (de Baar et al., 1990; Martin et al., 1991; Chavez et al., 1991; Coale et al., 1996) and the half-saturation constant for community Fe uptake has been estimated at ~ 0.1 nM in the equatorial Pacific (Coale et al., 1996). Phytoplankton blooms in the Southern Ocean have been observed following the receding sea ice during its seasonal melting (Smith and Nelson, 1985; Comiso et al., 1993; Moore et al., 1999). If the meltwater from the sea ice forms a shallow lens, then these calculations suggest that the Fe released from melting sea ice may alleviate algal Fe deficiency, enough to allow bloom development. But if the meltwater is mixed to depths greater than about 1 m, the increase in the Fe concentration will be small and possibly insignificant. Sedwick and Ditullio (1997) report surface-water dissolved Fe concentrations of 2.4 nM associated with receding sea ice in the Ross Sea. Their site was revisited 17 days later when it was ice-free. On the second visit, dissolved Fe concentrations had been reduced to 0.16-0.17 nM. While the sea ice was present, the mixed layer was approximately 25 m thick. Assuming that the sea ice was the source of the Fe, then to increase the mixed layer Fe by 2.3 nM, the sea ice would have to have contained 3.2 mg Fe m^{-2}. This is approximately 46 times the estimated annual atmospheric Fe flux for the Ross Sea. This implies that if the melting sea ice was responsible for the high initial Fe concentrations, it probably contained Fe from a source other than atmospheric dust. Several possibilities exist. The sea ice may have formed in Fe rich coastal seawater (e.g.: the south Ross Sea Polyna) and then circulated in the Ross Sea Gyre. In

addition, the snow might have contained dust from local sources (e.g., Mc Murdo Sound or the Victoria Land dry valleys). While the release of Fe from melting sea ice appears to be insignificant in terms of annual primary productivity in the Southern Ocean, relatively high Fe concentrations in the snow may be important to plankton communities living in the sea ice and to short-lived blooms of pelagic algae at the receding ice edge where high rates of production may be supported over periods of several days. Thus the data presented in this thesis do not support the second hypothesis, when considered on an annual basis, although the hypothesis is supported on a short-term (several-day) timescale.

4.3.4 Estimates of potential new production in Southern Ocean waters supported by atmospheric Fe deposition during the LGM

At present, the polar nutrient hypothesis and its variations (Sarmiento and Toggweiler, 1984; Knox and Mc Elroy, 1984; Siegenthaler and Wenk, 1984) appear best able to explain decreases in atmospheric CO_2 during Quaternary glaciations. These hypotheses contend that some factor present in the glacial ocean allowed phytoplankton to utilise presently unused nutrients, exporting large amounts of C to the deep ocean. In particular, the high nutrient, well ventilated, Southern Ocean has the greatest potential to affect atmospheric CO_2 levels (Sarimento and Orr, 1991). Martin (1990) hypothesised that Fe was the factor missing from the present-day Southern Ocean, but was present in larger amounts in the glacial ocean causing a major biological drawdown of atmospheric CO_2. Estimates of NP for the Southern

Ocean (Table 4.11) during the LGM were estimated from equations 4 and 5 assuming (1) a solubility of 30%, for atmospheric Fe(2) the Holocene estimate of upwelling N and Fe given in section 4.3.2, (3) an LGM atmospheric Fe flux of 0.816-2.15 mg m^{-2} yr^{-1} (see section 4.2.3), and (4) that this atmospheric Fe flux applies over the entire Southern Ocean (south of 50°S). The potential NP supported by the LGM atmospheric Fe fluxes estimated from the Law Dome data range between 0.16 and 5.92 mol C m^{-2} yr^{-1}. If the Fe input from upwelling is assumed to be the same as that estimated for the present-day (section 4.3.2), then the total NP could consume between 4-130% of the present-day Southern Ocean upwelling nitrate, as estimated by Francois et al. (1997). If this total NP is extrapolated over the Southern Ocean South of 50° S, the total NP comes to between 119-3392 Tg C yr^{-1}, approximately 69–2615 Tg C yr^{-1} greater than our estimate for the present day Southern Ocean. These estimates suggest that a large increase in NP of the glacial Southern Ocean could have resulted from an increase in the atmospheric Fe flux, consistent with hypothesis 3, based on our estimate of the Fe flux from the Law Dome cores. In addition, these estimates suggest that the atmospheric deposition of Fe was the dominant source of Fe, in glacial Southern Ocean waters assuming no increase in the velocity of upwelling over the region during the LGM.

Table 4.11 Potential new production in the glacial Southern Ocean supported by atmospheric and upwelled Fe inputs

LGM Atmospheric Fe flux ($mg\ m^{-2}\ yr^{-1}$)	C: Fe	Atmospheric Fe NP ($mol\ C\ m^{-2}\ yr^{-1}$)	Upwelling Fe NP ($mol\ C\ m^{-2}\ yr^{-1}$)	Total Fe NP ($mol\ C\ m^{-2}\ yr^{-1}$)	Southern Ocean, NP ($Tg\ C\ yr^{-1}$)	Percentage of potential NP (supported by N) (%)
0.86	33,000	0.16	0.10	0.26	119	4
2.15	33,000	0.39	0.10	0.49	224	9
0.86	93,000	0.44	0.28	0.72	329	12
2.15	93,000	1.10	0.28	1.38	631	24
0.86	100,000	0.47	0.30	0.77	352	13
2.15	100,000	1.18	0.30	1.48	677	26
0.86	500,000	2.37	1.50	3.87	1769	68
2.15	500,000	5.92	1.50	7.42	3392	131

Chapter 5

Conclusions

The concentration and apparent solubility of Fe in present-day and ancient East Antarctic snow has been determined to investigate whether the atmosphere is a significant source of soluble Fe to the surface waters of the Southern Ocean, or has been so during the past glacial period. This investigation focused on three testable hypotheses regarding the possible limitation of new phytoplankton production by iron deficiency in the present-day and LGM Southern Ocean, namely:

(1) The present-day atmospheric Fe flux to the Southern Ocean is insufficient to allow the complete use of upwelled nitrate by phytoplankton, assuming light-replete conditions.

(2) Antarctic sea ice may release a significant amount of Fe into the ocean during its melting; and

(3) The atmospheric Fe flux to the Southern Ocean during the LGM was high enough to sustain a large increase in new phytoplankton production relative to the present.

In this chapter, these hypotheses are tested using the data presented and discussed in chapters 3 and 4.

5.1 Hypothesis 1 - *The present-day atmospheric Fe flux to the Southern Ocean is insufficient to allow the complete use of upwelled nitrate by phytoplankton, assuming light-replete conditions*

The present-day atmospheric flux of TD-Fe onto East Antarctica and the surrounding oceanic region is estimated to be 0.07 mg Fe m^{-2} yr^{-1}, with an average of 30% of this Fe being readily soluble in meltwater. The maximum potential phytoplankton NP supported by the atmospheric deposition of Fe is estimated as 0.013-0.19 mol C m^{-2} yr^{-1} (Chapter 4), while the maximum potential phytoplankton NP supported by upwelling Fe was estimated as 0.1-1.5 mol C m^{-2} yr^{-1} and the total NP supported by both Fe sources 0.11-1.7 mol C m^{-2} yr^{-1}. In comparison Arrigo et al. (1998) estimated the average Southern Ocean PP to be 10 mol C m^{-2} yr^{-1}. These results indicate that for the present day, the atmosphere is a minor source of Fe to the Southern Ocean compared to that supplied from other sources such as upwelling and resuspended sediments. If the estimated potential NP supported by atmospheric and upwelling Fe fluxes are combined over the surface area of the entire Southern Ocean south of 50°S, the total potential NP for this region is estimated to be 69-777 Tg C yr^{-1}, which is up to 18% of the total primary production estimated for the Southern Ocean (Arrigo et al., 1998). This amount of NP could consume, at most, 30% of the surface water nitrate, assuming an upwelling rate for nitrate of 12g N m^{-2} yr^{-1}

(Francois et al., 1998) and a Redfield C:N assimilation ratio for Southern Ocean phytoplankton. Thus, on the basis of these estimates, the data presented in this thesis clearly support the hypothesis that the atmospheric Fe flux into the present-day Southern Ocean is insufficient to allow phytoplankton to utilise all available surface water nitrate.

5.2 Hypothesis 2 - ***Antarctic sea ice may release a significant amount of Fe into the ocean during its melting***

A maximum estimate of the Fe released from sea ice during the seasonal meltback would be the same as the estimated average atmospheric flux; i.e., 0.07 mg Fe m^{-2} yr^{-1}, and the resulting maximum phytoplankton NP is estimated to be 0.013-0.19 mol C m^{-2} yr^{-1}. Assuming the atmosphere to be the main source of Fe to the sea ice, other than the seawater itself, the data presented here indicate that Antarctic sea ice is not a significant source of Fe to Southern Ocean surface waters, on an annual basis. However, if wind mixing is minimal and the meltwater remains in a shallow surface layer (i.e., ~1 m) for a considerable amount of time (~1 day or more), the released Fe could conceivably increase the concentration of the surface water to approximately 4 nM, sufficient to allow phytoplankton to bloom. Such events may be an important component of the Southern Ocean biological pump because they may account for a disproportionately large export flux for a given rate of primary production (Buessler, 1998). Thus the data presented in this thesis do not support the second hypothesis, when considered on an annual basis, although the hypothesis is supported on a short

term (several-day) timescale. This conclusion only considers the atmosphere-derived Fe associated with sea ice, however, it should be noted that a significant amount of sea ice may be formed from Fe-rich seawater in coastal polynas, where vertical mixing supplies Fe-rich bottom waters into surface waters (Sedwick et al., 1999 (in press)). Therefore, further studies of the Fe input from sea ice should focus on the Fe content of the sea ice itself: as well as Fe contained in snow cover, and also the potential for polynas to introduce Fe into pelagic surface waters via production and advection of sea ice away from coastal regions.

5.3 Hypothesis 3 - *The atmospheric Fe flux to the Southern Ocean during the LGM was high enough to sustain a large increase in new phytoplankton production relative to the present*

In this study the atmospheric flux of Fe to the coastal Law Dome region was found to have been higher than during the late Holocene by a factor of 16-41 (using a minimum and maximum estimate of the LGM snow accumulation rate). The potential maximum NP production resulting from the LGM atmospheric flux is estimated to 0.2-5.9 mol C m^{-2} yr^{-1}. If the NP supported by upwelling Fe is assumed to be the same as for the present-day Southern Ocean, then the total NP is estimated to be 0.3-7.4 mol C m^{-2} yr^{-1}, which could consume 4-131% of the present-day surface water nitrate. If this potential increase in NP (total) is integrated over the entire Southern Ocean south of 50°S, the potential annual NP amounts to 119-3392 Tg C, an approximate 69-2615 Tg C increase in new production compared to the present-

day Southern Ocean estimate based on both atmospheric and upwelling Fe inputs. Thus the data in this thesis clearly support the hypothesis that the atmospheric flux to the Southern Ocean was significantly higher during the LGM, from which it can be inferred that a significantly higher level of algal new production was supported compared with that estimated for the present-day.

Bibliography

Anderson, G.C., and F.M.M. Morel, The influence of aqueous iron chemistry on the uptake of iron by the coastal diatom Thalassiosira weissflogii, *Limnology and Oceanography*, *27*, 789-813, 1982.

Anderson, R.F., N. Kumar, R.A. Mortlock, P.N. Froelich, P. Kubik, B. Dittrich-Hannen, and M. Suter, Late-Quaternary changes in productivity of the Southern Ocean, *Journal of Marine Systems*, *17*, 497-514, 1998.

Anderson, K.K., and P.D. Ditlevsen, Glacial/interglacial variations of meridonal transport and washout of dust: A one-dimensional model, *Journal of Geophysical Research*, *103* (D8), 8955-8962, 1998.

Andreae, M.O., Climatic effects of changing atmospheric levels, in *World Survey of Climatology*, edited by A. Henderson-Sellers, Elsevier, Amsterdam, 1995.

de Angelis, M., M. Legrand, J.R. Petit, N.I. Barkov, Y.S. Kurotkevitch, and V.M. Kotlyakov, Soluble and insoluble impurities along the 950 m. deep Vostok ice core (Antarctica) climatic implications, *Journal of Atmospheric Chemistry*, *1*, 215-239, 1984.

de Angelis, M., N.I. Barkov, and V.N. Petrov, Aerosol concentrations over the last climatic cycle (160 KYR) from an Antarctic ice core, *Nature*, *325*, 318-321, 1987.

Arrigo, K.R., D. Worthen, A. Schnell, and M.P. Lizotte, Primary production in Southern Ocean waters, *Journal of Geophysical Research*, *103* (C8), 15587-15600, 1998.

de Baar, H.J.W., A.G.J. Buma, R.F. Nolting, C.C. Gerhard, G. Jacques, and P.J. Treguer, On iron limitation of the Southern Ocean: experimental observations in the Weddell and Scotia Seas, *Marine Ecology Progress Series*, *65*, 105-122, 1990.

de Baar, H.J.W., J.T.M. de Jong, D.C.E. Bakker, B.M. Löscher, C. Veth, U. Bathmann, and V. Smetacek, Importance of iron for plankton blooms and carbon dioxide drawdown in the Southern Ocean, *Nature*, *373*, 412-415, 1995.

de Baar, H.J.W., J.T.M. de Jong, R.F. Nolting, K.R. Timmermans, M.A. van Leeuwe, U. Bathmann, M. Rutgers van der Loeff, and J. Sildam, Low dissolved Fe and the absence of diatom blooms in remote Pacific waters of the Southern Ocean, *Marine Chemistry*, *57*, 137-161, 1999.

Barbante, C., T. Bellomi, G. Mezzadri, P. Cescon, G. Scarponi, C. Morel, S. Jay, K. Van de Velde, C. Ferrai, and C.F. Boutron, Direct determination of heavy metals at picogram per gram levels in Greenland and Antarctic snow by double focussing inductively coupled plasma mass spectrometry, *Journal of Analytical Atomic Spectrometry*, *12*, 925-931, 1997.

Barnola, J.M., D. Raynaud, Y.S. Korokevich, and C. Lorius, Vostok ice core provides a 160,000-year record of atmospheric CO_2, *Nature*, *39* (6138), 408-414, 1987.

Basile, I., F.E. Grousset, and N.I. Barkov, Patagonian origin of glacial dust deposited in East Antarctica (Vostok and Dome C) during glacial stages 2, 4 and 6, *Earth and Planetary Science Letters*, *146* (3/4), 573-589, 1997.

Behrenfeld, M.J., and P.G. Falkowski, Photosynthetic rates derived from satellite-based chlorophyll concentration, *Limnology and Oceanography*, 42(1), 1-20, 1997.

Berner, W., B. Stauffer, and. H. Oeschger, Information on the CO_2 cycle from ice core studies, *Radiocarbon*, *22* (2), 227-235, 1980.

Bolshov, M.A., C.F. Boutron, F.M. Ducroz, U. Gorlach, O.N. Kompanetz, S.N. Rudniev, and B. Hutch, Direct ultratrace determination of cadmium in Antarctic and Greenland snow and ice by laser atomic flourescence spectrometry, *Analytica Chimica Acta, 251*, 169-175, 1991.

Boutron, C., M. Echevin, and C. Lorius, Chemistry of polar snows: estimation of rates of deposition in Antarctica, *Geochimica et Cosmochimica Acta, 36*, 1029-1041, 1972.

Boutron, C., and C. Lorius, Trace elements content in East Antarctica snow sample, in *Symposium on Isotopes and Impurities in Snow and Ice, UGGI*, 1975.

Boutron, C., S. Martin, and C. Lorius, Composition of aerosols deposited in snow at the South Pole: time dependency and sources, in *Proceedings of the 9th International conference on Atmospheric Aerosols, Condensation and Ice Nuclei*, Pergamon press, Galway, Ireland, 1977.

Boutron, C., Influence des aerosols naturels et anthropogeniques sur la geochimie des neiges polaires, pp. 130-193, Universite Scientifique et Medicale de Grenoble, Grenoble, France, 1978.

Boutron, C., Alkali and alkaline earth enrichments in aerosols deposited in Antarctic snows, *Atmospheric Environment, 13*, 919-924, 1979a.

Boutron, C., Past and present day tropospheric fallout fluxes of Pb, Cd, Cu, Zn, and Ag in Antarctica and Greenland, *Geophysical Research Letters*, *6* (3), 159-162, 1979b.

Boutron, C., and C. Lorius, Trace metals in Antarctic snows since 1914, *Nature*, *277* (5697), 551-554, 1979.

Boutron, C., Respective influence of global pollution and volcanic eruptions on the past variations of the trace metals content of Antarctic snows since 1880's, *Journal of Geophysical Research*, *85* (C12), 7426-7432, 1980.

Boutron, C., Nouvelles donnees sur le contenu en metaux traces des neiges de l'Antarctique, du Groenland et de l'ile de Devon, *Zeitschrift Fur Gletscherkunde und Glazialgeologie*, *17* (1), 79-113, 1981.

Boutron, C., Atmospheric trace-metals in the snow layers deposited at the South Pole from 1928 to 1977, *Atmospheric Environment*, *16*, 2451-2459, 1982.

Boutron, C.F., and Patterson.C. C., The occurrence of lead in Antarctic recent snow, firn deposited over the last two centuries and prehistoric ice, *Geochimica et Cosmochimica Acta*, *47*, 1355-1367, 1983.

Boutron, C.F., Atmospheric heavy metals in the snow and ice layers deposited in Antarctica and Greenland from prehistoric times to present, in *Heavy Metals in the Environment*, edited by G. Miller, pp. 174-177, CEP Consultants Ltd, Heidelberg, 1983.

Boutron, C.F., and F.M. Batifol, Assessing laboratory procedures for the decontamination of polar snow or ice samples for the analysis of toxic metals and metalloids, *Annals of Glaciology*, *7*, 1-11, 1985.

Boutron, C.F., and C.C. Patterson, Lead concentration changes in Antarctic ice during the Wisconsin Holocene transition, *Nature*, *323*, 222-225, 1986.

Boutron, C.F., and C.C. Patterson, Relative levels of natural and anthropogenic lead in recent Antarctic snow, *Journal of Geophysical Research*, *92* (ND7), 8454-8464, 1987.

Boutron, C.F., C.C. Patterson, V.N. Petrov, and N.I. Barkov, Preliminary data on changes of lead concentrations in Antarctic ice from 155,000 to 26,000 years BP, *Atmospheric Environment*, *21*, 1197-1202, 1987.

Boutron, C.F., C.C. Patterson, and N.I. Barkov, Assessing the quality of thermally drilled deep Antarctic ice cores for trace elements analysis, in *Ice Core Drilling: Proceedings of the Third International Workshop on Ice Drilling Technology*, edited by C. Rado, and D. Beaudoing, Genoble, France, 1988.

Boutron, C.F., U. Grolach, J.P. Candelone, M.A. Bolshov, and R.J. Delmas, Decrease in anthropogenic Lead, cadmium and zinc in Greenland snows since the late 1960's, *Nature, 353*, 153-156, 1991.

Boutron, C.F., S.N. Rudniev, M.A. Bolshov, V.G. Koloshnikov, C.C. Patterson, and N.I. Barkov, Changes in cadmium concentrations in Antarctic ice and snow during the past 155,000 Years, *Earth and Planetary Science Letters, 117*, 431-441, 1993.

Boutron, C.F., J.P. Candelone, and S. Hong, Past and recent changes in the large-scale tropospheric cycles of lead and other heavy metals as documented in Antarctic and Greenland snow and ice: a review, *Geochemica et Cosmochimica Acta, 58* (15), 3217-3225, 1994.

Boyd, P., A. Watson, and C. Law, Spotlight is on iron at international SOIREE in Southern Ocean, *US JGOFS Newsletter*, February,10-11, 1999

Broecker, W.S., and G.M. Henderson, The sequence of events surrounding Termination II and their implications for the cause of glacial-interglacial CO_2 changes, *Paleoceanography, 13*, 353-364, 1998.

Bromwich, D.H., J.F. Carrasco, Z. Liu, and R. Tzeng, Hemispheric atmospheric variations and oceanographic impacts associated with katabatic surges across the Ross Ice Shelf, Antarctica, *Journal of Geophysical Research, 98* (D7), 13045-13062, 1993a.

Bromwich, D.H., T.R. Parish, A. Pellegrini, C.R. Stearns, and G.A. Weidner, Spatial and temporal characteristics of intense katabatic winds at Terra Nova Bay, Antarctica, in *Antarctic Meteorology and Climatology : Studies Based on Automatic Weather Stations*, edited by D.H. Bromwich, and C.R. Stearns, American Geophysical Union, Washington, D.C, 1993b.

Bromwich, D.H., J.F. Carrasco, and J. Turner, A downward developing mesoscale cyclone over the Ross Ice Shelf during winter, *The Global Atmosphere and Ocean System, 4*, 125-147, 1996.

Bromwich, D.H., and Z. Liu, An observational study of the katabatic wind confluence zone near Siple Coast, West Antarctica, *Monthly Weather Review, 124*, 462-477, 1996.

Buat-Menard, P., The ocean as a sink for particles, in *The Role of Air-Sea Exchange in Geochemical Cycling*, edited by P. Buat-Menard, 165-183, Reidel, Norwell, 1986.

Budd, W.F., and R.J.M. Rowden-Rich, Finite element analysis of two dimensional longitudinal section flow on Law Dome, *ANARE Research Note*, *28*, 153-162, 1985.

Bull, C., Snow Accumulation in Antarctica, in *Research in the Antarctic*, edited by L.O. Quam, pp. 367-421, American Association for the Advancement of Science, Washington, D.C., 1971.

Candelone, J.P., S. Hong, and C.F. Boutron, An improved method for decontaminating polar snow or ice cores for heavy metal analysis, *Analytical Chimica Acta*, *299*, 9-16, 1994.

Chavez, F.P., K.R. Buck, K.H. Coale, J.H. Martin, G.R. DiTullio, N.A. Welschmeyer, A.C. Jackson, and R.T. Barber, Growth rates, grazing, sinking, and iron limitation of equatorial Pacific phytoplankton, *Limnology and Oceanography*, *36*, 1816-1833, 1991.

Chavez, F.P., and J.R. Toggweiler, Physical estimates of global new production: The upwelling contribution, in *Upwelling in the Ocean*, edited by C.P. Summerhayes, K.C. Emeis, M.V. Angel, R.L. Smith, and B. Zeitzschel, Wiley, New York, 1995.

Chester, R., The marine mineral aerosol, in *The Role of Air-Sea Exchange in Geochemical Cycling*, edited by P. Buat-Ménard, 443-476, Reidel Publishing Company, Dordrecht Holland, 1985.

Chester, R., and K.J.T. Murphy, Metals in the marine atmosphere, in *Heavy Metals in the Marine Environment*, edited by R.W. Furness, and P.S. Rainbow, 27-49, CRC Press, Boca Raton, 1990.

Chisholm, S.W., and F.M.M. Morel, What controls phytoplankton production in nutrient-rich areas of the open sea?, *Limnology and Oceanography*, *36*, 1507-1965, 1991.

Coale, K.H., K.S. Johnson, S.E. Fitzwater, M. Gordon, S. Tanner, F.P. Chavez, F. Ferioli, C. Sakamoto, P. Rogers, F. Millero, P. Steinberg, P. Nightingale, D. Cooper, W.P. Cochlan, M.R. Landry, J. Constantinou, G. Rollwagen, A. Trasvina, and R. Kudela, A massive phytoplankton bloom induced by an ecosystem-scale iron fertilization experiment in the equatorial Pacific Ocean, *Nature*, *383*, 495-501, 1996.

Coale, K.H., K.S. Johnson, S.E. Fitzwater, S.P.G. Blain, T.P. Stanton, and T.L. Coley, IronEx-I, an in situ iron-enrichment experiment: experimental design, implementation and results, *Deep Sea Research II*, *45*, 919-945, 1998.

Comiso, J.C., C.R. Mc Clain, C.W. Sullivan, J.P. Ryan, and C.L. Lenoard, Coastal zone scanner pigment concentrations in the Southern Ocean and relationships to geophysical surface features, *Journal of Geophysical Research, 98* (C2), 2419-2451, 1993.

Cragin, J.H., M.M. Herron, C.C.J. Langway, and G. Klouda, Interhemispheric comparison of changes in the composition of atmospheric precipitation during the late Cenozoic era, in *Polar oceans*, edited by M.J. Dunbar, 617-631, Arctic Institute of North America, Montreal, 1977.

Cullather, R.I., D.H. Bromwich, and M.L. Van Woert, Spatial and temporal variability of Antarctica precipitation from atmospheric methods, *Journal of Climate, 11*, 334-367, 1998.

Cunningham, W.C., and W.H. Zoller, The chemical composition of remote area aerosols, *The Journal of Aerosol Science, 12*, 367-384, 1981.

Currie, L.A., International recommendations offered on analytical detection and quantification concepts and nomenclature, *Analytica Chimica Acta, 391* (2), 105-126, 1999.

Davidson, C.I., Mechanisms of wet and dry deposition of atmospheric contaminants to snow surfaces, in *The Environmental Record in Glaciers and Ice Sheets*, edited by H. Oeschger, and C. Langway, 29-51, Wiley and Sons, New York, 1989.

Davidson, C.I., M.H. Bergin, and H.D. Kuhns, The deposition of particles and gases to ice sheets, in *Chemical Exchange Between the Atmosphere and Polar Snow*, edited by E.W. Wolff, and R.C. Bales, 275-301, Springer-Verlag, Berlin, 1996.

Delmas, R.J., Environmental information from ice cores, *Reviews of Geophysics, 30*, 1-21, 1992.

Dick, A.L., and D.A. Peel, Trace elements in Antarctic air and snowfall, *Annals of Glaciology, 7*, 12-19, 1985.

Dick, A.L., Trace elements in Antarctic snow and air, PhD thesis, UK, 1987.

Dick, A.L., Concentrations and sources of metals in the Antarctic Peninsula aerosol, *Geochimica et Cosmochimica Acta, 55*, 1827-1836, 1991.

Donaghay, P.L., P.S. Liss, R.A. Duce, D.R. Kester, A.K. Hanson, T. Villareal, N.W. Tindale, and D.J. Gifford, The role of episodic atmospheric nutrient inputs in the chemical and biological dynamics of oceanic ecosystems, *Oceanography, 4*, 62-70, 1991.

Duce, R.A., The impact of atmospheric nitrogen, phosphorus and iron species on marine biological productivity, in *The Role of Air-Sea Exchange in Geochemical Cycling*, edited by P. Buat-Ménard, 443-476, Reidel Publishing Company, Dordrecht Holland, 1986.

Duce, R., and N.W. Tindale, Atmospheric transport of iron and its deposition in the ocean, *Limnology and Oceanography*, *36*, 1715-1726, 1991.

Duce, R.A., P.S. Liss, J.T. Merril, E.L. Atlas, P. Buat-Menard, B.B. Hicks, J.M. Miller, J.M. Prospero, R. Arimoto, T.M. Church, W. Ellis, J.N. Galloway, L. Hansen, T.D. Jickells, A.H. Knap, K.H. Reinhardt, B. Schneider, A. Soudine, J.J. Tokos, S. Tsunogai, R. Wollast, and M. Zhou, The atmospheric input of trace species to the world ocean, *Global Biogeochemical Cycles*, *5*, 193-259, 1991.

Duce, R.A., Sources, distributions and fluxes of mineral aerosols and their relationship to climate, in *Aerosol Forcing of Climate: Report of the Dahlem Workshop on Aerosol Forcing of Climate*, edited by R.J. Charlson, and J. Heintzenburg, 43-72, Berlin, John Wiley and Sons, 1995.

Dugdale, R., and F. Wilkerson, Nutrient limitation of new production in the sea, in *Primary Production and Biogeochemical Cycles in the Sea*, edited by P.G. Falkowski, and A.D. Woodhead, 107-122, Plenum press, New York, 1992.

Edwards, R., P.N. Sedwick, V. Morgan, C.F. Boutron, and S. Hong, Iron in ice cores from Law Dome, East Antarctica: implications for past deposition of aerosol iron, *Annals of Glaciology*, *27*, 365-370, 1998.

Etheridge, D.M., and C.W. Wookey, Ice core drilling at a high accumulation area of Law Dome, Antarctica,1987, in *Ice Core Drilling: Proceedings of the Third International Workshop on Ice Drilling Technology*, 10-14, Grenoble, France, 1988.

Etheridge, D.M., G.I. Pearman, and F. de Silva, Atmospheric trace-gas variations as revealed by air trapped in an ice core from Law Dome, Antarctica, *Annals of Glaciology*, *10*, 28-33, 1988.

Falkowski, P.G., R.T. Barber, and V. Smetacek, Biogeochemical controls and feedbacks on ocean primary production, *Science*, *281*, 200-206, 1998.

Francois, R., M.A. Altabet, E.F. Yu, D.M. Sigman, M.P. Bacon, M. Frank, G. Bohrmann, G. Bareille, and L.D. Labeyrie, Contribution of Southern Ocean surface water stratifcation to low atmospheric CO_2 concentrations during the last glacial period, *Nature*, *389*, 929-935, 1997.

Gaudichet, A., J.R. Petit, R. Lefevre, and C. Lorius, An investigation by analytical transmission electron microscopy of individual insoluble microparticles from Antarctic (Dome C) ice core samples, *Tellus, 38B*, 250-261, 1986.

Gaudichet, A., M. de Angelis, R. Lefevre, J.R. Petit, Y.S. Korotkevich, and V.N. Petrov, Mineralogy of insoluble particles in the Vostok Antarctic ice core over the last climatic cycle (150 kyr), *Geophysical Research Letters, 15*, 1471-1474, 1988.

Gillette, D.A., Production of dust that may be carried great distances, in *Desert Dust: Origin, Characteristics, and Effect on Man*, edited by T.L. Péwé, 11-27, Geological Society of America, special paper, Boulder Colarado, 1981.

Gordon, A.L., H.W. Taylor, and D.T. Georgi, Antarctic oceanographic zonation, in *Polar Oceans*, edited by M. J. Dunbar, 45-85, Arctic institute of North America, Calgary, 1977.

Gorlach, U., and C.F. Boutron, Preconcentration of lead, cadmium, copper and zinc in water at the pg g^{-1} level by non-boiling evaporation, *Analytica Chimica Acta, 236*, 391-398, 1990.

Goudie, A.S., and N.J. Middleton, The changing frequency of dust storms in space and time, *Climate Change, 20*, 197-225, 1992.

Greene, R.M., R.J. Geider, and P.G. Falkowski, Effect of iron limitation on photosynthesis in a marine diatom, *Limnology and Oceanography*, *36*, 1772-1782, 1991.

Griffin, J.J., H. Windom, and E.D. Goldberg, The distribution of clay minerals in the world ocean, *Deep Sea Research*, *15*, 433-459, 1968.

Grotov, A.S., D.A. Nechaev, G.G. Panteleev, and M.I. Yaremchuk, Large scale circulation in the Bellingshausen and Amundsen Seas as a variational inverse of climatological data, *Journal of Geophysical Research*, 103 (C6), 13011-13022, 1998.

Grousset, F.E., P.E. Biscaye, M. Revel, J.R. Petit, K. Pye, S. Joussaume, and J. Jouzel, Antarctic (Dome C) ice-core dust at 18 k.y. B.P.: isotropic constraints on origins, *Earth and Planetary Science Letters*, 111, 175-182, 1992.

Hamilton, W.L., Microparticle deposition on polar ice sheets, pp. 81, Ohio State University, Columbus, Ohio, USA, 1969.

Hamley, T.C., V.I. Morgan, R.J. Thwaites, and X.Q. Gao, An ice-core drilling site at Law Dome summit Wilkes land, Antarctica, *Anare Research Notes*, *37*, 1-34, 1986.

Hanappe, F., M. Vosters, E. Picciotto, and S. Deutsch, chimie des neiges Antarctiques et taux de deposition de matiere extraterrestre deuxieme article, *Earth and Planetary Letters*, *4*, 487-496, 1968.

Heimann, M., P. Monfray, and G. Polian, Modeling the long-range transport of ^{222}Rn to Subantarctic and Antarctic areas, *Tellus*, *42B*, 83-99, 1990.

Helbling, E.W., V. Villafane, and O. Holm-Hansen, Effect of iron on productivity and size distribution of Antarctic phytoplankton, *Limnology and Oceanography*, *36*, 1879-1885, 1991.

Higham, M., C. M., A. Ruddell, and I. Allison, Snow-accumulation distribution in the interior of the Lambert Glacier basin, Antarctica, *Annals of Glaciology*, *25*, 412-417, 1997.

Hirayama, K., and N. Unohara, Spectrophotometric catalytic determination of an ultratrace amount of iron(III) in water based on the oxidation of N, N-dimethyl-p-phenylenediamine by hydrogen peroxide, *Analytical Chemistry*, 60, 2573-2577, 1988.

Hoppema, H., E. Fahrbach, M.C. Stoll, and H.J.W. de Baar, Annual uptake of atmospheric CO_2 by the Weddell Sea derived from a surface layer balance, including estimations of entrainment and new production, *Journal of Marine Systems*, 19, 219-333, 1999.

Jacobs, S., and S. Comiso, Satellite, passive microwave sea ice observations and oceanic processes in the Ross Sea, Antarctica, *Journal of Geophyscial Research*, 94 (C12), 18,195-18,211, 1989.

Jouzel, J., N.I. Barkov, and J.M. Barnola, Extending the Vostok ice-core record of paleoclimate to the penultimate glacial period, *Nature*, 364, 407-412, 1993.

Jun, L., T. H. Jacka, and V. Morgan, Crystal-size and microparticle record in the ice core from Dome Summit South, Law Dome, East Antarctica, *Annals of Glaciology*, *27*, 343-349, 1998.

Knox, F., and M.B. McElroy, Changes in atmospheric CO_2: Influence of marine biota at high latitude, *Journal of Geophysical Research*, 89, 4629-4637, 1984.

Kolber, Z.S., R.T. Barber, K.H. Coale, S.E. Fitzwater, R.M. Greene, K.S. Johnson, S. Lindley, and P.G. Falkowski, Iron limitation of phytoplankton photosynthesis in the equatorial Pacific Ocean, *Nature*, *371*, 145-149, 1994.

Kottmeier, C., and B. Fay, Trajectories in the Antarctic lower troposphere, *Journal of Geophysical Research, 103* (D9), 10947-10959, 1998.

Kumar, N., R.F. Anderson, R.A. Mortlock , P.N. Froelich, P. Kubik, B. Dittrich-Hannen, and M. Suter, Increased biological productivity and export production in the glacial Southern Ocean, *Nature, 378*, 675-680, 1995.

Ishii, M., H.Y. Inoue, H. Matsueda, and E. Tanoue, Close coupling between seasonal biological production and dynamics of dissolved inorganic carbon in the Western Pacific ocean sector of the Antarctic ocean, *Deep-Sea Research Part I, 45*, 1187-1209, 1998.

Laj, P., G. Ghermandi, R. Cecchi, V. Maggi, C. Riontino, S. Hong, J.P. Candelone, and C.F. Boutron, Distribution of Ca, Fe, K, and S between soluble and insoluble material in the Greenland ice core project ice core, *Journal of Geophysical Research, 102* (C12), 26615-26624, 1997.

Lambert, G., B. Ardouin, and J. Sanak, Atmospheric transport of trace elements toward Antarctica, *Tellus, 42B*, 76-82, 1990.

Landing, W.M., C. Haraldsson, and N. Paxeus, Vinyl polymer agglomerate based transition metal cation-chelating ion-exchange resin containing the 8-hydroxyquinoline functional group, *Analytical Chemistry*, *58*, 3031-3035, 1986.

Ledley, T.S., Snow on sea ice: competing effects in shaping climate, *Journal of Geophysical Research*, *96* (D9), 17195-17208, 1991.

van Leeuwe, M.A., R. Scharek, H.J.W. de Baar, J.T.M. de Jong, and L. Goeyens, Iron enrichment experiments in the Southern Ocean: physiological responses of plankton communities, *Deep Sea Research II*, *44*, 189-297, 1997.

Leinen, M., and M. Sarnthein, *Paleoclimatology and Paleometeorology: Modern and Past Patterns of Global Atmospheric Transport*, Kluwer Academic Pub, Dordrecht, 1989.

Lindley, S.T., and R.T. Barber, Phytoplankton response to natural and experimental iron addition, *Deep Sea Research II*, *45*, 1135-1150, 1998.

Loscher, B.M., H.J.W. de Baar, J.T.M. deJong, C. Veth, and F. Dehairs, The distribution of Fe in the Antarctic Circumpolar Current, *Deep Sea Research II*, *44*, 143-187, 1997.

Losno, R., J.L. Colin, N. Le Bris, G. Bergametti, T. Jickells, and B. Lim, Aluminium solubility in rainwater and molten snow, *Journal of Atmospheric Chemistry*, 17, 29-43, 1993.

Lorius, C., J. Jouzel, C. Ritz, L. Merlivat , and N. Barkov, A 150,000-year climatic record from Antarctic ice, *Nature*, 316, 591-596, 1985.

Lorius, C., Polar ice cores: a record of climatic and environmental changes, in *Global Changes of the Past*, edited by R.S. Bradley, 261-294, UCAR/OIES, Boulder, USA, 1989.

Maenhaut, W., W.N. Zoller , R.A. Duce, and G.L. Hoffman, Concentrations and size distributions of particulate trace elements in the South Pole atmosphere, *Journal of Geophysical Research, 84* (2421-2431), 1979.

Maggi, V., and J.R. Petit, Atmospheric dust concentration record from the Hercules Névé firn core, northern Victoria Land, Antarctica, *Annals of Glaciology, 27*, 355-359, 1998.

Maring, H.B., and R.A. Duce, The impact of atmospheric aerosols on trace metal chemistry in open ocean surface seawater, 1, Aluminum, *Earth and Planetary Science Letters, 84*, 381-392, 1987.

Marshall, E.W., The stratigraphic distribution of particulate matter in the firn at Byrd Station, Antarctica, *Antarctic Research, 7*, 185-196, 1962.

Mart, L., Seasonal variations of Cd, Pb, Cu and Ni levels in snow from the eastern Artic Ocean, *Tellus, 35B*, 131-141, 1983.

Martin, J.H., and S.E. Fitzwater, Iron deficiency limits phytoplankton growth in the north-east Pacific subarctic, *Nature, 331*, 341-343, 1988.

Martin, J.H., R.M. Gordon, and S.E. Fitzwater, VERTEX: phytoplankton/iron studies in the Gulf of Alaska, *Deep Sea Research part A, 36*, 649, 1989.

Martin, J.H., Glacial-interglacial CO_2 change: The iron hypothesis, *Paleoceanography, 5* (1), 1-13, 1990.

Martin, J.H., R.M. Gordon, and S.E. Fitzwater, Iron in Antarctic waters, *Nature, 345*, 156-158, 1990a.

Martin, J.H., R.M. Gordon, and S.E. Fitzwater, Iron deficiency limits phytoplankton growth in Antarctic waters, *Global Biochemical Cycles, 4*, 5-12, 1990b.

Martin, J.H., R.M. Gordon, and S.E. Fitzwater, The case for iron, *Limnology and Oceanography, 36*, 1793-1802, 1991.

Martin, J.H., K.H. Coale, K.S. Johnson, S.E. Fitzwater, R.M. Gordon, S.J. Tanner, C.N. Hunter, V.A. Elrod, J.L. Nowicki, T.L. Coley, R.T. Barber, S. Lindley, A.J. Watson, K. Vanscoy, L. CS., M.I. Liddicoat, R. Ling, T. Stanton, J. Stockel, C. Collins, A. Anderson, R. Bidigare, M. Ondrusek, M. Latasa, F.J. Millero, and K. Lee, Testing the iron hypothesis in ecosystems of the equatorial Pacific Ocean, *Nature*, 371, 123-129, 1994.

Massom, R.A., V.I. Lytle, A.P. Worby, and I. Allison, Winter snow cover variability on East Antarctic sea ice, *Journal of Geophysical Research*, 103 (C11), 24,837-24,855, 1998.

Mayewski, P.A., M.S. Twickler, S.I. Whitlow, L.D. Meeker, Q. Yang, J. Thomas, K. Kreutz, P.M. Grootes, D.L. Morse, E.J. Steig, E.D. Waddington, E. Saltzman, P.Y. Whung, and K. Taylor, Climate change during the last deglaciation in Antarctica, *Science*, 272, 1636-1638, 1996.

Measures, C.I., J. Yuan, and J.A. Resing, Determination of iron in seawater by flow injection analysis using in-line preconcentration and spectrophotometric detection, *Marine Chemistry*, 50, 1-10, 1995.

Moens, L., P. Verrept, R. Dams, U. Greb, G. Jung, and B. Laser, New high resolution inductively coupled plasma mass spectrometry technology applied for the determination V, Fe, Cu, Zn and Ag in human serum, *Journal of Analytical Atomic Spectrometry*, 9, 1075, 1994.

Moens, L., F. Vanhaecke, J. Riondato, and R. Dams, Some Figures of merit of a double focussing inductively coupled plasma mass spectrometer, *Journal of Analytical Atomic Spectrometry*, 10, 569, 1995.

Moody, J.R., and R.M. Lindstrom, Selection and cleaning of plastic containers for storage of trace element samples, *Analytical Chemistry*, 49, 2264-2267, 1977.

Moore, R.M., J.E. Milley, and A. Chatt, The potential for biological mobilization of trace elements from aeolian dust in the ocean and its importance in the case of iron, *Oceanologica Acta*, 7, 221-228, 1984.

Moore, J.K., M.R. Abbott, J.G. Richman, W.O. Smith, J. Cowles, K.H. Coale, W.D. Gardner, and R.T. Barber, Seawifs satellite ocean color data from the Southern Ocean, *Geophysical Research Letters*, 26 (10), 1465-1468, 1999.

Morales, C., The airborne transport of Saharan dust: A review, *Climate Change*, 9, 219-241, 1985.

Morel, F.M.M., J.G. Rueter, and N.M. Price, Iron nutrition of phytoplankton and its possible importance in the ecology of ocean regions with high nutrient and low biomass, *Oceanography*, 4, 56-61, 1991.

Morgan, V.I., and A.P. McCray, Enhanced shear zones in ice flow implications for ice cap modeling and core dating, *ANARE Research Note*, 28, 4-9, 1985.

Morgan, V.I., I.D. Goodwin, D.M. Etheridge, and C.W. Wookey, Evidence from Antarctic ice cores for recent increases in snow accumulation, *Nature*, 354, 58-60, 1991.

Morgan, V.I., C.W. Wookey, J. Li, T.D. van Ommen, W.M. Skinner, and M.F. Fitzpatrick, Site information and initial results from deep ice drilling on Law Dome, Antarctica, *Journal of Glaciology*, 43, 3-10, 1997.

Mosley-Thompson, E., and L.G. Thompson, Microparticle analysis of the Ross Ice Shelf Q-13 core and preliminary results from the J-9 core, *Annals of Glaciology*, 3, 211-215, 1982.

Murozumi, M., J.T. Chow, and C. Patterson, Chemical concentrations of pollutant lead aerosols, terrestrial dusts and sea salts in Greenland and Antarctica snow strata, *Geochimica et Cosmochimica Acta*, 33, 1247-1294, 1969.

Neftel, A., H. Oeschger, J. Schwande, B. Stauffer, and R. Zumbrunn, Ice core sample measurements give atmospheric CO2 content during the past 40,000 years, *Nature*, 295, 220-223, 1982.

Ng, A., and C. Patterson, Natural concentrations of lead in Arctic and Antarctic ice, *Geochimica et Cosmochimica Acta*, 45, 2109-2121, 1981.

Nunes Vaz, R.A., and G.W. Lennon, Physical Oceanorgraphy of the Prydz bay region of Antarctic waters, *Deep Sea Research I*, 43, 603-641, 1996.

van Ommen, T.D., and V. Morgan, Calibrating the ice core paleothermometer using seasonality, *Journal of Geophysical Research, 102* (D8), 9351-9357, 1997.

Parish, T.R. and D. H., Bromwich, Continental-scale simulation of the Antarctic katabatic wind regime, *Journal of Climate*, 4, 135-146, 1991.

Parkinson, C., Southern Ocean sea ice distributions and extents, *Philosophical Transactions of the Royal Society of London*, 338, 243-250, 1992.

Patterson, C.C., and D.M. Settle, The reduction of order of magnitude errors in lead analyses of biological materials and natural waters by evaluation and controlling the extent and sources of industrial lead contamination introduced during sample collection and analysis, in *Accuracy in Trace Analysis: Sampling, Sample Handling and Analysis*, edited by P. LaFleur, 321-351, National Bureau of Standards, 1976.

Petit, J.R., M. Briat , and A. Royer, Ice age aerosol content form East Antarctic ice core samples and past wind strength, *Nature*, 293, 391-394, 1981.

Petit, J.R., L. Mounier, J. Jouzel, Y.S. Korotkevich, V.I. Kotlyakov, and C. Lorius, Palaeoclimatological and chronological implications of the Vostok core dust record, *Nature*, *343*, 56-58, 1990.

Péwé, T.L., Desert dust: an overview, in *Desert Dust: Origin, Characteristics, and Effect on Man*, edited by T. L. Péwé, 1-11, Geological Society of America, special paper, Boulder Colarado, 1981.

Price, N.M., B.A. Ahner, and F.M.M. Morel, The equatorial Pacific Ocean: grazer-controlled phytoplankton populations in an iron limited ecosystem, *Limnology and Oceanography*, 35, 652-662, 1994.

Prospero, J.M., Aeolian transport to the world ocean, in *The Sea*, edited by C. Emiliani, 801-974, Wiley Interscience, New York, 1981a.

Prospero, J.M., Arid regions as sources of mineral aerosols in the marine atmosphere, in *Desert Dust: Origin, Characteristics, and Effect on Man*, edited by T.L. Péwé, 11-26, Geological Society of America, special paper, Boulder, Colarado, 1981b.

Pye, K., *Aeolian Dust and Dust Deposits*, Academic Press, London, 1987.

Rea, D.K., The paleoclimatic record provided by eolian deposition in the deep sea: the geologic history of the wind, *Reviews of Geophysics*, 32, 159-195, 1994.

Ram, M., and R. Gayley, Insoluble particles in Antarctic ice; back-ground aerosol size distribution and diatom concentration, *Journal of Geophysical Research*, 93 (D7), 8378-8382, 1988.

Rathburn, A.E., J.J. Pichon, M.A. Ayress, and P. De Deckker, Microfossil and stable-isotope evidence for changes in late Holocene paleoproductivity and paleoceanographic conditions in the Prydz Bay region of Antarctica, *Paleogeography, Paleoclimatology, Paleoecology*, 131, 485-510, 1997.

Raven, J., The iron and molybdenum use efficiencies of plant growth as a function of different energy, carbon and nitrogen sources, *New Phytology, 109*, 297-287, 1988.

Raven, J., Predictions of Fe and Mn use efficiencies of phototrophic growth as a function of light availability for growth and of C assimilation pathway, *New Phytology*, *116*, 1-18, 1990.

Redfield, A.C., The biological control of chemical factors in the environment, *American Scientist*, 46, 205-221, 1958.

Resing, J.A., and C.I. Measures, Fluorometric determination of Al in seawater by flow injection analysis with in-line preconcentration, *Analytical Chemistry*, 66, 4105-4111, 1994.

Rich, H.W., and F.M.M. Morel, Availability of well defined iron colloids to the marine diatom *Thalassiosira weisflogii*, *Limnology and Oceanography*, 35, 652-662, 1990.

Rosman, K.J., R.W. Chisholm, C.F. Boutron, J.P. Candelone, and C.C. Patterson, Anthropogenic lead isotopes in Antarctica, *Geophysical Research Letters*, 21, 2669-2672, 1994.

Royer, A., M. de Angelis, and J.R. Petit, A 30000 year record of physical and optical properties of microparticles from an east Antarctic ice core and implications for paleoclimate reconstruction models, *Climatic Change*, 5, 381-412, 1983.

Rubin, S.I., T. Takahashi, D.W. Chipman, and J.G. Goddard, Primary productivity and nutrient utilization ratios in the Pacific sector of the Southern Ocean based on seasonal changes in seawater chemistry, *Deep Sea Research I*, 45, 1211-1234, 1998.

Sarmiento, J.L., and J.R. Toggweiler, A new model for the role of the oceans in determining atmosphere PCO_2, *Nature*, 308, 621-624, 1984.

Sarmiento, J.L., and J.C. Orr, Three-dimensional simulations of the impact of Southern Ocean nutrient depletion on atmospheric CO_2 and ocean chemistry, *Limnology and Oceanography*, 36, 1928, 1991.

Sarmiento, J.L., and U. Siegenthaler, New production and the global carbon cycle, in *Primary Productivity and Biogeochemical Cycles in the Sea*, edited by P.G. Falkowski, and A.D. Woodhead, 317-333, Plenum Press, New York, 1992.

Schütz, L.W., J.M. Prospero, P. Buat-Menard, R.A.C. Carvalho, R. Harriss, N.Z. Heidam, and R. Jaenicke, The long range transport of mineral aerosols: Group report, in *The Large-Scale Transport of Natural and contaminant Substances*, edited by A.H. Knap, 197-229, Kluwer Academic Pub, Dordrecht, 1990.

Sedwick, P.N., and G.R. Ditullio, Regulation of algal blooms in Antarctic shelf waters by the release of iron from melting sea ice, *Geophysical Research Letters*, 24, 2515-2518, 1997.

Sedwick, P.N., P.R. Edwards, D.J. Mackey, F.B. Griffiths, and J.S. Parslow, Iron and manganese in surface waters of the Australian Subantarctic region, *Deep Sea Research I*, 44, 1239-1253, 1997.

Sedwick, P.N., DiTullio, G. R. and Mackey, D.J., Iron and manganese in the Ross Sea, Antarctica: Seasonal iron limitation in Antarctic shelf waters, *Journal of Geophysical Research*, in press 1999.

Selavka, C.M., K.S. Jiao, and I.S. Krull, Construction and comparison of open tubular reactors for post-column reaction detection in liquid chromatography, *Analytical Chemistry*, *59*, 2221-2224, 1987.

Shaw, G.E., Considerations on the origin and properties of the Antarctic aerosol, *Review of Geophysics and Space Physics*, *17*, 1983-1998, 1979.

Shimamura, T., M. Iwashita, Y. Takaku, I. Akabane, A. Tsumura, and S. Yamasaki, Determination of the trace elements in a Mizuho ice core sample by a combination of conventional and high resolution inductively coupled plasma mass spectrometry, *Polar Meteorology and Glaciology*, *9*, 33-34, 1995.

Siegenthaler, U., and T. Wenk, Rapid atmospheric CO_2 variations and ocean circulation, *Nature*, *308*, 624-626, 1984.

Skoog, D.A., *Principles of Instrumental Analysis*, Saunders College Publishing, Fort Worth, 1984.

Smith, W.O., Jr., and D.M. Nelson, Phytoplankton bloom produced by a receding ice edge in the Ross Sea: Spatial coherence with the density field, *Science*, *227*, 163-166, 1985.

Smith, W.O.J., Nutrient distributions and new production in polar regions: parallels and contrasts between the Arctic and Antarctic, *Marine Chemistry*, *35*, 245-257, 1991.

Sowers, T., M. Bender, and D. Raynaud, The $\delta^{18}O$ of atmospheric O_2 from air inclusions in the Vostok ice core: timing of CO_2 and ice volume changes during the penultimate deglaciation, *Paleoceanography*, *6*, 679-696, 1991.

Sunda, W.G., D.G. Swift, and S.A. Huntsman, Low iron requirement in oceanic plankton, *Nature*, *351*, 55, 1991.

Sunda, W.G., and S.A. Huntsman, Iron uptake and growth limitation in oceanic and coastal phytoplankton, *Marine Chemistry, 50*, 189-206, 1995.

Suttie, E.D., and E.W. Wolff, Seasonal input of heavy metals to Antarctic snow, *Tellus, 44B*, 351-157, 1992.

Suttie, E.D., and E.W. Wolff, The local deposition of heavy metal emissions from point sources in Antarctica, *Atmospheric Environment, 27*, 1833-1841, 1993.

Taylor, L.D., and J. Gliozzi, Distribution of particulate matter in the firn at Byrd station, Antarctica, in *Antarctic Snow and Ice Studies*, edited by M. Mellor, 267-277, American Geophysical Union, Washington, D.C., 1964.

Taylor, S.R., and S.M. McClennan, The continental crust: its composition and evolution, 66-67, Blackwell scientific publications, Oxford, 1985.

Tegen, I., and I. Fung, Contribution to the atmospheric mineral aerosol load from land surface modification, *Journal of Geophysical Research, 100* (D9), 18,707-18,726, 1995.

Townsend, A.T., and R. Edwards, Ultratrace analysis of Antarctic snow and ice samples using high resolution inductively coupled plasma mass spectrometry, *Journal of Analytical Atomic Spectrometry, 13*, 463-468, 1998.

Tschopel, P., L. Kotz, W. Schulz, G. Veber, and G. Tolg, Causes and elimination of systematic errors in the determination of elements in aqueous solutions in the ng mL^{-1} and pg mL^{-1} range, *Fresenius Zeitschrift für Analytische Chemie*, *302*, 1-14, 1980.

Tsoar, H., and K. Pye, Dust transport and the question of desert loess formation, *Sedimentology*, *34*, 139-153, 1987.

Tuncel, G., N.K. Aras, and W.H. Zoller, Temporal variations and sources of elements on the South Polar atmosphere: 1 Nonenriched and moderately enriched elements, *Journal of Geophysical Research*, *94* (D3), 13,025-13,038, 1989.

Vandal, G.M., W.F. Fitzgerald, C.F. Boutron, and J.P. Candelone, Variations in mercury deposition to Antarctica over the past 34,000 years, *Nature*, *362*, 621-623, 1993.

Wagenbach, D., U. Gorlach, K. Moser, and K.O. Munnich, Coastal Antarctic aerosol: the seasonal pattern of its chemical composition and radionuclide content, *Tellus*, *40B*, 426-436, 1988.

Wells, M.L., N.G. Zorkin, and A.G. Lewis, The role of colloid chemistry in providing a source of iron to phytoplankton, *Journal of Marine Research*, *41*, 731-746, 1983.

Westerlund, S., and P. Ohman, Iron in the water column of the Weddell Sea, *Marine Chemistry*, *35*, 199-217, 1991.

Winograd, I.J., J.M. Landwehr, K.R. Ludwig, T.B. Coplen, and A.C. Riggs, Duration and structure of the past four interglaciations, *Quaternary Research*, *48*, 141-154, 1997.

Wolff, E.W., M.P. Landy, and D.A. Peel, Preconcentration of cadmium, lead and zinc in water at the 10-12 g/g level by adsorption onto tungsten wire followed by flameless atomic absorption spectrometry, *Analytical Chemistry*, *53*, 1566-1570, 1981.

Wolff, E.W., and D.A. Peel, The record of global pollution in polar snow and ice, *Nature*, *313*, 535-540, 1985.

Wolff, E.W., Signals of atmospheric pollution in polar snow and ice, *Antarctic Science*, *2*, 189-205, 1990.

Wolff, E.W., and E.D. Suttie, Antarctic snow record of Southern Hemisphere lead pollution, *Geophysical Research Letters*, *21*, 781, 1994.

Wolff, E.M., and D.A. Peel, Assessing global and local pollution for heavy metals in Antarctica, in *Analusis Magazine*, 22, 41-43, 1994.

Wolff, E.W., M.R. Legrand, and D. Wagenbach, Coastal Antarctic aerosol and snowfall chemistry, *Journal of Geophysical Research, 103* (D9), 10927-10934, 1998.

Worby, A.P., and R.A. Massom, Structure and properties of sea ice and snow cover in East Antarctic pack ice, Hobart, Tasmania, Antarctic CRC, 7, 1995.

Worby, A.P., R.A. Massom, I. Allison, V.I. Lytle, and P. Heil, East Antarctic sea ice: A review of its structure, properties and drift, *Antarctic Research Series, 74*, 41-67, 1998.

Yung, Y.L., T. Lee, C.H. Wanf, and Y.T. Shieh, Dust: a diagnostic of the hydrologic cycle during the Last Glacial Maximum, *Science, 271*, 962-963, 1996.

Zhu, X.R., J.M. Prospero, and F.J. Millero, Diel variability of soluble Fe(II) and soluble Fe in North African dust in the trade winds at Barbados, *Journal of Geophysical Research, 102* (D17,), 21,297-21,305, 1997.

Zhuang, G.S., R.A. Duce, and D.R. Kester, The solubility of atmospheric iron in the surface seawater of the open ocean, *Journal of Geophysical Research, 95*, 16207-16216, 1990.

Zoller, W.H., E.S. Gladney, and R.A. Duce, Atmospheric concentrations and sources of trace metals at the South Pole, *Science*, *183*, 198-200, 1973.

Appendix

A.1 Snow data

Trace-metal concentration data for snow samples collected from Antarctic sea ice and continental sites are presented in the following tables. Trace-metal concentrations are shown in picograms per gram (pg g^{-1}). Samples are named as:

site ID –pit number – sample number.

Abbreviations used in the tables are:

n.a. = not analysed

b.d.l. = below detection limit

Table A.1 Prydz Bay total-dissolvable metals

Sample ID	Sample depth from surface (cm)	Salinity (‰)	TD-Fe (pg g^{-1})	TD-Mn (pg g^{-1})	TD-Al (pg g^{-1})
Site: N **Lat:** 64.57° S **Long:** 74.98° E **Date:** 21/9/94					
N-1/1	15-20	1	610 ± 30	n.a.	n.a.
N-1/2	8-13	2	1330 ± 60	n.a.	n.a.
N-1/3	2-7	2	980 ± 30	n.a.	n.a.
N-2/1	5-10	0	1530 ± 120	170 ± 10	4400 ± 340

Sample ID	Sample depth from surface (cm)	Salinity (‰)	TD-Fe (pg g^{-1})	TD-Mn (pg g^{-1})	TD-Al (pg g^{-1})
N-2/2	6-11	0	200 ± 20	b.d.l.	170 ± 30
N-2/3	7-12	0	690 ± 30	n.a.	n.a.
N-2/4	0-18	2	90 ± 10	n.a.	n.a.
N-2/5	0-18	3	770 ± 10	n.a.	n.a.
N-3/1	0-18	1	70 ± 10	n.a.	n.a.
N-3/2	0-18	1	70 ± 10	n.a.	n.a.
Site: O **Lat:** 64.90° S **Long:** 75.00° E **Date:** 21/9/94					
O-1/1	2-7	0	750 ± 30	n.a.	n.a.
O-1/2	4-9	0	1080 ± 30	n.a.	n.a.
O-1/3	5-10	1	1260 ± 30	n.a.	n.a.
O-1/4	0-18	1	810 ± 10	n.a.	n.a.
O-1/5	0-18	1	270 ± 10	n.a.	n.a.
O-2/1	4-9	0	630 ± 30	10 ± 5	1310 ± 110
O-2/2	2-7	0	1430 ± 100	n.a.	n.a.
O-2/3	2-7	0	390 ± 20	b.d.l	190 ± 30
Site: U **Lat:** 66.12° S **Long:** 75.32° E **Date:** 23/9/94					
U-1/1	2-7	0	1080 ± 30	n.a.	n.a.
U-1/2	0-13	0	240 ± 15	n.a.	n.a.
U-1/3	0-13	1	150 ± 10	n.a.	n.a.
U-2/1	0-5	0	390 ± 20	n.a.	n.a.
U-2/3	0-18	0	640 ± 5	n.a.	n.a.
U-2/4	0-18	1	460 ± 20	n.a.	n.a.
U-3/1	4-9	2	680 ± 20	n.a.	n.a.
U-3/2	0-18	1	270 ± 10	n.a.	n.a.

Sample ID	Sample depth from surface (cm)	Salinity (‰)	TD-Fe (pg g^{-1})	TD-Mn (pg g^{-1})	TD-Al (pg g^{-1})
U-3/3	0-18	1	320 ± 10	n.a.	n.a.
U-4/1	4-9	1	180 ± 20	n.a.	n.a.
U-4/2	0-18	2	280 ± 10	n.a.	n.a.
U-4/3	0-18	1	460 ± 10	n.a.	n.a.
Site: V **Lat:** 66.30 °S **Long:** 75.72 °E **Date:** 23/9/94					
V-1/1	5-10	0	1770 ± 50	n.a.	n.a.
V-1/2	9-14	0	390 ± 20	n.a.	n.a.
V-1/3	6--11	0	870 ± 80	n.a.	n.a.
V-2/1	6-11	0	510 ± 20	n.a.	n.a.
V-2/2	4-9	1	400 ± 10	20 ± 10	930 ± 90
V-2/3	4-9	1	270 ± 20	b.d.l	430 ± 40
V-2/4	0-18	1	230 ± 10	n.a.	n.a.
V-2/5	0-18	1	1090 ± 10	n.a.	n.a.
V-2/6	0-18	1	260 ± 10	n.a.	n.a.

Table A.2 Princess Elizabeth Land total-dissolvable metals

Sample ID	Sample depth from surface (cm)	TD-Fe (pg g^{-1})	TD-Mn (pg g^{-1})	TD-Al (pg g^{-1})
Site: LGB70 **Lat:** 70.57 °S **Long:** 76.91 °E **Elevation:** 1650 m (ASL) **Date:** 18/11/94				
LGB 70-1/1	2-7	480 ± 20	20 ± 10	920 ± 120
LGB 70-1/2	10-15	1550 ± 70	n.a.	n.a.
LGB 70-2/1	2-7	740 ± 30	20 ± 10	1290 ± 160
LGB 70-2/2	10-15	610 ± 20	20 ± 10	1230 ± 160
LGB 70-t2/3	0-18	170 ± 10	n.a.	n.a.
LGB 70-3/1	10-15	310 ± 20	20 ± 5	560 ± 80
Site: LGB59 **Lat:** 73.43° S **Long:** 76.86° E **Elevation:** 2520 m (ASL) **Date:** 4/12/94				
LGB 59-1/1	2-7	2310 ± 80	90 ± 10	n.a.
LGB 59-1/2	10-15	1550 ± 70	40 ± 10	n.a.
LGB 59-2/1	2-7	350 ± 20	n.a.	n.a.
LGB 59-2/2	10-15	870 ± 10	n.a.	n.a.
LGB 59-3/1	2-7	750 ± 20	30 ±10	2880 ± 340
LGB 59-3/2	10-15	2950 ± 80	10 ± 5	1170 ± 150
Site: LGB53 **Lat:** 74.90 °S **Long:** 74.52 °E **Elevation:** 2430 m (ASL) **Date:** 12/12/94				
LGB 53-1/1	2-7	320 ± 10	15 ± 5	1220 ± 155
LGB 53-1/2	10-15	710 ± 10	n.a.	n.a.
LGB 53-1/3	0-18	620 ± 15	n.a.	n.a.
LGB 53-1/4	0-18	430 ± 10	n.a.	n.a.
LGB 53-2/1	2-7	1860 ± 20	30 ± 10	1510 ± 190
LGB 53-2/2	10-15	2790 ± 40	n.a.	n.a.
LGB 53-3/1	2-7	310 ± 10	15 ± 5	670 ± 100
LGB 53-3/2	10-15	375 ± 10	20 ± 5	620 ± 100
Site: LGB46 **Lat:** 75.85° S **Long:** 71.50° E **Elevation:** 2413 m (A.S.L.) **Date:** 22/12/94				

Sample ID	Sample depth from surface (cm)	TD-Fe (pg g^{-1})	TD-Mn (pg g^{-1})	TD-Al (pg g^{-1})
LGB 46-1/1	0-18	390 ± 5	n.a.	n.a.
LGB 46-1/2	2-7	415 ± 10	15 ± 5	1855 ± 225
LGB 46-1/3	10-15	475 ± 10	n.a.	n.a.
LGB 46-2/1	2-7	380 ± 20	10 ± 5	700 ± 100
LGB 46-2/2	10-20	515 ± 20	20 ± 5	900 ± 120
LGB 46-3/1	2-7	270 ± 5	n.a.	n.a.
LGB 46-3/2	10-15	830 ± 15	30 ± 10	5680 ± 670
LGB 46-3/3	0-18	845 ± 25	n.a.	n.a.
LGB 46-3/4	0-18	730 ± 10	n.a.	n.a.

Table A.3 Dumont d'Urville Sea total-dissolvable metals

Sample ID	Sample depth from surface(cm)	Salinity (‰)	TD-Fe (pg g^{-1})	TD-Mn (pg g^{-1})	TD-Al (pg g^{-1})
Site: A **Lat:** 64.60° S **Long:** 140.33° E **Date:** 02/08/95					
A-1/1	0-5	0	50 ± 5	n.a.	n.a.
A-1/2	0-5	0	64 ± 5	b.d.l.	b.d.l.
A-2/1	0-5	1	30 ± 5	b.d.l.	b.d.l.
A-2/2	0-5	1	30 ± 5	b.d.l.	b.d.l.
A-3/1	0-5	0	40 ± 5	n.a.	n.a.
A-3/2	8-13	1	20 ± 5	n.a.	n.a.
A-3/3	16-21	1	20 ± 5	n.a.	n.a.
A-3/4	24-29	2	20 ± 5	n.a.	n.a.
A-3/5	32-37	4.5	125 ± 5	n.a.	n.a.
A-4/1	0-5	1	95 ± 5	n.a.	n.a.
A-4/2	0-5	1.5	70 ± 5	n.a.	n.a.
A-5/1	0-5	0	270 ± 5	b.d.l	b.d.l
A-5/2	0-5	0	4110 ± 200	40 ± 5	350 ± 40
A-6/1	0-5	0	120 ± 5	n.a.	n.a.
A-6/2	0-5	0	5000 ± 200	n.a.	n.a.
Site: B **Lat:** 64.88 °S **Long:** 141.07 °E **Date:** 02/08/95					
B-1/1	16-21	5	50 ± 5	n.a.	n.a.
B-1/2	0-5	0	170 ± 5	n.a.	n.a.
B-1/3	8-13	0	25 ± 5	n.a.	n.a.
B-2/1	Snow slush from lead	10	120 ± 5	n.a.	n.a.

Sample ID	Sample depth from surface(cm)	Salinity (‰)	TD-Fe (pg g^{-1})	TD-Mn (pg g^{-1})	TD-Al (pg g^{-1})
Site: S **Lat:** 64.97° S **Long:** 141.45° E **Date:** 03/08/95					
S-1/1	0-5	0	140 ± 10	n.a.	n.a.
S-1/2	0-5	0	70 ± 5	b.d.l.	55 ± 30
S-1/3	11-17	4	30 ± 5	n.a.	n.a.
S-1/4	11-17	3	80 ± 5	n.a.	n.a.
S-1/5	21-26	11	120 ± 5	b.d.l.	40 ± 30
S-1/6	21-26	11	80 ± 5	n.a.	n.a.
S-1/7	29-38	3	80 ± 5	n.a.	n.a.
S-1/8	29-38	3	80 ± 5	n.a.	n.a.
Site: K **Lat:** 64.93° S **Long:** 141.25° E **Date:** 04/08/95					
K-1/3	3-8	1	90 ± 5	n.a.	n.a.
K-1/4	3-8	1	80 ± 5	n.a.	n.a.
Site: H-2 **Lat:** 65.00° S **Long:** 140.21° E **Date:** 09/08/95					
H2-1/1	2-7	0	260 ± 5	n.a.	n.a.
H2-1/2	2-7	0	400 ± 5	n.a.	n.a.
H2-1/3	9-14	3	90 ± 5	n.a.	n.a.
H2-1/4	9-14	5	25 ± 5	n.a.	n.a.
H2-1/5	16-21	3	350 ± 10	n.a.	n.a.
H2-1/6	16-21	6	230 ± 5	n.a.	n.a.

Table A.4 Ross Sea total-dissolvable metals

Sample ID	Sample depth bellow surface(cm)	Salinity (‰)	TD-Fe (pg g^{-1})	TD-Mn (pg g^{-1})	TD-Al (pg g^{-1})
Site: 1 **Lat:** 69.52° S **Long:** 170.6° W **Date:** 10/11/94					
1-2/1	0-18 cm	16	710 ± 15	n.a.	n.a.
1-2/2	0-18 cm	14	790 ± 15	n.a.	n.a.
Site: 2 **Lat:** 75.00° S **Long:** 170.67° W **Date:** 28/11/94					
2-1/1	0-17 cm	0	1170 ± 30	30 ± 5	1035 ± 85
2-1/2	0-17 cm	0	720 ± 20	25 ± 5	855 ± 70
Site: 3 **Lat:** 76.45° S **Long:** 175.52° W **Date:** 02/12/94					
3-1/1	0-5 cm	13	920 ± 20	n.a.	n.a.
3-1/2	.0-5 cm	11	1050 ± 50	n.a.	n.a.

Table A.5 Soluble Fe

Sample ID	TD-Fe (pg g^{-1})	TF-Fe (pg g^{-1})	Filter Blank (pg g^{-1})	Soluble Fe fraction (%)
Prydz Bay				
N-2/2	199 ± 20	30 ± 5	b.d.l.	10
N-2/5	770 ± 10	320 ± 10	b.d.l.	40
N-2/6	90 ± 15	65 ± 10	b.d.l.	70
N-3/1	70 ± 5	10 ± 5	b.d.l.	20
N-3/2	70 ± 10	20 ± 5	b.d.l.	20
O-2/4	810 ± 30	90 ± 10	b.d.l.	10
U-1/2	150 ± 5	70 ± 5	b.d.l.	50
U-1/3	240 ± 10	160 ± 5	b.d.l.	70
U-2/1	640 ± 5	75 ± 5	b.d.l.	10
U-3/2	270 ± 10	80 ± 5	b.d.l.	30
U-3/3	320 ± 5	230 ± 10	b.d.l.	70
U-4/2	280 ± 5	225 ± 5	b.d.l.	80
U-4/3	460 ± 10	50 ± 5	b.d.l.	10
V-2/4	235 ± 10	140 ± 5	b.d.l.	60
V-2/5	1090 ± 10	105 ± 10	b.d.l.	10
V-2/6	260 ± 10	60 ± 10	b.d.l.	25
Princess Elizabeth Land				
LGB 53-2/2	2790 ± 40	615 ± 10	b.d.l.	20
LGB 59-1/3	430 ± 10	385 ± 10	b.d.l.	90
LGB 59-1/4	620 ± 15	375 ± 10	b.d.l.	60
LGB 46-3/4	730 ± 10	190 ± 10	b.d.l.	30
LGB 46-3/3	845 ± 20	505 ± 10	b.d.l.	60

A2 Ice-core trace metal data

Table A.6 Ice-core total-dissolved metals

Core ID	Depth below ice cap (m)	Age ≈BP (1997)	Time span	TD-Fe (pg g^{-1})	TD-Mn (pg g^{-1})	TD-Al (pg g^{-1})
DSS core sections						
DSS 28A-1	46.64 - 46.82	56	summer autumn	140 ± 10	n.a.	n.a.
DSS 28A-2	46.82 - 46.98	56	winter	35 ± 10	n.a.	n.a.
DSS 28A-3	46.98 -47.08	56	spring	60 ± 10	n.a.	n.a.
DSS 28A-4	47.17- 47.54	57	summer autumn	80 ± 10	b.d.l	90 ± 20
DSS 41-B	72.95 – 73.20	88	winter	30 ± 5	b.d.l	50 ± 15
DSS 940	895.74 -895.99	2729	~ 2 years	30 ± 5	b.d.l	20 ± 10
DSS 1165-1	1106.76-1106.94	8518	~ 16 years	110 ± 5	n.a	n.a
DSS 1165-2	1106.94-1107.04	8530	~ 10 years	70 ± 5	n.a	n.a
DE08 core sections						
DE08 55A	96.01- 96.29	69	summer autumn	250 ± 5	20 ± 10	295 ± 335
DE08 55b(a)	96.41 - 96.55	70	autumn	340 ± 5	20 ± 10	320 ± 35
DE08 55b(b)	96.55 – 96.69	70	winter	100 ± 5	b.d.l	70 ± 20
DE08 77A(a)	136.02 – 136.16	102	winter	55 ± 5	b.d.l	b.d.l
DE08 77A(b)	136.16 – 136.30	102	spring	60 ± 5	b.d.l	b.d.l
DE08 85-A	150.90 – 151.42	115	winter	30 ± 5	n.a	n.a
DE08 108-A	192.80 – 193.08	155	summer	75 ± 5	b.d.l	50 ± 15
BHC1 core sections						
BHC1 129-1	256.28-256.39	~ 15000	10	3020 ± 110	n.a	n.a
BHC1 129-2	256.39-256.48	~ 15000	10	2015 ± 90	n.a	n.a

Core ID	Depth below ice cap (m)	Age ≈BP (1997)	Time span	TD-Fe (pg g^{-1})	TD-Mn (pg g^{-1})	TD-Al (pg g^{-1})
BHC1 129-3	256.48-256.59	~ 15000	10	1710 ± 90	n.a	n.a
BHC1 129-4	256.59-256.77	~ 15000	10	3905 ± 130	n.a	n.a
BHC1 129-5	256.77-256.87	~ 15000	10	3740 ± 130	n.a	n.a
BHC1 132A	262.14–262.28	~18000	~ 10 years	6700 ± 200	n.a	n.a
BHC1 137B-1	271.76–271.84	~30000	>10 years	1200 ± 80	n.a	n.a
BHC1 137B-2	271.84–271.91	~30000	>10 years	1230 ± 80	n.a	n.a
BHC1 137B-3	271.91–271.99	~30000	>10 years	750 ± 70	n.a	n.a
BHC1 137B-4	271.99–272.065	~30000	>10 years	1410 ± 80	n.a	n.a
BHC1 137B-5	272.065–272.145	~30000	>10 years	1045 ± 75	n.a	n.a

Table A.7 Ice-core decontamination profiles

Sample layer	Approx. layer depth (cm)	TD-Fe (pg g^{-1})	TD-Al (pg g^{-1})
DSS 28A-L1	4.0 –3.0	4155 ± 590	n.a
DSS 28A-L2	3.0-2.5	1210 ± 50	n.a
DSS 28A-L3	2.5 –2.0	140 ± 10	n.a
DSS 28A-L4	2.0-1.5	110 ± 10	n.a
DSS 28A inner sub-sample	1.5-0.0	80 ± 15	n.a
DE08 -55b-L1	4.0-3.5	5270 ± 140	5470 ± 350
DE08 55b-L2	3.5-2.5	215 ± 10	240 ± 40
DE08 55b-L3	2.5-2.0	440 ± 5	210 ± 30
DE08 55b inner sub sample average	2.0-0.0	215 ± 10	195 ± 30
DSS 1165-L1	2.75-2.5	73620± 2010	n.a.
DSS 1165-L2	2.5-2.0	755 ± 15	n.a.
DSS 1165-L3	2.0-1.5	640 ± 15	n.a.
DSS 1165-L4	1.5-1.0	190 ± 10	n.a.
DSS 1165 inner sub sample average	1.0-0.0	90 ± 5	n.a.
BHC1 132A- L1	4.0 –3.0	19400 ± 1000	n.a
BHC1 132A- L2	3.0-2.5	9700 ± 250	n.a
BHC1 132A- L3	2.5 –2.0	6900 ± 200	n.a
BHC1 132A- L4	2.0-1.5	6900 ± 200	n.a
BHC1 132A inner sample	1.5-0.0	6700 ± 200	n.a
BHC1 137B-L1	4.0 –3.0	8810 ± 800	n.a
BHC1 137B-L2	3.0-2.5	1530 ± 80	n.a.
BHC1 137B-L3	2.5 –2.0	1045 ± 75	n.a.

Sample layer	Approx. layer depth (cm)	TD-Fe (pg g^{-1})	TD-Al (pg g^{-1})
BHC1 137B-L4	2.0-1.5	1270 ± 80	n.a.
BHC1 137B inner sub-sample average	1.5-0.0	1125 ± 170	n.a.

A.3 Enrichment factors

Abbreviations

EF = enrichment factor relative to the earth's crust

Table A.8 Elemental enrichment factors

Sample ID	Fe EF	Mn EF
Prydz Bay snow samples		
N-2/1	0.4	2.3
N-2/2	1.4	na
O-2/1	0.6	0.5
O-2/3	2.5	2.3
V-2/2	0.5	1.0
V-2/3	0.7	1.7
Princess Elizabeth Land snow samples		
LGB 70-1/1	0.6	1.2
LGB 70-2/1	0.7	1.1
LGB 70-2/2	0.6	1.2
LGB 70-3/1	0.7	1.9
LGB 59-3/1	0.4	0.5
LGB 59-3/2	3.0	0.5
LGB 53-1/1	0.4	0.7
LGB 53-2/1	1.4	1.1
LGB 53-3/1	0.6	1.3
LGB 53-3/2	0.7	1.6
LGB 46-1/2	0.2	0.5

Sample ID	Fe EF	Mn EF
LGB 46-2/1	0.6	1.0
LGB 46-3/2	0.1	0.3
Dumont d'Urville Sea snow samples		
A-5/2	14	7
S-1/5	4.0	na
S-1/2	1.4	na
Ross Sea		
2-1/1	1.3	1.6
2-1/2	1.0	1.7
Law Dome ice-core samples		
DSS 108-A	1.7	
DE08 55A	1.1	3.3
DE08 55b(a)	1.3	3.6
DE08 55b(b)	1.7	
DSS 1254	1.3	1.0
DSS 28A-4	1.1	
DSS 41-B	0.8	
DSS 940	2.0	